UNIVERSITY OF CINCINNATI

DATE: November 25, 2003

I, Wendi L. Fleeman ,

hereby submit this as part of the requirements for the degree of:

Doctorate of Philosophy (Ph.D.)

in:

Chemistry

It is entitled:

Self-Quenching and Cross-Quenching Reactions of Platinum(II)Diimine Complexes

Approved by:

Dr. William Connick

Dr. William Heineman

Dr. Michael Baldwin

SELF-QUENCHING AND CROSS-QUENCHING REACTIONS OF PLATINUM(II) DIIMINE COMPLEXES

A dissertation submitted to the

Division of Research and Advanced Studies
of the University of Cincinnati

in partial fulfillment of the
requirements for the degree of

DOCTORATE OF PHILOSOHPY (Ph.D.)

In the Department of Chemistry
of the College of Arts and Sciences

2003

by

Wendi L. Fleeman

B.A., Transylvania University, 1998
M.S., University of Cincinnati, 2000

Committee Chair: Dr. William B. Connick

Abstract

Neutral square planar platinum(II) diimine complexes undergo self-quenching in fluid solution, characterized by an increase in the emission decay rate with concentration. The corresponding quenching rates (10^9-10^{10} $M^{-1}s^{-1}$) are nearly diffusion limited. The accumulated evidence suggests that an excited platinum complex, (M*) reacts with a ground-state complex, (M), to form an excimer, (M_2*), which rapidly relaxes to give two ground-state complexes. These complexes possess many attractive properties for use in application such as DNA recognition and chemical sensing. However, because the self-quenching rates are nearly diffusional, this behavior presents serious problems for applications demanding a long-lived excited state. As a result, there is great interest in learning to control the self-quenching behavior.

Three possible interactions have been proposed to stabilize the excimer: (*i*) diimine-diimine interactions, (*ii*) metal-metal interactions, and (*iii*) a combination of these interactions. Efforts to distinguish between these possibilities have been hampered by short lifetimes and low quantum yields of the excimers. Consequently, we have turned our efforts toward cross-quenching reactions which are similar to self-quenching with the distinction that the excited monomer, M*, reacts with a different ground-state complex, Q, presumably to form an exciplex, MQ*.

Through steady-state and time-resolved cross-quenching studies of Pt(tmphen)(tdt) with quenchers having various steric and electronic properties, we were able to investigate the mechanism of quenching. Rapid rates of cross-quenching (10^9-10^{10} $M^{-1}s^{-1}$) were only observed when the quencher was another platinum(II) diimine complex. Energy transfer and outer-sphere electron transfer were ruled out as possible

quenching mechanisms based on the driving forces for these reactions. The effects of both steric and electronic properties of the platinum(II) diimine quenchers on the observed rate constants have been examined in detail. The accumulated data are consistent with metal-metal interactions playing a critical role in cross-quenching.

To my family

Acknowledgements

Through my years at UC, I have met many individuals who have contributed to the completion of my Ph.D. degree. First, I would like to thank my advisor, Bill Connick for his constant encouragement in helping me to achieve above and beyond what I might have thought possible, not only as a chemist but also as a person. I would also like to thank my committee members, Bill Heineman and Michael Baldwin for their efforts throughout the many stages of my graduate career.

I have also greatly appreciated the support and encouraging words of the Connick group. I especially would like to thank Hershel, who has been there since the beginning, for his way positive attitude, his willingness to answer any and all questions, and his willingness to help in any situation. I would also like to thank P.J. for all the help she has provided while writing my thesis and I wish her success in her future endeavors with quenching.

Finally, I would like to thank the most important people in my life. Close to the beginning of my graduate career, I encountered a sad moment in life. My dad unexpectedly passed away, leaving me to question the importance of graduate school. However, in everything I ever tried to do or succeeded in, my dad was there to cheer me on. Therefore, without his love and support, as well as the continued love, support, and understanding of my husband, mom, sister, nieces, and brother-in-law, I do not believe I would have succeeded in this endeavor.

Table of Contents

List of Tables

List of Schemes

List of Figures

Table of Abbreviations

bdt	1,2 benzenedithiolate
tdt	3,4-toluenedithiolate
bpy	2,2'-bipryridine
dmbpy	4,4'-dimethyl bipryridine
dbbpy	4,4'-di-*t*-butyl bipryridine
dpbpy	4,4'-diphenyl bipyridine
phen	1,10-phenanthroline
dmphen	4,7-dimethyl phenanthroline
dpphen	4,7-diphenyl phenanthroline
2,9-dmphen	2,9-dimethyl phenanthroline
tmphen	3,4,7,8-tetramethyl phananthroline
dppz	dipyrido[3,2-a:2',3'-c]phenazine
Mes	2,4,6-trimethyl phenyl
dppH	2,9-diphenyl-1,10-phenanthroline
tpy	terpyridine
LF	ligand field
R	8.314 J/mol·K
T	temperature
PEG	poly(ethylene glycol)

Chapter 1

Introduction

In the last fifteen years, square planar platinum(II) diimine complexes have been studied extensively due to their rich spectroscopic and photophysical properties, including, for some complexes, room-temperature fluid solution emission, which originates from a long-lived predominantly triplet excited state.[1-31] These complexes consist of a diimine ligand, such as 2,2'-bipyridine (bpy) or 1,10-phenanthroline (phen), chelated to a platinum metal center along with two ancillary ligands (L). In this document, we will focus our comments on neutral complexes with anionic ancillary ligands, though much of this discussion applies to charged complexes. The ancillary ligands are typically neutral groups, such as amines, or anionic ligands, such as Cl^- or CN^-. These complexes possess several attractive properties such as long-lived excited states, tunability of their excited-state energies, different orbital character that gives rise to different excited-state properties, and powerful photo-reducing/photo-oxidizing power.[1-3,11,20-22,32-39] Consequently, there is growing interest in the use of these complexes as photocatalysts, molecular photochemical devices, and luminescent probes for chemical sensing and biological systems such as DNA.[7,9,29,40-44] Notably, the open coordination sites around the metal center in these compounds suggest that molecular properties, such as absorption and emission of light, may be significantly perturbed by interactions with the surrounding medium. Moreover, these sites offer platforms for activation of multielectron substituents or for self-assembly to produce supramolecular structures and macroscopic assemblies.

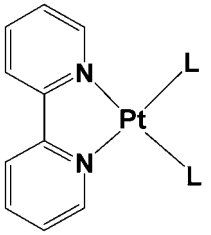

The orbital character of the lowest emissive excited state of these complexes depends on the nature of the anionic ancillary ligands:

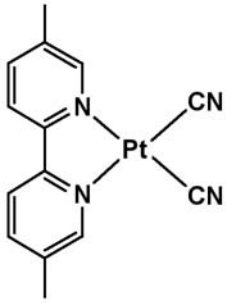

$Pt(5,5'\text{-dmbpy})(CN)_2$

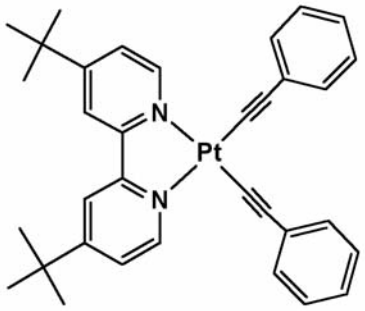

$Pt(dbbpy)(C{\equiv}CC_6H_5)_2$

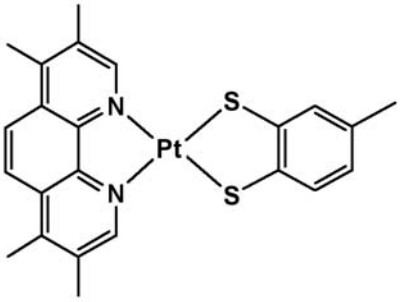

Pt(tmphen)(tdt)

In the case of cyanide groups, the colorless compounds (*e.g.*, $Pt(5,5'\text{-dmbpy})(CN)_2$) exhibit green emission characteristic of a ligand-centered $^3(\pi\text{-}\pi^*)$ excited state. Substitution with phenyl acetylide groups results in yellow complexes (*e.g.*, $Pt(dbbpy)(C{\equiv}CC_6H_5)_2$) with orange or red emission characteristic of a spin-forbidden metal-to-ligand charge transfer state. In the case of dithiolate ligands such as 1,2-toluenedithiolate, the red-violet compounds (*e.g.*, Pt(tmphen)(tdt)) exhibit solvent-sensitive red to near infrared emission. The observed emission is characteristic of a lowest excited-state having significant dithiolate-to-diimine charge transfer character, often identified as a metal-mixed-ligand-to-ligand charge transfer state (MMLLCT). As a result, by simply varying the ancillary ligands it is possible to tune the excited-state energies of these complexes from approximately 1.7 to 2.8 eV and the excited state-lifetimes from the nanosecond to tens of microseconds timescales. This tunability further augments the potential utility of these diimine complexes in photochemical applications. As a result, numerous investigations have been undertaken with the aim of understanding the factors governing the spectroscopic, photophysical and photochemical properties of these chromophores.

One of the most intriguing properties of these complexes and the focus of this discussion was discovered in 1989, when Che and coworkers[10] observed that the emission lifetime of Pt(5,5′-dmbpy)$(CN)_2$ is concentration dependent. The observed behavior is consistent with an excited-state self-quenching reaction in which an excited platinum complex (M*) reacts with a ground-state complex (M) to form an excimer (M_2*):

$$M^* + M \rightarrow M_2^* \rightarrow 2M$$

The excimer rapidly relaxes to give two ground-state complexes and the stored light energy is squandered as heat. The observed rate of emission decay (k') was found to decrease linearly with concentration, corresponding to a rapid self-quenching reaction (k_i =5.24 x 10^5 s^{-1} and k_{sq}= 4.8 x 10^9 $M^{-1}s^{-1}$):

$$k' = k_i + k_{sq}[Pt] \qquad (1)$$

Since this earliest observation, several groups[5-7,9,12,28,45-47] have noted similar self-quenching behavior for other platinum diimine complexes, and in some instances, emission from the excimer was observed (Table 1.2). However, it was not until 1999 that Eisenberg and coworkers[14] presented evidence suggesting self-quenching is a general phenomenon, *characteristic of all fluid-solution emitting platinum(II) diimine complexes, regardless of the lowest emissive triplet excited state of the compound*. Thus, this behavior is characteristic of platinum(II) diimine complexes and is not observed for octahedral luminophores, such as $Ru(bpy)_3^{2+}$.

Because self-quenching rates are nearly diffusion limited, ranging from 10^9 to 10^{10} $M^{-1}s^{-1}$, this behavior presents serious practical problems for applications demanding a long-lived excited state in fluid solution. Accordingly, there is considerable interest in understanding and learning to control this behavior. A major obstacle is that the structure of the excimer is unknown, and

the exact nature of the stabilizing intermolecular interactions is uncertain. Possible modes of association include *(i)* diimine-diimine interactions, *(ii)* metal-metal interactions and *(iii)* a combination of these interactions. All three interactions have been proposed to play a role in excimer formation (Scheme 1.1).[1,13,20-22,32,48]

Scheme 1.1. Proposed modes of association of an excited platinum(II) diimine complex with a ground-state complex.

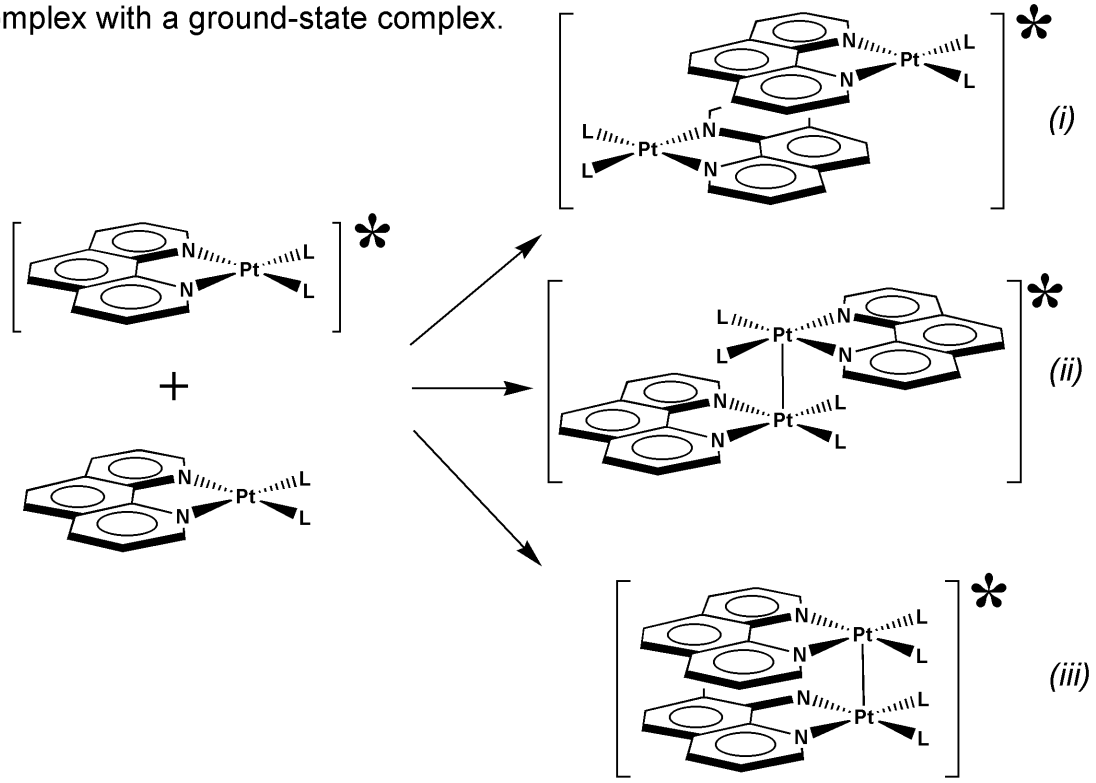

However, all three interactions also occur in crystals and solution aggregates of these complexes,[1,13,20-22,32,48] making it difficult to predict which mode of association will dominate excited-state association.

While direct characterization of the excimer seems an attractive approach to answering this question, these efforts often are hampered by the apparent short lifetimes and low emission quantum yields of the excimers as compared to those of the monomers.[5-7,14,28,31,45,47] Moreover, poor solubility of the monomers and possible ground-state aggregation at high

concentrations hinder characterization. Indeed, several attempts have been made to characterize the nature of the excimer. For example, George, Weinstein, and coworkers[49] recorded the fluid solution time-resolved infrared spectrum (TRIR) of the $Pt(dpphen)(CN)_2$ excimer. Their results show that the ν(CN) stretch of the excimer is only slightly shifted(~ 5 cm^{-1}) from that of the ground-state complex. This result is most consistent with an excimer stabilized by diimine-diimine interactions, however no firm conclusions were reached. Moreover, it is not obvious that all platinum(II) diimine excimers will be supported by the same intermolecular interactions.

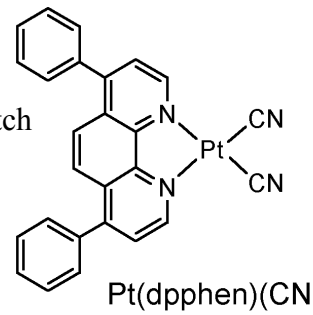

$Pt(dpphen)(CN)_2$

These considerations have led to investigations of cross-quenching reactions as an indirect means of elucidating the mechanism of association involved in self-quenching. A cross-quenching reaction is similar to its self-quenching counterpart with the distinction that the excited monomer, M*, reacts with a different ground-state complex, Q, presumably to form an exciplex, MQ*:

$$M^* + Q \rightarrow MQ^* \rightarrow M + Q$$

Employing this strategy the photophysical behavior of a *single* chromophore can be explored in the presence of a wide variety of possible quenchers (Q). For our studies, Pt(tmphen)(tdt) was chosen as the chromophore due to several attractive properties. These include a long lifetime, a relatively high quantum yield, and a low-energy absorption band allowing for selective excitation of the chromophore and not the quencher complex.

Before describing the cross-quenching investigations with the Pt(tmphen)(tdt) chromophore, aimed at elucidating the interactions involved in excimer formation of Pt(II) diimine complexes, we examine the accumulated photophysical and photochemical data for this

class of complexes in Chapter 2. Specifically, we assess the available self-quenching data for a series of platinum diimine chromophores with varying steric and electronic properties (Table 1.1), and we examine the associated implications for the quenching mechanism. Interestingly, we find no firm evidence of a correlation between the rate of self-quenching and orbital character or the energy of the monomer emissive state. Similarly, no direct correlation was observed between the calculated driving forces for electron transfer and the self-quenching rates, indicating little or no dependence upon electronic properties. However, self-quenching rates appear to be influenced by the steric bulk of substituents on the diimine ligands, although the effects are modest when compared to other excimers and exciplexes.[50] Finally, the kinetics of self-quenching are rigorously examined in order to assess the nature of the excimer and strength of the excimer association. Overall, the evidence provided by self-quenching alone does conclusively implicate the interactions stabilizing the excimer.

As a result, in Chapters 3-6, we explore the cross-quenching reactions of the Pt(tmphen)(tdt) chromophore in an effort to elucidate the mechanism of quenching. In Chapter 3 we report the synthesis of the chromophore and quencher complexes as well as the characterization techniques employed. This chapter also includes details about the electronic structures of the synthesized complexes and how these properties affect the cross-quenching experimental design. For example, we explore how the electronic structures of the quencher complexes determine selection of appropriate quenchers and wavelength of excitation of the chromophore to avoid energy-transfer quenching and the inner-filter effect. We also examine the redox properties of the chromophore and the majority of the quenchers, as well as the structures of four complexes characterized by X-ray crystallography.

In Chapter 4, the steady-state and time-resolved cross-quenching experiments with Pt(tmphen)(tdt) are described. This chapter also details the types of complexes used to investigate the three suggested modes of association. Organic aromatic molecules were used to investigate the efficiency of quenchers lacking a platinum center. Several platinum complexes without diimine ligands were investigated as quenchers to assess how these ligands influence exciplex formation. Finally, platinum(II) diimine complexes with an array of diimine ligands and anionic ancillary ligands were examined as possible quenchers. Surprisingly, it was found that rapid rates (10^9-10^{10} $M^{-1}s^{-1}$), comparable to those observed for self-quenching reactions, were only observed when the quencher was another platinum(II) diimine complex.

In Chapter 5, we discuss the variations in cross-quenching rates and correlations with properties of platinum(II) diimine quenchers. The quenchers are divided into three classes according to the type of diimine ligand: bipyridine and phenanthroline quenchers, dppz quenchers (dppz=dipyrido[3,2-*a*:2',3'-*c*]phenazine), and those containing electron-withdrawing groups on either the diimine or ancillary ligands. The rates of quenching with the bipyridine and phenanthroline complexes are dependent upon the steric bulk around the metal center of the complex. Increasing steric bulk around the metal center results in slower quenching with rates as slow as 10^7 $M^{-1}s^{-1}$. The dppz quenchers do not strictly follow either steric or electronic factors, and no significant changes are observed with variations in either. On the other hand, platinum(II) bipyridine and phenanthroline quenchers with electron-withdrawing ancillary ligands are most dependent upon electronic properties, exhibiting some of the slowest quenching rates (~10^7 $M^{-1}s^{-1}$) suggesting a dependence on electronic properties. Chapter 5 also includes a detailed analysis of the kinetics of cross-quenching based on the assumptions made in Chapter 2 concerning self-quenching.

Chapter 6 examines the accumulated data from self-quenching and cross-quenching reactions, in order to assess the mechanism of quenching. For each class of compounds the possible quenching mechanisms are discussed. The rates for the bipyridine and phenanthroline class of quenchers are dependent on changes in steric properties around the metal center in a manner that is consistent with metal-metal association. To better understand how electronic factors would influence metal-metal interactions, we examine the charge-transfer interactions that are believed to stabilize associated ground-state complexes and extend this analysis to the exciplexes. Electronic factors that favor metal-metal interaction will tend to stabilize the excimer and accelerate quenching. The two most important factors are σ-donor and π-acceptor properties of the ligands, and we show the quenching data for all quenchers, with the exception of the dppz complexes, are consistent with these considerations and support the conclusion that the exciplex is stabilized by metal-metal interactions. In contrast, the dppz complexes quench the emission from Pt(tmphen)(tdt) by formation of a different exciplex, or alternatively, by an entirely different mechanism.

Table 1.1. Self-quenching Data for Pt(II) Diimine Complexes.

Compound	Solvent	Emissive State	λ_{max} (nm)[a]	k_{sq} (10^9 $M^{-1}s^{-1}$)	τ_0 (ns)
Pt(dbbpy)$(CN)_2$[b]	$(CH_2Cl)_2$	$^3(\pi\text{-}\pi^*)$	490[c]	0.9	2900
Pt(dmbpy)$(CN)_2$[d]	CH_3CN	$^3(\pi\text{-}\pi^*)$	502[c]	4.8	6300
Pt(dpphen)$(CN)_2$[e]	PEG	$^3(\pi\text{-}\pi^*)$	530	~6[f]	100
	CH_2Cl_2	$^3(\pi\text{-}\pi^*)$	520	0.5	13000
Pt(dbbpy)$(C\equiv CC_6H_5)_2$[g]	CH_3CN	^{3}MLCT	570	1.4 ± 0.2	691
Pt(dbbpy)$(C\equiv CC_6H_4F)_2$[g]	CH_3CN	^{3}MLCT	570	1.6 ± 0.1	663
Pt(dbbpy)$(C\equiv CC_6H_4CH_3)_2$[g]	CH_3CN	^{3}MLCT	592	1.0 ± 0.2	440
Pt$(C_6H_5C\equiv$Cphen$)(C\equiv CC_6H_5)_2$[g]	CH_3CN	^{3}MLCT	590	4.2 ± 0.3	5600
Pt(phen)$(C\equiv CPh)_2$[h]	CH_3CN	^{3}MLCT	575	6.3	904
	CH_2Cl_2	^{3}MLCT	565	3.3	1888
Pt(phen)$(C\equiv CC_6H_4F)_2$[h]	CH_3CN	^{3}MLCT	584	6.7	814
Pt$(CH_3$phen$)(C\equiv CC_6H_5)_2$[g]	CH_3CN	^{3}MLCT	575	5.5 ± 0.2	972
Pt(phen)$(C\equiv CC_6H_4CH_3)_2$[h]	CH_3CN	^{3}MLCT	578	6.2	549
Pt(Brphen)$(C\equiv CC_6H_5)_2$[g]	CH_3CN	^{3}MLCT	605	4.6 ± 0.2	366
Pt(Clphen)$(C\equiv CC_6H_5)_2$[g]	CH_3CN	^{3}MLCT	605	5.5 ± 0.7	390
Pt(tmphen)(tdt)[h]	CH_2Cl_2	^{3}MMLLCT	675[i]	4.2	1911
Pt(bpy)(bdt)[j]	CH_3CN	^{3}MMLLCT	700[i]	9.5	460
	$CHCl_3$	^{3}MMLLCT	705[i]	4.0	560
Pt(dbbpy)(tdt)[h]	CH_2Cl_2	^{3}MMLLCT	720[i]	1.0	489
Pt(dmbpy)(tdt)[h]	CH_2Cl_2	^{3}MMLLCT	720[i]	2	360
Pt(phen)(tdt)[h]	CH_2Cl_2	^{3}MMLLCT	730[i]	4.7	580
Pt(5,5'-dmbpy)$(C\equiv CC_6H_5)_2$[k]	CH_2Cl_2	^{3}MLCT	545	2.79	1600
Pt(4,4'-dbbpy)$(C\equiv CC_6H_5)_2$[k]	CH_2Cl_2	^{3}MLCT	554	0.29	1300
Pt(4,4'-dmbpy)$(C\equiv CC_6H_5)_2$[k]	CH_2Cl_2	^{3}MLCT	554	2.20	1200
Pt(4,4'-dpbpy)$(C\equiv CC_6H_5)_2$[k]	CH_2Cl_2	^{3}MLCT	580	1.84	1000
Pt(tmphen)$(C\equiv CC_6H_5)_2$[k]	CH_2Cl_2	^{3}MLCT	522	2.90	2700
Pt(5,6-dmphen)$(C\equiv CC_6H_5)_2$[k]	CH_2Cl_2	^{3}MLCT	554	3.46	2300
Pt(5-mphen)$(C\equiv CC_6H_5)_2$[k]	CH_2Cl_2	^{3}MLCT	558	3.86	2000
Pt(phen)$(C\equiv CC_6H_5)_2$[k]	CH_2Cl_2	^{3}MLCT	561	3.68	1900
Pt(5-pphen)$(C\equiv CC_6H_5)_2$[k]	CH_2Cl_2	^{3}MLCT	563	2.32	2000
Pt(4,7-dpphen)$(C\equiv CC_6H_5)_2$[k]	CH_2Cl_2	^{3}MLCT	570	1.36	2800

Pt(4,4'-dbbpy)(C≡C-C≡C_6H_5)$_2$ [k]	CH_2Cl_2	^{3}MLCT	536	1.00	1100
[Pt(Thpy)(pz)]$_2$ [l]	CH_2Cl_2	^{3}MLCT	559 [c]	0.035	15500
[Pt(Thpy)(aza)]$_2$ [l]	CH_2Cl_2	^{3}MLCT	561 [c]	—— [n]	3100
[Pt(Thpy)(bzim)]$_3$ [l]	CH_2Cl_2	^{3}MLCT	560 [c]	0.030	10900
Pt(bpy)(C≡CC_6H_4-2,2-dipyridylamine)$_2$ [m]	CH_2Cl_2	^{3}MLCT	571	—— [n]	1300
Pt(phen)(C≡CC_6H_4-2,2-dipyridylamine)$_2$ [m]	CH_2Cl_2	^{3}MLCT	590	—— [n]	6100

[a]Corrected emission maximum unless specified. [b]Ref 5. [c]Structured emission. [d]Ref 10. [e]Ref 28, 26. [f]Self-quenching rate obtained from the quenching half-concentration, assuming that $k_{MD} << k_D$ [g]Ref 18. [h]Ref 14, estimated errors for k_{sq} are ±0.1to ±0.2. [i]Uncorrected emission maximum. [j]Ref 12. [k]Ref 9. [l]Ref 51. [m]Ref. 47. [n]No k_{sq} reported.

Table 1.2. Excimer emissions of platinum(II) diimine complexes.[i]

Compound	Solvent	Monomer			Excimer			
		Emissive State	τ (ns)	λ_{max}(nm)	τ_D (ns)	λ_{max} (nm)	FWHM[g] (cm^{-1})	ΔE (cm^{-1})[h]
Pt(dpphen)$(CN)_2$[a]	PEG	$^3(\pi\text{-}\pi^*)$	100	530[f]	~ 100	630	~ 3500	4500
	CH_2Cl_2	$^3(\pi\text{-}\pi^*)$	13000	520[f]	~ 3000	665	~ 4000	5900
Pt(dppby)$(CN)_2$[b]	$CH_3CH_2Cl_2$	$^3(\pi\text{-}\pi^*)$	2900	485[f]	~ 40	565	~ 3600	6700
[Pt(dppH)(CH_3CN)]$(Cl_4$[c]	CH_2Cl_2	^{3}MLCT	2600	550[f]	~ 900	~ 700	~ 4400	3500
Pt(phen)$(C\equiv CPh)_2$[d]	CH_2Cl_2	^{3}MLCT	904	565	~ 100	~ 750	~ 2800	6700
Pt$(C_6H_3C\equiv C$phen$)(C?CC_5$[e]	CH_3CN	^{3}MLCT	5600	590	—	~ 750	~ 2600	7000

[a]Ref 45,52. [b]Ref. 53. [c]Ref. 7. [d]Ref. 16. [e]Ref. 19. [f]structured emission. [g]FWHM=full-width at half maximum intensity. [h]$\Delta E = E_{0,0} - \nu_{max}$(excimer). [i] Fluid solution eximer emission has been reported by Wang and coworkers (Ref 47) for two other complexes, Pt(bpy)$(C\equiv CC_6H_4$-2,2'-dipyridylamine$)_2$ and Pt(phen)$(C\equiv CC_6H_4$-2,2'-dipyridylamine$)_2$. However, a detailed description of the photophysical analyses was not provided.

References

1. Miskowski, V. M.; Houlding, V. H. *Inorg. Chem.* **1989**, *28*, 1529-1533.
2. Miskowski, V. M.; Houlding, V. H. *Inorg. Chem.* **1991**, *30*, 4446-4452.
3. Miskowski, V. M.; Houlding, V. H.; Che, C.-M.; Wang, Y. *Inorg, Chem.* **1993**, *32*, 2518-2524.
4. Vogler, C.; Schwederski, B.; Klein, A.; Kaim, W. *J. Organomet. Chem.* **1992**, *436*, 367-378.
5. Wan, K.-T.; Che, C.-M.; Cho, K.-C. *J. Chem. Soc., Dalton Trans.* **1991**, 1077-1080.
6. Chan, C.-W.; Che, C.-M.; Cheng, M.-C.; Wang, Y. *Inorg. Chem.* **1992**, *31*, 4874-4878.
7. Chan, C. W.; Lai, T. F.; Che, C. M.; Peng, S. M. *J. Am. Chem. Soc.* **1993**, *115*, 11245-11253.
8. Chan, C. W.; Cheng, L. K.; Che, C.-M. *Coord. Chem. Rev.* **1994**, *31*, 87-97.
9. Chan, S.-C.; Chan, M. C. W.; Wang, Y.; Che, C.-M.; Cheung, K.-K.; Zhu, N. *Chem. Eur. J.* **2001**, *7*, 4180-4190.
10. Che, C.-M.; Wan, K.-T.; He, L.-Y.; Poon, C.-K.; Yam, V. W.-W. *J. Chem. Soc., Chem. Commun.* **1989**, 943-945.
11. Connick, W. B.; Henling, L. M.; Marsh, R. E.; Gray, H. B. *Inorg. Chem.* **1996**, *35*, 6261-6265.
12. Connick, W. B.; Gray, H. B. *J. Am. Chem. Soc.* **1997**, *119*, 11620-11627.
13. Connick, W. B.; Marsh, R. E.; Schaefer, W. P.; Gray, H. B. *Inorg. Chem.* **1997**, *36*, 913-922.
14. Connick, W. B.; Geiger, D.; Eisenberg, R. *Inorg. Chem.* **1999**, *38*, 3264-3265.
15. Connick, W. B.; Miskowski, V. M.; Houlding, V. H.; Gray, H. B. *Inorg. Chem.* **2000**, *39*, 2585-2592.
16. Cummings, S. D.; Eisenberg, R. *J. Am. Chem. Soc.* **1996**, *118*, 1949-1960.

17. Dungey, K. E.; Thompson, B. D.; Kane-Magiore, N. A. P.; Wright, L. L. *Inorg. Chem.* **2000**, *39*, 5192-5196.

18. Hissler, M.; Connick, W. B.; Geiger, D. K.; McGarrah, J. E.; Lipa, D.; Lachicotte, R. J.; Eisenberg, R. *Inorg. Chem.* **2000**, *39*, 447-457.

19. Hissler, M.; McGarrah, J. E.; Connick, W. B.; Geiger, D. K.; Cummings, S. D.; Eisenberg, R. *Coord. Chem. Rev.* **2000**, *208*, 115-37.

20. Kato, M.; Sasano, K.; Kosuge, C.; Yamazaki, M.; Yano, S.; Kimura, M. *Inorg. Chem.* **1996**, *35*, 116-123.

21. Kato, M.; Kosuge, C.; Morii, K.; Ahn, J. S.; Kitagawa, H.; Mitani, T.; Matsushita, M.; Kato, T.; Yano, S.; Kimura, M. *Inorg. Chem.* **1999**, *38*, 1638-1641.

22. Kato, M.; Kozakai, M.; Fukagawa, C.; Funayama, T.; Yamauchi, S. *Mol. Cryst. Liq. Cryst.* **2000**, *343*, 353-358.

23. Klein, A.; Hausen, H. D.; Kaim, W. *J. Organomet. Chem.* **1992**, *440*, 207-217.

24. Klein, A.; Kaim, W. *Organometallics* **1995**, *14*, 1176-1186.

25. Klein, A.; Kaim, W.; Waldhor, E.; Hausen, H.-D. *J. Chem. Soc. Perkin Trans.* **1995**, *2*, 2121-2126.

26. Klein, A.; Scheiring, T.; Kaim, W. *Z. Anorg. Allg. Chem.* **1999**, *625*, 1177-1180.

27. Klein, A.; McInnes, E. J. L.; Kaim, W. *J. Chem. Soc., Dalton Trans.* **2002**, 2371-2378.

28. Kunkely, H.; Vogler, A. *J. Am. Chem. Soc.* **1990**, *112*, 5625-5627.

29. Liu, H. Q.; Peng, S. M.; Che, C.-M. *J. Chem. Soc., Chem. Comm.* **1995**, 509-510.

30. Liu, H. Q.; Cheung, T. C.; Che, C.-M. *J. Chem. Soc., Chem. Comm.* **1996**, 1039-1040.

31. Lu, W.; Chan, M. C. W.; Cheung, K. K.; Che, C. M. *Organometallics* **2001**, *20*, 2477-2486.

32. Bailey, J. A.; Hill, M. G.; Marsh, R. E.; Miskowski, V. M.; Schaefer, W. P.; Gray, H. B. *Inorg. Chem.* **1995**, *34*, 4591-4599.

33. Houlding, V. H.; Miskowski, V. M. *Coord. Chem. Rev.* **1991**, *111*, 145-152.

34. Biedermann, J.; Wallfahrer, M.; Gliemann, G. *J. Luminesc.* **1987**, *37*, 323-329.

35. Weiser-Wallfahrer, M.; Gliemann, G. *Z. Naturforsch.* **1990**, *45b*, 652-657.

36. Biedermann, J.; Gliemann, G.; Klement, U.; Range, K.-J.; Zabel, M. *Inorg. Chem.* **1990**, *29*, 1884-1888.

37. Biedermann, J.; Gliemann, G.; Klement, U.; Range, K.-J.; Zabel, M. *Inorg. Chim. Acta* **1990**, *171*, 35-40.

38. Biedermann, J.; Gliemann, G.; Klement, U.; Range, K.-J.; Zabel, M. *Inorg. Chim. Acta* **1990**, *169*, 63-70.

39. Crosby, G. A.; Kendrick, K. R. *Coord. Chem. Rev.* **1998**, *171*, 407-417.

40. Drew, S. M.; Janzen, D. E.; Buss, C. E.; Macewan, D. I.; Dubline, K. M.; Mann, K. R. *J. Am. Chem. Soc.* **2001**, *123*, 8414-8415.

41. Bielli, E.; Gidney, P. M.; Gillard, R. D.; Heaton, B. T. *J. Chem. Soc., Dalton Trans.* **1974**, 2133-2139.

42. Shih, K.-C.; Herber, R. H. *Inorg. Chem.* **1992**, *31*, 5444-5449.

43. Kato, M.; Omura, A.; Toshikawa, A.; Kishi, S.; Sugimoto, Y. *Angew. Chem. Int. Ed.* **2002**, *41*, 3183.

44. Buss, C. E.; Mann, K. R. *J. Am. Chem. Soc.* **2002**, *124*, 1031-1039.

45. Pettijohn, C. N.; Jochnowitz, E. B.; Chuong, B.; Nagle, J. K.; Vogler, A. *Coord. Chem. Rev.* **1998**, *171*, 85-92.

46. Lai, S. W.; Chan, M. C. W.; Cheung, K. K.; Peng, S. M.; Che, C. M. *Organometallics* **1999**, *18*, 3991-3997.

47. Kang, Y.; Lee, J.; Song, D.; Wang, S. *J. Chem. Soc. Dalton Trans.* **2003**, 3493-3499.

48. Buchner, R.; Cunningham, C. T.; Field, J. S.; Haines, R. J.; McMillin, D. R.; Summerton, G. C. *J. Chem. Soc., Dalton Trans.* **1999**, *5*, 711-717.

49. Kuimova, M. K.; Melnikov, M. Y.; Weinstein, J. A.; George, M. W. *J. Chem. Soc., Dalton Trans.* **2002**, 2857-2861.

50. Birks, J. B. *Photophysics of Aromatic Molecules*; Wiley-Interscience: London, 1970.

51. Lai, S. W.; Chan, M. C. W.; Cheung, K. K.; Peng, S. M.; Che, C. M. *Organometallics.* **1999**, *18*, 3991-3997.

52. Kunkely, H.; Vogler, A. *J. Am. Chem. Soc.* **1990**, *112*, 5625-5627.

53. Wan, K.-T.; Che, C.-M.; Cho, K.-C. *J. Chem. Soc., Dalton Trans.* **1991**, 1077-1080.

Chapter 2

Photophysical and Photochemical Properties of Platinum(II) Diimine Complexes

I. Electronic Structures

Platinum(II) diimine complexes often exhibit intense, long-lived emissions in the solid-state and fluid solution. In solid samples or at very high concentrations, intermolecular interactions (*e.g.*, Pt···Pt, ligand···ligand) can directly influence the nature of the lowest excited states. The spectroscopic and photophysical properties of those systems have been discussed by Miskowski[1-4] and others.[5-13] The following comments are restricted to the lowest, predominantly triplet excited states of discrete monomers.

Scheme 2.1. Orbital energy level diagram for $Pt(bpy)X_2$.

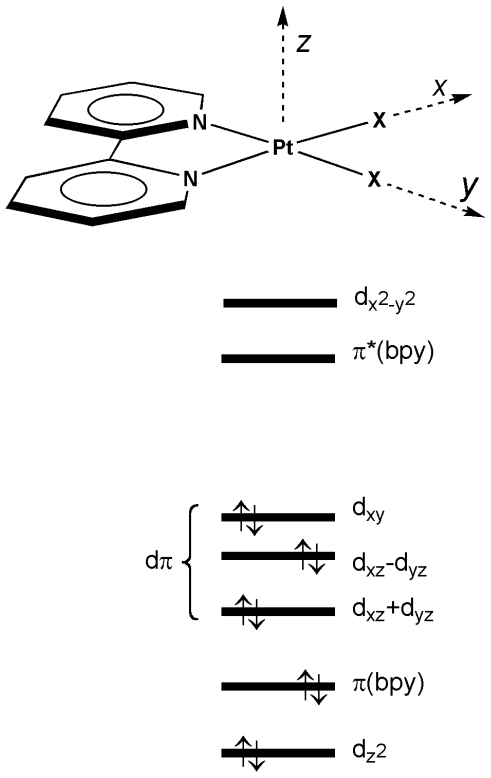

From molecular orbital considerations (Scheme 2.1),[1,14] the highest occupied levels are expected to be predominantly metal-centered with *d* orbital character or diimine ligand-centered with π orbital character. Similarly, the lowest unoccupied levels are expected to have $d_{x^2-y^2}$ or

π*(diimine) character. The order of the resulting lowest diimine-localized $^3(\pi\text{-}\pi^*)$ states and metal-centered ligand field states (^{3}LF) depends on the nature of the anionic ancillary ligands (Scheme 2.2). Strong σ-donor ligands destabilize LF states, resulting in a high-energy, structured emission originating from a $^3(\pi\text{-}\pi^*)$ excited state, as observed for Pt(dbbpy)$(CN)_2$ (emission in CH_2Cl_2 solution: 456, 489, 519, 560sh nm at 298 K; Figure 2.1a).[15,16] In contrast, complexes with weak σ-donor ligands, illustrated by Pt(bpy)Cl_2 (solid-state emission: λ_{max}=641 nm; FWHM=4000 cm^{-1}; τ=500 ns at 250 K), often exhibit a Stokes-shifted, weak, broad emission originating from a ^{3}LF state.[1]

The presence of low-lying $^3(\pi\text{-}\pi^*)$ and ^{3}LF states suggests the proximity of a triplet metal-to-ligand charge-transfer (^{3}MLCT) [*d*(Pt)→ π*(diimine)] state. Indeed, moderately intense ^{1}MLCT transitions (ε~3-4,000 $M^{-1}cm^{-1}$) are often observed to the red of the $^1(\pi\text{-}\pi^*)$ bands. These considerations have led Miskowski and coworkers[2,14] to propose two strategies for tuning the electronic structures of these complexes depending on the nature of the ancillary ligands (Scheme 2.2). In the case of weak σ donors, illustrated by Pt(3,3'-$(CO_2Me)_2$bpy))Cl_2 (solid-state emission: λ_{max}=556sh, 587, 667sh nm; τ=350 ns at 300 K), substitution of electron withdrawing groups on the diimine stabilizes the ligand π* levels relative to the antibonding

Scheme 2.2. Qualitative representation of the excited-state energies of Pt(diimine)X_2 complexes.

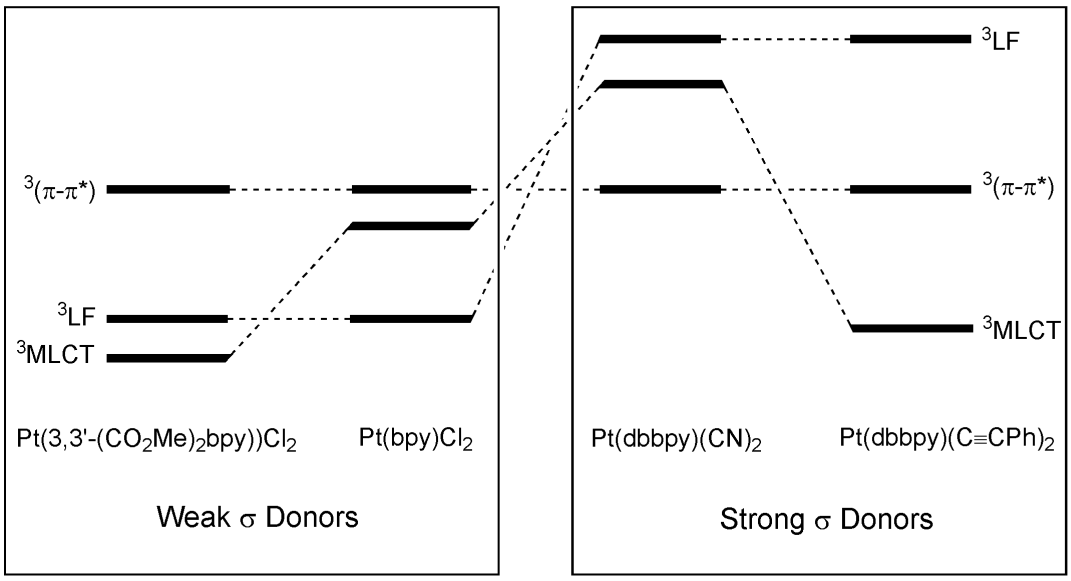

$d_{x^2-y^2}$ level, resulting in a lowest ^{3}MLCT state.[2] In the case of strong σ donor ligands, as observed for Pt(diimine)R_2 (R=alkyl, aryl, arylacetylide, 3,5-dimethyl-pyrazolate)[14,17-21] strongly electron-donating ligands effectively destabilize the filled *d* levels relative to the diimine π levels resulting in a lowest ^{3}MLCT state (*e.g.*, Pt(dbbpy)(C≡CPh)$_2$, Scheme 2.2).

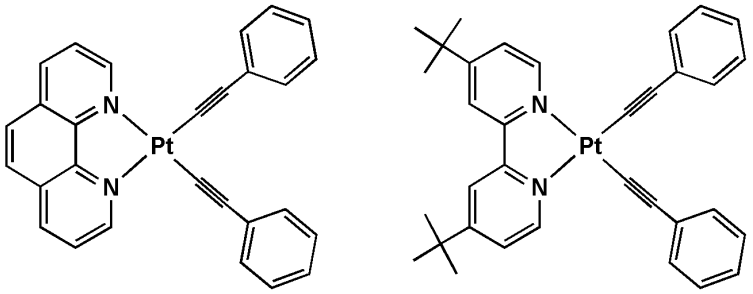

Pt(phen)(C≡CPh)$_2$ Pt(dbbpy)(C≡CPh)$_2$

An intriguing situation arises when non-innocent ligands, such as dithiolates are coordinated to the Pt center. Complexes such as Pt(tmphen)(tdt) (λ_{max}=535 nm, 7160 $M^{-1}cm^{-1}$, CH_2Cl_2; 526 nm, DMSO; Figure 2.1c) exhibit a broad, solvent-sensitive, charge-transfer absorption band shifted to the red of the lowest ^{1}MLCT absorption bands. Studies by Eisenberg[22,23] and others[24-30] have established that the highest occupied levels in these complexes have considerable dithiolate ligand character, and the lowest unoccupied levels have mostly diimine ligand character. Because of the extensive mixing of the Pt and dithiolate levels, the low-energy band has been assigned as a mixed-metal-ligand(dithiolate)-to-ligand(diimine) charge transfer (MMLLCT) transition.[31,32] Intense emission from these complexes is proposed to originate from the corresponding ^{3}MMLLCT state (Pt(tmphen)(tdt): λ_{max}=720 nm in CH_2Cl_2; (Figure 2.1c). Thus, these molecules share a converse relationship with asymmetric mixed-valence complexes (*e.g.*, $(CN)_5Ru^{II}(CN)Ru^{III}(NH_3)_5^-$)[33] popularized in studies of intramolecular electron transfer. The ligands assume the roles of donor (dithiolate) and acceptor (diimine), and the metal acts as the bridge mediating electronic coupling. Therefore, it is

possible to describe the non-radiative excited-state decay process using the Energy Gap Law[22,34] or semi-classical electron-transfer theory.[35]

The remarkable intensity of the MMLLCT absorption band (6,000-19,000 $M^{-1}cm^{-1}$),[22,32] as compared to ^{1}MLCT transitions,[29] may be a result of coupling to the intense d→p transitions of platinum. Alternatively, ligand-metal orbital mixing may facilitate partial delocalization across the metal center, giving the complex some of the π-delocalization character attributed to nickel(II) analogues.[36] The lowest triplet component of this charge transfer, presumably buried in the broad absorption band, remains elusive and never has been directly identified in absorption or excitation spectra, even at low temperature. Nevertheless, as expected for the MMLLCT states, the apparent singlet-triplet splitting (~1,000 cm^{-1}) is smaller than observed for MLCT states (3,000-4,000 cm^{-1}), indicating a greater degree of charge separation.[29]

II. Fluid Solution Emission

The fact that many platinum diimine complexes are only weakly emissive or non-emissive in fluid solution is not fully understood. Of the preceding, only some of those with lowest ^{3}(π-π*), ^{3}MLCT, or ^{3}MMLLCT states have been found to exhibit long-lived emission in room-temperature solution. The absence of fluid solution emission from a ^{3}LF state is consistent with rapid non-radiative decay, as expected for an excited-state geometry that is very different from that of the ground state due to the antibonding nature of the $d_{x^2-y^2}$ level. In fact, the presence of thermally accessible ^{3}LF states frequently has been suggested in order to account for the absence of fluid solution emission from platinum diimine complexes with lowest ^{3}(π-π*), ^{3}MLCT, or ^{3}MMLLCT states. While likely correct in certain instances, this explanation cannot account for the observed wide variations in σ-donor strength of ancillary ligands and energies of the lowest excited states. Strong interactions with solvent and/or non-totally symmetric

distortions also are expected to play an important role in non-radiative decay, and these mechanisms can be expected to depend strongly on the orbital character of the excited state.[2,14,32,37]

A closer examination of the luminescent complexes in Table 2.1 reveals some interesting trends. The $E_{0,0}$ energies decrease along the emitting $^3(\pi\text{-}\pi*)$, ^{3}MLCT, ^{3}MMLLCT series, ranging from ~2.7 to 1.7 eV. Very generally speaking, the longest emission lifetimes and quantum yields also appear to slightly decrease along this series. In fluid solution, complexes with lowest $^3(\pi\text{-}\pi^*)$ excited states tend to have the longest lifetimes, in part because of somewhat reduced spin-orbit coupling. Of these, the di(cyanide) derivatives seem most often to give rise to fluid solution emission. Complexes with a lowest ^{3}MLCT state appear to have slightly longer lifetimes and larger emission quantum yields than those with a lowest ^{3}MMLLCT state. Of the ^{3}MLCT emitters, only the di(arylacetylide) complexes frequently exhibit long-lived solution emission, perhaps because of the nature of the partially occupied Pt *d* orbital and/or the reduction in ligand rotational motion near the metal center. Complexes with a cyclometalating diimine ligand, such as $Pt(dpp)(CH_3CN)^+$ (dppH=2,9-diphenyl-1,10-phenanthroline) also apparently emit from a lowest ^{3}MLCT excited state in fluid solution, albeit with relatively short lifetimes (<150 ns) (Table 2.1). Of the complexes with a lowest ^{3}MMLLCT state, those with a toluenedithiolate (tdt^{2-}) ligand seem to exhibit the longest lifetimes in fluid solution, almost surely in part because the emissive state is strongly stabilized with respect to the LF states. For these reasons, fluid solution emission studies have tended to focus on complexes with cyanide, arylacetylide and/or toluenedithiolate ligands such as those listed in Table 2.1.

III. Self-Quenching

Attractive properties such as long-lived excited states, tunability of excited-state energies, variations in orbital character of the lowest excited states, and powerful photo-reducing/photo-oxidizing power have prompted investigations aimed at understanding the factors governing the spectroscopic, photophysical and photochemical properties of these chromophores. As early as 1989, Che and coworkers determined that the emission lifetime of one of the diimine complexes, Pt(5,5′-dmbpy)$(CN)_2$, is concentration dependent.[38] The observed behavior is consistent with an excited-state self-quenching reaction in which an excited platinum complex (M*) reacts with a ground-state complex (M) to form an excimer (M_2*):

$$M^* + M \rightarrow M_2^* \rightarrow 2M \quad (1)$$

The excimer rapidly relaxes to give two ground-state complexes and the stored light energy is squandered as heat. The observed rate of emission decay ($k'=1/\tau$) was found to decrease linearly with concentration, corresponding to a rapid self-quenching reaction (k_i= 5.23 x 10^5 $s^{-1}$and k_{sq}=4.8 x 10^9 $M^{-1}s^{-1}$):

$$k' = k_i + k_{sq}[Pt] \quad (2)$$

While the predicted excited-state lifetime at infinite dilution ($\tau=1/k_i$=6.3 μs) is long, the observed lifetime in concentrated solutions is severely attenuated by the nearly diffusion limited self-quenching reaction (k_{sq}=4.8 x 10^9 $M^{-1}s^{-1}$). The following year, Kunkely and Vogler[39]reported that, with increasing concentration, the green emission from Pt(dpphen)$(CN)_2$ (λ_{max}=530 nm) in polyethylene glycol is gradually replaced by a red emission (λ_{max}=630 nm), attributed to an excimer. Subsequently, Che and co-workers[15] reported self-quenching (k_{sq}=0.9 x 10^9 $M^{-1}s^{-1}$) accompanied by excimer emission from solutions of Pt(dbbpy)$(CN)_2$. Transient emission measurements indicate that the excimer luminescence reaches its maximum intensity

approximately 100 ns after excitation with a short laser flash, confirming the notion that the excimer is not a ground-state aggregate.

Since this earliest observation, several groups have noted similar self-quenching behavior for other platinum(II) diimine complexes, and in several instances, emission from the excimer was observed.[15,39-43] However, it was not until 1999 that Eisenberg and coworkers presented evidence suggesting self-quenching is a general phenomenon, *characteristic of all fluid-solution emitting platinum(II) diimine complexes (Table 2.1), regardless of the lowest emissive triplet excited state of the compound*.[16]

Because self-quenching rates are nearly diffusion limited, ranging from 10^9 to 10^{10} $M^{-1}s^{-1}$, this behavior presents serious practical problems for applications demanding precise control of a long-lived excited state in fluid solution. Accordingly, there is considerable interest in understanding and learning to control this behavior.

Scheme 2.3. Proposed modes of association.

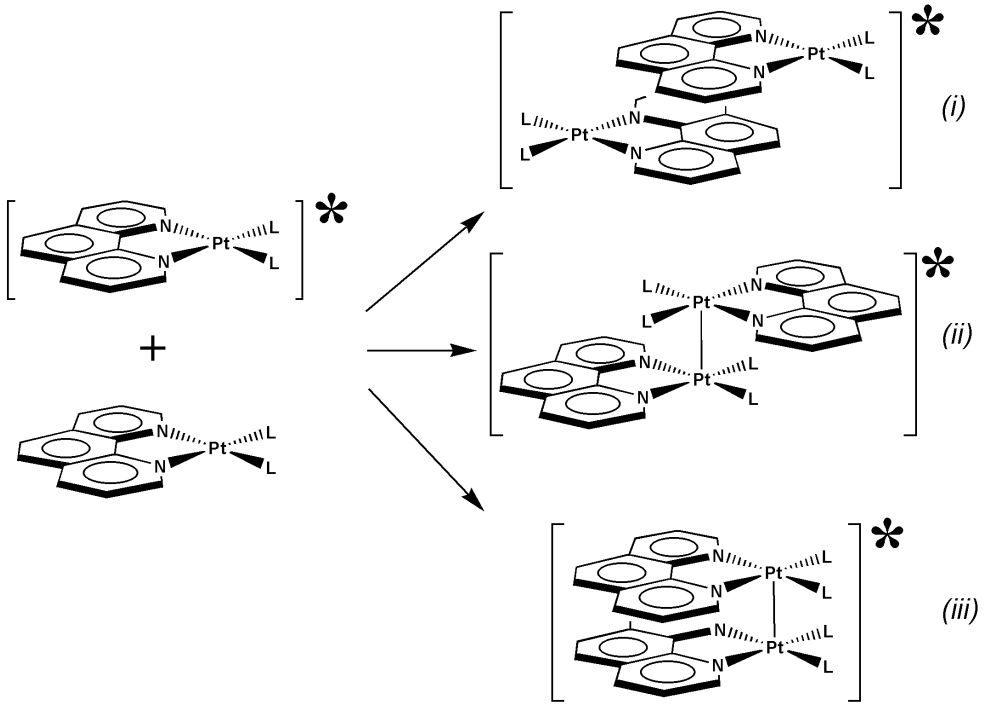

A major obstacle is that the structure of the excimer is unknown, and the exact nature of the stabilizing intermolecular interactions is uncertain. Possible modes of association include *(i)* diimine-diimine interactions, *(ii)* metal-metal interactions, or alternatively, *(iii)* a combination of these interactions (Scheme 2.3). Indeed, all three interactions occur in crystals and solution aggregates of these complexes, making it difficult to assess which will dominate excited-state association.[1,10,13,43-45]

For each complex, the transient emission decay is well described by a single-exponential function. The corresponding rate of decay (k') exhibits a linear dependence on concentration according to equation (2). For neutral complexes (Table 2.1), the resulting self-quenching rates (k_{sq}) range from ~10^9 to ~10^{10} $M^{-1}s^{-1}$, indicating a very efficient reaction. Since the unimolecular excited-state decay rates ($k_i=1/\tau$) are relatively slow (~10^6 s^{-1}), the self-quenching reaction plays a significant role in deactivation for concentrations greater than ~10 to 100 μM. Therefore, it is not surprising that self-quenching has not yet been reported for complexes with very short fluid solution lifetimes (τ<100 ns; $k_i>10^7$ s^{-1}).[21] Limited solubility, weak emission and short lifetimes are expected to restrict the range of accessible concentrations and observable emission decay rates.

Inspection of Table 2.1 provides some insight into the nature of this reaction. There is no firm correlation between the self-quenching rate and the orbital character or energy of the monomer emissive state, suggesting that, within this series, quenching may be independent of the electronic structure of the monomer. Nevertheless, it should be noted that all three classes of complexes share a common electronic property, namely a lowest energy unoccupied diimine π^* orbital. On the other hand, it is readily apparent that bulky substituents on the diimine ligand slow the self-quenching reaction. For example, the *t*-butyl groups of dbbpy appear to reduce the

self-quenching rate by a factor of ~5. Unfortunately, there is limited information concerning the steric effects of the ancillary anionic ligands. Similarly, the solvent dependence of these reactions has not yet been examined in detail. However, there is mounting evidence to suggest that halogenated solvents tend to slow self-quenching by ~50%, regardless of the nature of the monomer excited state. This decrease is slightly greater than expected from viscosity considerations for a diffusion-controlled process.[46,47] From Stokes law of diffusion, we expect the rate of quenching to be inversely proportional to the viscosity of the solvent, and we predict a 17% decrease in the self-quenching rate on going from CH_3CN to CH_2Cl_2 (15ºC: η=0.375, CH_3CN; 0.449, CH_2Cl_2).[47] It also should be noted that charged complexes exhibit self-quenching rates that are slower than observed for neutral complexes, as might be expected from Coulombic repulsions. However, the ionic strength dependence of these reactions has not yet been investigated.

The accumulated evidence suggests that self-quenching is a dynamic process, resulting from a collisional encounter between an excited complex and a ground-state complex. The absorption spectra of the compounds in Table 2.1 are reported to obey Beer's Law over the investigated concentrations. Similarly, the excitation spectra are in good agreement with the absorption spectra. For several complexes, the observed decay rates (k')[48] and quantum yields[40] are known to be insensitive to excitation wavelength, indicating that self-quenching is not a static process. Also, these rates are invariant over modest ranges of excitation power (~0.5-2 mJ/pulse), suggesting that self-quenching is not dominated by triplet-triplet annihilation.[16,29]

There also is little evidence to support the notion that self-quenching occurs by electron-transfer. From constructing a Latimer diagram for each complex as shown in Figure

2.2, and utilizing the following equation representing the oxidation and reduction potentials of an excited platinum complex reacting with a ground state platinum complex, we were able to calculate the driving forces for photoinduced oxidation and reduction.

$$Pt^* + Pt \rightarrow Pt^+ + Pt^- \quad (3)$$

Using the excited-state redox potentials and $E_{0,0}$ values (estimated from the maximum of the emission intensity at 77 K) reported by Cummings and Eisenberg,[22] Che and coworkers, and Eisenberg and coworkers[20] we have estimated the photoinduced electron-transfer reaction driving forces (ΔG) (Figure 2.2, Table 2.2) for nine of the compounds in Table 2.1.

For the dithiolate complexes with lowest MMLLCT states and Pt(dbbpy)$(CN)_2$ with a lowest π-π^* state, the reaction is endergonic (ΔG=0.011 to 0.15 eV), whereas the reaction is slightly exergonic (ΔG=-0.03 to +0.30 eV) for the di(arylacetylide) complexes. If charge transfer plays a significant role, the self-quenching rate is expected to increase with driving force. However, Figure 2.2 does not give any indication of a relationship between the two parameters, and any correlation is maybe masked by steric effects. A similar analysis of cross-quenching rates is discussed in Chapter 5.

IV. Excimer Formation

Fluid solution excimer emission has been reported for five platinum diimine complexes with lowest $^3(\pi-\pi^*)$ or ^{3}MLCT monomer excited states (Table 2.3).[15,16,20,39,40,42] Wang and coworkers have reported fluid solution excimer emission for two additional complexes, Pt(bpy)$(C\equiv CC_6H_4$-2,2-dipyridylamine$)_2$ and Pt(phen)$(C\equiv CC_6H_4$-2,2-dipyridylamine$)_2$, however the complete characterization of the electronic and photophysical properties of these complexes was not provided.[49] In each case, concentrated solutions give rise to a new emission band, shifted to the red of the monomer emission. There is considerable evidence to support the view

that the emission does not arise from ground-state aggregation.[50] Notably, Che and coworkers[15] reported that the excitation spectrum for the red excimer emission from concentrated solutions of $Pt(dbbpy)(CN)_2$ agrees with the excitation spectrum for the green monomer emission from dilute solutions. Moreover, time-resolved studies have established that, following excitation with a short laser pulse, the excimer emission intensity increases with time.[15] In the case of 10^{-4} M $Pt(phen)(C{\equiv}CPh)_2$, the transient monomer emission signal at 566 nm shows single-exponential kinetics following a laser flash, whereas the excimer emission signal at 750 nm is biexponential, reaching its maximum intensity ~150 ns *after the laser flash* (Figure 2.1b).[16] Unfortunately, direct characterization of these excimers has been somewhat hampered by their apparent short lifetimes and low emission quantum yields as compared to the excited monomers. Moreover, poor solubility of the monomer has hindered characterization studies at high concentrations. In most instances, the observed excimer emission signal decays at nearly the same rate as the monomer emission, as expected for a relatively short-lived species.[51] One exception is the $Pt(dpphen)(CN)_2$ excimer, which decays (~100 ns) at a similar rate to the monomer (100 ns) in a polyethylene glycol solution.[42] Even in a CH_2Cl_2 solution, the excimer lives almost three times longer than any of the other reported complexes,[42] providing a rare opportunity to directly characterize this species. George, Weinstein, and coworkers have monitored the monomer-excimer equilibrium for $Pt(dpphen)(CN)_2$ in CH_2Cl_2 room-temperature fluid solution using time-resolved infrared spectroscopy (TRIR).[52] The TRIR spectrum shows that the ν(CN) bands shift slightly (5 cm^{-1}) to higher frequency upon formation of the monomer excited state. This shift is much smaller than observed for $Ru(bpy)_2(CN)_2$ (35 cm^{-1}), which is known to have a lowest MLCT. This result is consistent with the view that $Pt(dpphen)(CN)_2$ has a lowest ligand-

centered π-π* excited state. The TRIR kinetic traces exhibit biexponential behavior, with the longer-lived species (100 μs) attributed to the excited monomer and the shorter-lived species (3 μs) attributed to excimer. The difference between the spectrum at 400 ns (monomer and excimer) and that recorded at 20 μs (purely monomer) after excitation provide an approximate TRIR spectrum for the $Pt(dpphen)(CN)_2$ excimer. No firm conclusion or generalization about the mechanism of excimer association in the $Pt(dpphen)(CN)_2$ complex was reported, although the results are most consistent with an excimer stabilized by diimine-diimine interactions.

Steady-state emission spectra provide some additional insight into the nature of the emitting species. The emission profiles are characteristically broad (FWHM ~ 2,800 to 4,400 cm^{-1}) and unstructured.[53] The data in Table 2.1 indicate that the emission maxima span a wide range of energies, suggesting that the emission energy is dependent on the ligands surrounding the platinum center. For example, $Pt(dbbpy)(CN)_2$ excimer emission maximizes at 565 nm (Figure 2.1a), whereas $Pt(phen)(C{\equiv}CPh)_2$ excimer emission maximizes at 750 nm (Figure 2.1b) in methylene chloride solution.[16] The red shift in the excimer emission relative to the monomer emission is represented by ΔE in Table 2.3, corresponding to the difference between the monomer emission $E_{0,0}$ and the excimer peak transition energy. The large shifts (3500-7000 cm^{-1}) are comparable to those found for organic aromatics (*e.g.*, benzene, 5700; naphthalene, 6500; 9-methyl-anthracene, ~6900; pyrene, ~6000 cm^{-1}),[47] suggesting comparably strong intermolecular interactions (> 5 kcal/mol). In addition, the solution excimer emission profiles are similar to those observed from room-temperature solid samples of platinum diimine complexes. For example, $[Pt(phen)_2]Cl_2$ exhibits a low-energy ligand-ligand excimer emission that is very sensitive to moisture and sample history (λ_{max}=~530-640 nm; ΔE=~3,300-6,600 cm^{-1}, FWHM ~2,400-4,200 cm^{-1}). Similarly, discrete $Pt(tpy)Cl^+$ dimers and extended chains of

platinum diimine complexes with short Pt-Pt interactions exhibit low-energy and slightly asymmetric emission profiles (λ_{max}=~600-780 nm; ΔE=~4,500-9,400 cm^{-1}, FWHM ~2,000-4,300 cm^{-1}).[1,3,4,44,53,54] Interestingly, both ligand-ligand and Pt-Pt interactions are present in the ground-state structure of the head-to-tail isomer $[Pt(dbbpy)(\mu\text{-}pyS)]_2^{2+}$ (Pt-Pt, 2.917[2] Å), resulting in a weak, symmetric emission in methylene chloride solution (λ_{max}=~603 nm; FWHM ~2,400-4,200 cm^{-1}, τ=320 ns).[55]

Excimer emission quantum yields are not available for any of the complexes listed in Table 2.3. Nevertheless, from the relative intensities of the monomer and excimer emissions,[15,20,39,40,42] it appears that complexes with lowest $^3(\pi\text{-}\pi^*)$ monomer states have higher quantum yields than those with lowest ^{3}MLCT monomer states, consistent with Energy Gap Law behavior.[34] This decrease in quantum yield could account for the fact that excimer emission has not been reported for a diimine dithiolate complex. Additionally, the trend in emission energies in Table 2.1 suggests emission from those complexes will lie to the red of 800 nm, where multialkali photocathode photomultiplier tubes are relatively insensitive.

V. Quenching Kinetics

Formation of a metastable M_2^* excimer suggests the possibility of the reverse reaction, namely dissociation to reform the excited monomer (M*) and a ground-state complex (M). This situation is illustrated in Scheme 2.4, in which k_{abs}, k_M, k_{MD}, and k_D represent unimolecular rate constants, and k_{DM} is the bimolecular rate constant for formation of the excimer. A similar model was used by Birks to describe monomer/excimer fluorescence kinetics of aromatic hydrocarbons, with the chief distinction being that, in the present case, the excited platinum complexes have predominantly triplet spin character. Unfortunately, the kinetics parameters

have not been fully determined for any of the complexes in Table 2.1, and present estimates of k_D (=$1/\tau_D$, Table 2.2), k_{DM} and k_{MD} should be regarded as approximate.

Scheme 2.4. Model describing self-quenching and excimer formation.

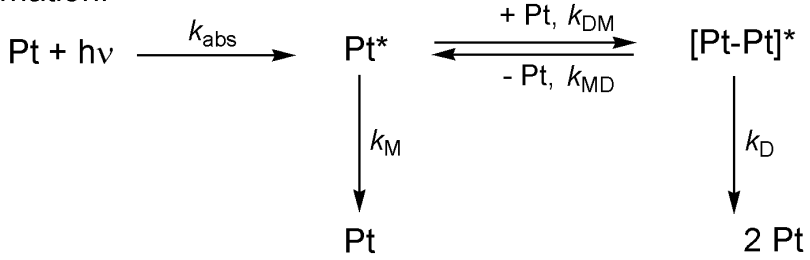

This model predicts biexponential kinetics for monomer emission decay, according to the solutions to two simultaneous differential equations describing the concentration of excited monomer and dimer with respect to time.

$$\frac{d[Pt^*]}{dt} = k_{MD}[Pt_2^*] - (k_M + k_{DM}[Pt])[Pt^*]$$

$$\frac{d[Pt_2^*]}{dt} = k_{DM}[Pt^*][Pt] - (k_D + k_{MD})[Pt_2^*]$$

The two analytical solutions for these equations, obtained from Laplace transformations, give [Pt*] and [Pt_2*] as functions of time:

$$[Pt^*] = \frac{[Pt^*]_0}{\lambda_2 - \lambda_1}[(\lambda_2 - X)(e^{-\lambda_1 t} + (X - \lambda_1)e^{-\lambda_2 t})$$

$$[Pt_2^*] = \frac{k_{DM}[Pt][Pt^*]_0}{\lambda_2 - \lambda_1}(e^{-\lambda_1 t} - e^{-\lambda_2 t})$$

where: $\lambda_{1,2} = \frac{1}{2}\left[k_M + k_{DM}[Pt] + k_D + k_{MD} \mu \sqrt{(k_D + k_{MD} - k_M - k_{DM}[Pt])^2 + 4k_{MD}k_{DM}[Pt]}\right]$ (3)

or $\lambda_{1,2} = \frac{1}{2}\left[X + Y \mu \sqrt{(Y - X)^2 + 4k_{MD}k_{DM}[Pt]}\right]$ (4)

where $X=k_M + k_{DM}[Pt]$ and $Y=k_D + k_{MD}$

However, each of the compounds listed in Table 2.1 exhibits single-exponential emission decay kinetics over the investigated concentration ranges (~10^{-6}-10^{-3} M). The predicted time-dependences of the emissions provide a possible explanation for this behavior.[56] The intensity of monomer fluorescence, $i_M(t)$, is given by:

$$i_M(t) = \frac{k_{FM}[Pt^*]}{[Pt^*]_0} \quad (5)$$

$$\text{or } \frac{k_{FM}(\lambda_2 - X)}{\lambda_2 - \lambda_1}(e^{-\lambda_1 t} + \frac{X - \lambda_1}{\lambda_2 - X}e^{-\lambda_2 t}) \quad (6)$$

where $[Pt^*]_0$ is the concentration of platinum at time zero after the arrival of the excitation pulse. Similar results for the intensity of the excimer, $i_D(t)$, are found, where both functions predict biexponential decay and obey the following proportionalities, respectively:[57]

$$i_M(t) \propto e^{-\lambda_1 t} + Ae^{-\lambda_2 t} \quad (7)$$

$$i_D(t) \propto e^{-\lambda_1 t} - e^{-\lambda_2 t} \quad (8)$$

where:

$$A = \frac{k_M + k_{DM}[Pt] - \lambda_1}{\lambda_2 - k_M + k_{DM}[Pt]}$$

For the only two reported cases, Pt(dbbpy)$(CN)_2$ (4 x 10^{-3} M)[15] and Pt(phen)$(C{\equiv}CPh)_2$ (10^{-4} M),[16] fitting of the biexponential excimer emission decay gives values for λ_1 and λ_2 of ~10^6 and ~10^7 s^{-1}, respectively. For these rates, the predicted biexponential behavior of the monomer emission should have been evident in the transient monomer emission decay. To account for the observed single exponential decay, we consider the three conditions under which equation (7) reduces to a single exponential function.

In the first case, the two exponential terms in equation (7) decay at the same rate, *i.e.*, $\lambda_1 \approx \lambda_2$. This condition holds when,

$$X \approx Y >> \sqrt{4k_{MD}k_{DM}[Pt]}$$

In that case,

$$\lambda_1 \approx \lambda_2 \approx X \approx Y$$

X depends on [Pt], whereas Y does not. Therefore, this appears to be a fortuitous situation of single exponential decay that is unlikely to be realized over a wider range of [Pt]. Nevertheless, the situation is conceivable. Values of k_M ~5 x 10^5 s^{-1} and [Pt] ~10^{-4} M are typical. To account for observed self-quenching rates, ~10^9-10^{10} $M^{-1}s^{-1}$, k_{DM} must be ≥ 10^9 $M^{-1}s^{-1}$, corresponding to X≈$10^6 s^{-1}$. In order for X to exceed $\sqrt{4k_{MD}k_{DM}[Pt]}$ by at least an order of magnitude, k_{MD}<<2.5 x 10^5. This corresponds to:

$$K = \frac{k_{DM}}{k_{MD}} >> 4000$$

suggesting a tightly bound excimer.

In the second case, we consider the possibility that A>>1, and the emission decay is dominated by the second term in equation (7), corresponding to a rate equal to λ_2. This situation is satisfied when the following conditions are met:

$$X >> Y \qquad (9)$$

$$X >> \sqrt{4k_{MD}k_{DM}[Pt]} \qquad (10)$$

According to the condition specified by equation (10), equation (4) reduces to:

$$\lambda_2 \approx X = k_M + k_{DM}[Pt]$$

$$\text{where. } \lambda_1 << \lambda_2$$

This is an attractive result because the observed values of k' are linearly dependent on [Pt], as predicted for λ_2. As discussed above, the condition specified by equation (10) is satisfied for relatively small values of k_{MD} (<<10^6 s^{-1}), corresponding to a tightly bound excimer. On the other hand, the value of k_M is typically 10^6 s^{-1}. To account for the observed self-quenching rates ~10^9-10^{10} $M^{-1}s^{-1}$, k_{DM} must be ≥10^9 $M^{-1}s^{-1}$. Therefore, the conditions specified by equation (9) is satisfied by:

$$k_D + k_{MD} << 10^6 \ s^{-1}$$

Values of k_D<<$10^6 s^{-1}$are consistent with a relatively long-lived excimer and values of k_{MD}<<10^6 s^{-1} are consistent with a tightly bound excimer.

Lastly, in the third case, we consider the possibility that A<<1 and the emission decay is dominated by the first term in equation (3) corresponding to a rate equal to λ_1. This situation is satisfied when the following conditions are met:

$$Y >> X \quad (11)$$

$$|Y - X| \approx \sqrt{4k_{MD}k_{DM}[Pt]} \quad (12)$$

According to the condition of equation (11), $\lambda_1 \approx X$ and $\lambda_2 \approx Y$. This is an attractive result because the observed values of k' are linearly dependent on [Pt], as predicted for λ_1. According to equation (12), equation (7) reduces to

$$Y >> \sqrt{4k_{MD}k_{DM}[Pt]}$$

This equation may be satisfied under three possible conditions. If either $k_{MD} \approx k_{DM}[Pt]$ or $k_{MD} < k_{DM}[Pt]$, then $k_D >> k_{MD}$. This result suggests rapid relaxation of the excimer. If $k_{MD} > k_{DM}[Pt]$, the equation generally holds without restriction on values of k_D.

However, experimental evidence supports $k_D > k_{MD}$. In fact, using rate parameters obtained from modeling the emission decays for Pt(dbbpy)$(CN)_2$ and Pt(phen)$(C{\equiv}CPh)_2$, we have found that the monomer emission decay ($k'=\lambda_1$ or λ_2) scales linearly with concentration up to ~7 x 10^{-3} and ~3 x 10^{-3} M, respectively.[58] The observed linear dependence of the emission decay (k') on concentration for all of the complexes listed in Table 2.1, as described by equation (2), supports this interpretation and suggests $k_{sq} \sim k_{DM}$. Thus, it appears that these excimers are moderately stable (>4 kcal/mol), exhibiting relatively large k_{DM}/k_{MD} ratios, as recently suggested for Pt(dpphen)$(CN)_2$ (~3 x 10^4 M^{-1}).[42,59] Evidently, the low solubility of these metal complexes has prevented measurements of λ_1 (and λ_2) at higher concentrations where a non-linear dependence on concentration is expected. Clearly, reliable measurements at high concentrations are needed to evaluate these rate constants and assess the validity of Scheme 2.3. Moreover, variable temperature measurements are necessary to determine the excimer binding energies.

Integration of (7) with respect to time gives the quantum yield for monomer emission (Φ_M):

$$\Phi_M = \int_0^\infty i_M(t)dt$$

Evaluation from t=0 to t=∞ leads to the familiar result that the reciprocal of the monomer emission quantum yield (Φ_M) is linearly dependent on concentration for the diffusional quenching model in Scheme 2.4:[57]

$$\frac{1}{\Phi_M} = \frac{1}{\Phi_M^0} + \frac{k_{sq}}{\Phi_M^0 k_i}[Pt] \qquad (13)$$

where Φ_M^0 is the emission quantum yield at infinite dilution, and:

$$k_{sq} = \frac{k_{DM} k_D}{(k_D + k_{MD})} \qquad (14)$$

If $k_D >> k_{MD}$, as suggested above, this expression reduces to:

$$k_{sq} \sim k_{DM}$$

In fact, Φ_M has been reported to decrease with concentration, and equation (3) has been used to estimate Φ_M^0, using the self-quenching rate (k_{sq}) obtained from time-resolved emission measurements.[20,40] However, the validity of equation (3) has not been confirmed by independent quantum yield studies. Such investigations are warranted because they would help to evaluate the role (if any) of ground-state association, as well as provide corroborating support for the conclusion that the excimer is short-lived and/or tightly bound. The reciprocal of Φ_M is expected to show a quadratic dependence on concentration if both static and dynamic quenching mechanisms are active.[60]

VI. Summary

Self-quenching is a general property of platinum(II) diimine complexes exhibiting long-lived fluid solution emission. The accumulated evidence suggests a dynamic process, involving a diffusion-controlled collisional encounter between an excited complex and a ground-state complex to give a moderately stable excimer. The steady-state emission

spectroscopy and the observed kinetics are consistent with the mechanism in equation (1). The reaction is apparently insensitive to the nature of the lowest monomer excited-state, and variations in rates can be understood in terms of the steric demands of substituents on the diimine ligands. Bulky substituents interfere with quenching, though the effects are modest in comparison to other excimers and exciplexes.[47] The observed rates are not consistent with variations in electron-transfer driving force, suggesting that outer-sphere electron transfer does not contribute significantly to self-quenching. Finally, an analysis of the quenching kinetics suggest that the excimer is tightly bound and/or short- lived.

Table 2.1. Self-quenching Data for Pt(II) Diimine Complexes

Compound	Solvent	Emissive State	λ_{max} (nm)[a]	k_{sq} (10^9 $M^{-1}s^{-1}$)	τ_0 (ns)
Pt(dbbpy)$(CN)_2$[b]	$(CH_2Cl)_2$	$^3(\pi\text{-}\pi^*)$	490[c]	0.9	2900
Pt(dmbpy)$(CN)_2$[d]	CH_3CN	$^3(\pi\text{-}\pi^*)$	502[c]	4.8	6300
Pt(dpphen)$(CN)_2$[e]	PEG	$^3(\pi\text{-}\pi^*)$	530	~6[f]	100
	CH_2Cl_2	$^3(\pi\text{-}\pi^*)$	520	0.5	13000
Pt(dbbpy)$(C\equiv CC_6H_5)_2$[g]	CH_3CN	^{3}MLCT	570	1.4 ± 0.2	691
Pt(dbbpy)$(C\equiv CC_6H_4F)_2$[g]	CH_3CN	^{3}MLCT	570	1.6 ± 0.1	663
Pt(dbbpy)$(C\equiv CC_6H_4CH_3)_2$[g]	CH_3CN	^{3}MLCT	592	1.0 ± 0.2	440
Pt$(C_6H_5C\equiv C$phen$)(C\equiv CC_6H_5)_2$[g]	CH_3CN	^{3}MLCT	590	4.2 ± 0.3	5600
Pt(phen)$(C\equiv CPh)_2$[h]	CH_3CN	^{3}MLCT	575	6.3	904
	CH_2Cl_2	^{3}MLCT	565	3.3	1888
Pt(phen)$(C\equiv CC_6H_4F)_2$[h]	CH_3CN	^{3}MLCT	584	6.7	814
Pt$(CH_3$phen$)(C\equiv CC_6H_5)_2$[g]	CH_3CN	^{3}MLCT	575	5.5 ± 0.2	972
Pt(phen)$(C\equiv CC_6H_4CH_3)_2$[h]	CH_3CN	^{3}MLCT	578	6.2	549
Pt(Brphen)$(C\equiv CC_6H_5)_2$[g]	CH_3CN	^{3}MLCT	605	4.6 ± 0.2	366
Pt(Clphen)$(C\equiv CC_6H_5)_2$[g]	CH_3CN	^{3}MLCT	605	5.5 ± 0.7	390
Pt(tmphen)(tdt)[h]	CH_2Cl_2	^{3}MMLLCT	675[i]	4.2	1911
Pt(bpy)(bdt)[j]	CH_3CN	^{3}MMLLCT	700[i]	9.5	460
	$CHCl_3$	^{3}MMLLCT	705[i]	4.0	560
Pt(dbbpy)(tdt)[h]	CH_2Cl_2	^{3}MMLLCT	720[i]	1.0	489
Pt(dmbpy)(tdt)[h]	CH_2Cl_2	^{3}MMLLCT	720[i]	2	360
Pt(phen)(tdt)[h]	CH_2Cl_2	^{3}MMLLCT	730[i]	4.7	580
Pt(5,5'-dmbpy)$(C\equiv CC_6H_5)_2$[k]	CH_2Cl_2	^{3}MLCT	545	2.79	1600
Pt(4,4'-dbbpy)$(C\equiv CC_6H_5)_2$[k]	CH_2Cl_2	^{3}MLCT	554	0.29	1300
Pt(4,4'-dmbpy)$(C\equiv CC_6H_5)_2$[k]	CH_2Cl_2	^{3}MLCT	554	2.20	1200
Pt(4,4'-dpbpy)$(C\equiv CC_6H_5)_2$[k]	CH_2Cl_2	^{3}MLCT	580	1.84	1000
Pt(tmphen)$(C\equiv CC_6H_5)_2$[k]	CH_2Cl_2	^{3}MLCT	522	2.90	2700
Pt(5,6-dmphen)$(C\equiv CC_6H_5)_2$[k]	CH_2Cl_2	^{3}MLCT	554	3.46	2300
Pt(5-mphen)$(C\equiv CC_6H_5)_2$[k]	CH_2Cl_2	^{3}MLCT	558	3.86	2000
Pt(phen)$(C\equiv CC_6H_5)_2$[k]	CH_2Cl_2	^{3}MLCT	561	3.68	1900
Pt(5-pphen)$(C\equiv CC_6H_5)_2$[k]	CH_2Cl_2	^{3}MLCT	563	2.32	2000
Pt(4,7-dpphen)$(C\equiv CC_6H_5)_2$[k]	CH_2Cl_2	^{3}MLCT	570	1.36	2800
Pt(4,4'-dbbpy)$(C\equiv C\text{-}C\equiv C_6H_5)_2$[k]	CH_2Cl_2	^{3}MLCT	536	1.00	1100

[Pt(Thpy)(pz)]$_2$ [l]	CH_2Cl_2	^{3}MLCT	559 [c]	0.035	15500
[Pt(Thpy)(aza)]$_2$ [l]	CH_2Cl_2	^{3}MLCT	561 [c]	—— [n]	3100
[Pt(Thpy)(bzim)]$_3$ [l]	CH_2Cl_2	^{3}MLCT	560 [c]	0.030	10900
Pt(bpy)(C≡CC_6H_4-2,2-dipyridylamine)$_2$ [m]	CH_2Cl_2	^{3}MLCT	571	—— [n]	1300
Pt(phen)(C≡CC_6H_4-2,2-dipyridylamine)$_2$ [m]	CH_2Cl_2	^{3}MLCT	590	—— [n]	6100

[a]Corrected emission maximum unless specified. [b]Ref. 15. [c]Structured emission. [d]Ref. 38. [e]Ref. 40, 42. [f]Self-quenching rate obtained from the quenching half-concentration, assuming that $k_{MD} << k_D$ [g]Ref. 20. [h]Ref. 16, estimated errors for k_{sq} are ±0.1to ±0.2. [i]Uncorrected emission maximum. [j]Ref. 29. [k]Ref. 9. [l]Ref. 61. [m]Ref. 47. [n]No k_{sq} reported.

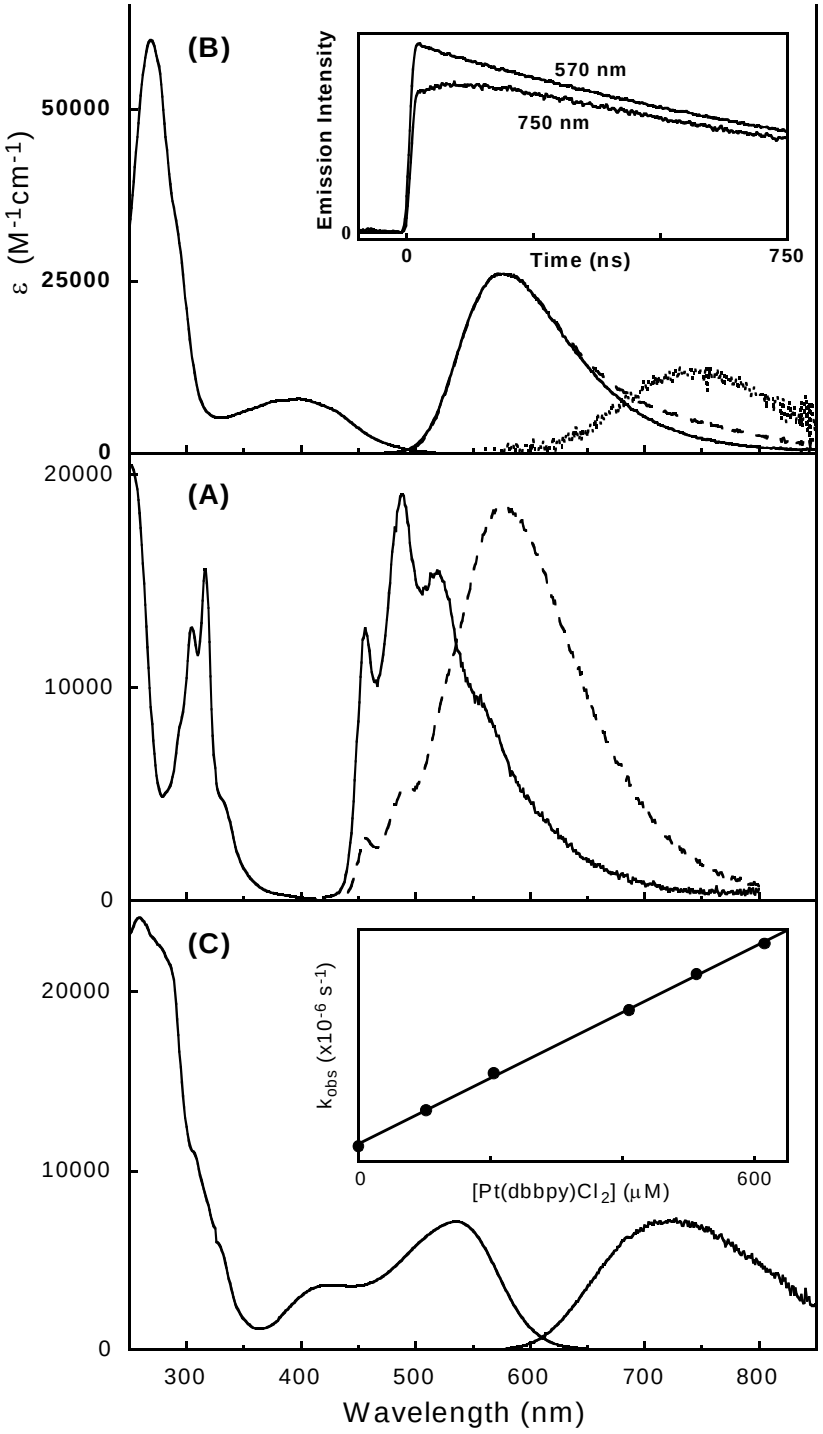

Figure 2.1. Absorption and emission spectra for (A) Pt(dbbpy)$(CN)_2$ (——0.01mM; - - -, 0.8 mM), (B) Pt(phen)$(C{\equiv}CPh)_2$ (- - -0.01mM; ····· 0.5 mM difference emission spectrum x 5), and (C) 0.02 mM Pt(tmphen)(tdt) in CH_2Cl_2. (B) inset shows the emission intensitites at 570 and 750 nm after laser excitation (λ_{ex}=460 nm). (C) Inset shows observed rate of emission decay ($k_{obs}=k''$) for Pt(tmphen)(tdt) as a function of Pt(dbbpy)Cl_2 concentration. Emission spectra are arbitrarily scaled.

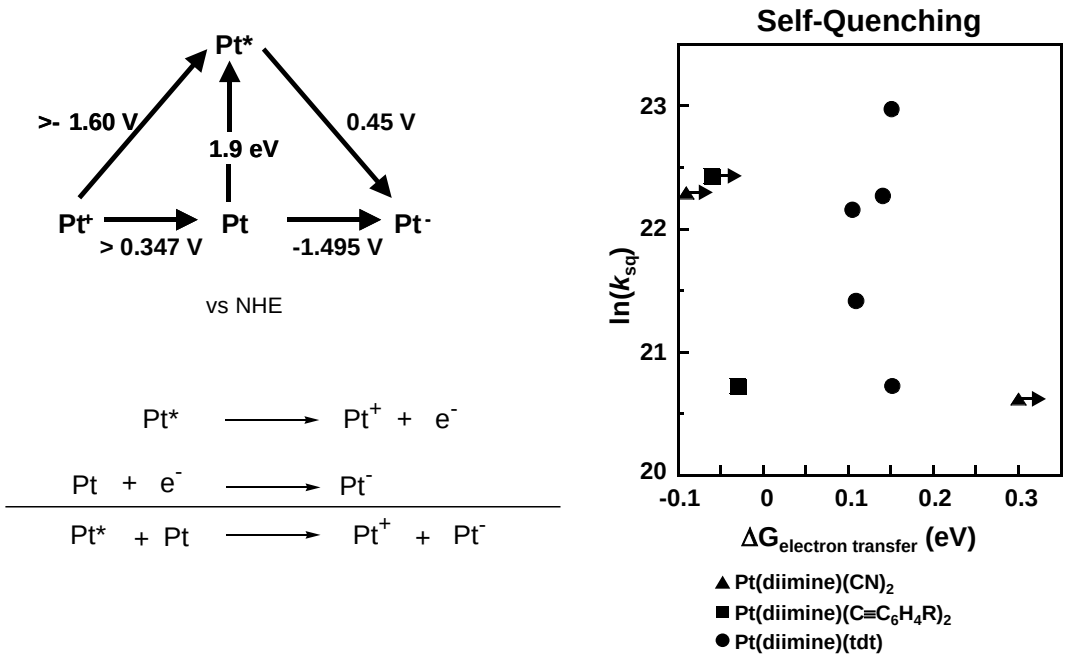

Figure 2.2. a) Latimer diagram for Pt(tmphen)(tdt) and the associated reduction and oxidation half-reactions as discussed from data in reference 22. b) Natural logarithim of self-quenching rate as a function of driving force (ΔG) for electron transfer: (▲) Pt(dbbpy)$(CN)_2$ (0.300 eV), Pt(dmbpy)$(CN)_2$ (> -0.090 eV); (■) Pt(dbbpy)$(CC_6H_4CH_3)_2$ (> -0.030 eV), Pt$(CH_3$phen$)(CCC_6H_5)_2$ (> -0.060 eV); (●) Pt(dbbpy)(tdt) (0.152 eV), Pt(bpy)(tdt) (0.151 eV), Pt(dmbpy)(tdt) (0.109 eV), Pt(tmphen)(tdt) (0.105 eV).

Table 2.2 Electrochemical Data and ΔG^e values for Pt(diimine) Complexes

Compound	Solvent	$E_{0,0}$ (eV)	$E(Pt^{+/0})$	$E(Pt^{0/-})$	$E(Pt^{*/-})$	$E(Pt^{+/*})$	ΔG (eV)	k_{sq} (10^9 $M^{-1}s^{-1}$)
$Pt(dbbpy)(CN)_2$[a]	CH_3CN	2.7	1.2	-1.2	1.5	-1.5	0.300	0.9
Pt(dbbpy)(tdt)[b]	DMF	1.93	0.389	-1.398	0.54	-1.55	0.152	1.0
Pt(bpy)(tdt)[b]	DMF	1.86	0.376	-1.339	0.52	-1.49	0.151	9.5
Pt(phen)(tdt)[b]	DMF	1.84	0.376	-1.319	0.52	-1.46	0.141	4.7
Pt(dmbpy)(tdt)[b]	DMF	1.87	0.390	-1.371	0.50	-1.48	0.109	2.0
Pt(tmphen)(tdt)[b]	DMF	1.94	0.347	-1.495	0.45	-1.60	0.105	4.2
$Pt(dmbpy)(CN)_2$[c]	DMF	2.6	≥1.1	-1.59	1.0	≥-1.5	-0.090	4.8
$Pt(CH_3phen)(C{\equiv}CC_6H_5)_2$[d]	CH_3CN	2.5	1.15	-1.41	1.09	-1.35	-0.060	5.5
$Pt(dbbpy)(C{\equiv}C_6H_4CH_3)_2$[d]	CH_3CN	2.52	1.18	-1.37	1.15	-1.34	-0.030	1.0

[a]Ref. 15. [b]Ref. 22. [c]Ref. 38. [d]Ref. 20. [e]ΔG is the electron-transfer driving force for the reaction described by equation 3.

Table 2.3. Excimer emissions of platinum(II) diimine complexes.[i]

Compound	Solvent	Monomer			Excimer			
		Emissive State	τ (ns)	λ_{max}(nm)	τ_D (ns)	λ_{max} (nm)	FWHM[g] (cm^{-1})	ΔE (cm^{-1})[h]
Pt(dpphen)$(CN)_2$[a]	PEG	$^3(\pi\text{-}\pi^*)$	100	530[f]	~ 100	630	~ 3500	4500
	CH_2Cl_2	$^3(\pi\text{-}\pi^*)$	13000	520[f]	~ 3000	665	~ 4000	5900
Pt(dppby)$(CN)_2$[b]	$CH_3CH_2Cl_2$	$^3(\pi\text{-}\pi^*)$	2900	485[f]	~ 40	565	~ 3600	6700
[Pt(dppH)(CH_3CN)](Cl_4)[c]	CH_2Cl_2	^{3}MLCT	2600	550[f]	~ 900	~ 700	~ 4400	3500
Pt(phen)$(C{\equiv}CPh)_2$[d]	CH_2Cl_2	^{3}MLCT	904	565	~ 100	~ 750	~ 2800	6700
Pt$(C_6H_5C{\equiv}C$phen$)(C{\equiv}CC_5)$[e]	CH_3CN	^{3}MLCT	5600	590	—	~ 750	~ 2600	7000

[a]Ref. 39,42. [b]Ref. 15. [c]Ref. 40. [d]Ref 16. [e]Ref 20. [f]structured emission. [g]FWHM=full-width at half maximum intensity. [h]$\Delta E = E_{0,0} - \nu_{max}$(excimer). [i] Fluid solution eximer emission has been reported by Wang and coworkers (Ref 49) for two other complexes, Pt(bpy)$(C{\equiv}CC_6H_4$-2,2'-dipyridylamine$)_2$ and Pt(phen)$(C{\equiv}CC_6H_4$-2,2'-dipyridylamine$)_2$. However, a detailed description of the photophysical analyses was not provided.

References

1. Miskowski, V. M.; Houlding, V. H. *Inorg. Chem.* **1989**, *28*, 1529-1533.
2. Miskowski, V. M.; Houlding, V. H.; Che, C.-M.; Wang, Y. *Inorg, Chem.* **1993**, *32*, 2518-2524.
3. Miskowski, V. M.; Houlding, V. H. *Inorg. Chem.* **1991**, *30*, 4446-4452.
4. Houlding, V. H.; Miskowski, V. M. *Coord. Chem. Rev.* **1991**, *111*, 145-152.
5. Biedermann, J.; Wallfahrer, M.; Gliemann, G. *J. Luminesc.* **1987**, *37*, 323-329.
6. Weiser-Wallfahrer, M.; Gliemann, G. *Z. Naturforsch.* **1990**, *45b*, 652-657.
7. Biedermann, J.; Gliemann, G.; Klement, U.; Range, K.-J.; Zabel, M. *Inorg. Chem.* **1990**, *29*, 1884-1888.
8. Biedermann, J.; Gliemann, G.; Klement, U.; Range, K.-J.; Zabel, M. *Inorg. Chim. Acta* **1990**, *171*, 35-40.
9. Biedermann, J.; Gliemann, G.; Klement, U.; Range, K.-J.; Zabel, M. *Inorg. Chim. Acta* **1990**, *169*, 63-70.
10. Kato, M.; Sasano, K.; Kosuge, C.; Yamazaki, M.; Yano, S.; Kimura, M. *Inorg. Chem.* **1996**, *35*, 116-123.
11. Connick, W. B.; Henling, L. M.; Marsh, R. E.; Gray, H. B. *Inorg. Chem.* **1996**, *35*, 6261-6265.
12. Crosby, G. A.; Kendrick, K. R. *Coord. Chem. Rev.* **1998**, *171*, 407-417.
13. Kato, M.; Kozakai, M.; Fukagawa, C.; Funayama, T.; Yamauchi, S. *Mol. Cryst. Liq. Cryst.* **2000**, *343*, 353-358.
14. Connick, W. B.; Miskowski, V. M.; Houlding, V. H.; Gray, H. B. *Inorg. Chem.* **2000**, *39*, 2585-2592.

15. Wan, K.-T.; Che, C.-M.; Cho, K.-C. *J. Chem. Soc., Dalton Trans.* **1991**, 1077-1080.

16. Connick, W. B.; Geiger, D.; Eisenberg, R. *Inorg. Chem.* **1999**, *38*, 3264-3265.

17. Klein, A.; Hausen, H. D.; Kaim, W. *J. Organomet. Chem.* **1992**, *440*, 207-217.

18. Chan, C. W.; Cheng, L. K.; Che, C.-M. *Coord. Chem. Rev.* **1994**, *31*, 87-97.

19. Klein, A.; Kaim, W. *Organometallics* **1995**, *14*, 1176-1186.

20. Hissler, M.; Connick, W. B.; Geiger, D. K.; McGarrah, J. E.; Lipa, D.; Lachicotte, R. J.; Eisenberg, R. *Inorg. Chem.* **2000**, *39*, 447-457.

21. Dungey, K. E.; Thompson, B. D.; Kane-Magiore, N. A. P.; Wright, L. L. *Inorg. Chem.* **2000**, *39*, 5192-5196.

22. Cummings, S. D.; Eisenberg, R. *J. Am. Chem. Soc.* **1996**, *118*, 1949-1960.

23. Zuleta, J. A.; Bevilacqua, J. M.; Proserpio, D. M.; Harvey, P. D.; Eisenberg, R. *Inorg. Chem.* **1992**, *31*, 2396-2404.

24. Miller, T. R.; Dance, G. *J. Am. Chem. Soc.* **1973**, *95*, 6970-6979.

25. Vogler, A.; Kunkley, H. *J. Am. Chem. Soc.* **1981**, *103*, 1559-1560.

26. Kumar, L.; Puthraya, K. H.; Srivastava, T. S. *Inorg. Chim. Acta* **1984**, *86*, 173-178.

27. Vogler, A.; Kunkely, H. *Comments Inorg. Chem.* **1990**, *9*, 201-220.

28. Zhang, Y.; Ley, K. D.; Schanze, K. S. *Inorg. Chem.* **1996**, *35*, 7102-7110.

29. Connick, W. B.; Gray, H. B. *J. Am. Chem. Soc.* **1997**, *119*, 11620-11627.

30. Wootton, J. L.; Zink, J. I. *J. Phys. Chem.* **1995**, *99*, 7251-7257.

31. Paw, W.; Cummings, S. D.; Mansour, M. A.; Connick, W. B.; Geiger, D. K.; Eisenberg, R. *Coord. Chem. Rev.* **1998**, *171*, 125-150.

32. Huertas, S.; Hissler, M.; McGarrah, J. E.; Lachicotte, R. J.; Eisenberg, R. *Inorg. Chem.* **2001**, *40*, 1183-1188.

33. Doorn, S. K.; Dyer, R. B.; Stoutland, P. O.; Woodruff, W. H. *J. Am. Chem. Soc.* **1993**, *115*, 6398-6405.

34. Kober, E. M.; Caspar, J. V.; Lumpkin, R. S.; Meyer, T. J. *J. Phys. Chem.* **1986**, *90*, 3722-34.

35. Marcus, R. A.; Sutin, N. *Biochim. Biophys. Acta* **1985**, *811*, 265-322.

36. Chen, C.-T.; Liao, S.-Y.; Lin, K.-J.; Chen, C.-H.; Lin, T.-Y. J. *Inorg. Chem.* **1999**, *38*, 2734-2741.

37. Crites Tears, D. K.; McMillin, D. R. *Coord. Chem. Rev.* **2001**, *211*, 195-205.

38. Che, C.-M.; Wan, K.-T.; He, L.-Y.; Poon, C.-K.; Yam, V. W.-W. *J. Chem. Soc., Chem. Commun.* **1989**, 943-945.

39. Kunkely, H.; Vogler, A. *J. Am. Chem. Soc.* **1990**, *112*, 5625-5627.

40. Chan, C. W.; Lai, T. F.; Che, C. M.; Peng, S. M. *J. Am. Chem. Soc.* **1993**, *115*, 11245-11253.

41. Chan, C.-W.; Che, C.-M.; Cheng, M.-C.; Wang, Y. *Inorg. Chem.* **1992**, *31*, 4874-4878.

42. Pettijohn, C. N.; Jochnowitz, E. B.; Chuong, B.; Nagle, J. K.; Vogler, A. *Coord. Chem. Rev.* **1998**, *171*, 85-92.

43. Connick, W. B.; Marsh, R. E.; Schaefer, W. P.; Gray, H. B. *Inorg. Chem.* **1997**, *36*, 913-922.

44. Buchner, R.; Cunningham, C. T.; Field, J. S.; Haines, R. J.; McMillin, D. R.; Summerton, G. C. *J. Chem. Soc., Dalton Trans.* **1999**, *5*, 711-717.

45. Kato, M.; Kosuge, C.; Morii, K.; Ahn, J. S.; Kitagawa, H.; Mitani, T.; Matsushita, M.; Kato, T.; Yano, S.; Kimura, M. *Inorg. Chem.* **1999**, *38*, 1638-1641.

46. Lide, D. R., Ed. *Handbook of Chemistry and Physics*; 48th ed.; CRC Press, Inc.: Boca Raton, 1999; Weast, R. C., Ed. *Handbook of Chemistry and Physics*; 48th ed.; CRC Press, Inc.: Cleveland, 1964.

47. Birks, J. B. *Photophysics of Aromatic Molecules*; Wiley-Interscience: London, 1970.

48. Connick, W. B.; Gray, H. B. *unpublished results*; Connick, W. B.; Eisenberg, R. *unpublished results.*

49. Kang, Y.; Lee, J.; Song, D.; Wang, S. *J. Chem. Soc. Dalton Trans.* **2003**, 3493-3499.

50. These statements should not be construed to mean that ground-state aggregation cannot occur in these systems. Aggregation (and accompanying static quenching) is expected at high concentrations, and careful control experiments are necessary to address this possibility.

51. Self-quenching and excimer kinetics data have been reported for acetonitrile solutions of Pt(dpp-CNN)$(CH_3CN)^+$ (ref. 39). However, inconsistencies in the reported values and figures make detailed interpretation of these data difficult.

52. Kuimova, M. K.; Mel'nikov, M. Y.; Weinstein, J. A.; George, M. W. *J. Chem. Soc., Dalton Trans.* **2002**, 2857-2861.

53. The excimer emission spectrum for Pt(CNN-dpp)$(CH_3CN)^+$ was obtained by subtracting the normalized emission spectrum of a dilute sample from that of a concentrated sample (ref. 9). The resulting emission profile has poorly resolved shoulders with ~1100-1500 cm^{-1} spacings, characteristic of ligand ring breathing modes. These shoulders are suspiciously coincident with sharp features in the dilute sample spectrum, and it is not obvious that they are present in the true excimer emission profile.

54. Bailey, J. A.; Hill, M. G.; Marsh, R. E.; Miskowski, V. M.; Schaefer, W. P.; Gray, H. B. *Inorg. Chem.* **1995**, *34*, 4591-4599.

55. Connick, W. B.; Miskowski, V. M.; Houlding, V. H.; Gray, H. B., *manuscript in preparation*.

56. The observed single-exponential decay kinetics for monomer emission also are consistent with the dynamic equilibrium condition k_{DM}[Pt], $k_{MD}>>k_M$, k_D. (Birks, J. B.; Braga, C. L.;

Lumb, M. D. *Proc. Roy. Soc. A* **1965**, *283*, 83-99) More data are necessary to assess this possibility.

57. Birks, J. B.; Dyson, D. J.; Munro, I. H. *Proc. Roy. Soc. A* **1963**, *275*, 575-588.
58. Model parameters: 4 x 10^{-3} M Pt(dbbpy)$(CN)_2$ in dichloroethane, k_M=3.4 x 10^5, k_D=9.1 x 10^6, k_{MD}=3.4 x 10^5 s^{-1}, and k_{DM}=9 x 10^8 s^{-1}; 10^{-4}M Pt(phen)$(C{\equiv}CPh)_2$ in methylene chloride, k_M=5.3 x 10^5, k_D=1.2 x 10^7, k_{MD}=2 x 10^5 s^{-1}, and k_{DM}=3.3 x 10^9 s^{-1}.
59. A similar situation, namely A<<1 and linear dependence of λ_1 on concentration (298 K, k_{DM}= 6.7 x 10^9 $M^{-1}s^{-1}$, k_{MD}=6.5 x 10^6 s^{-1}), is encountered for pyrene self-quenching at low to moderate concentrations (<2 x 10^{-3} M, ref. 60).
60. Demas, J. N. *Excited State Lifetime Measurements*; Academic Press: New York, 1983.60.
61. Lai, S. W.; Chan, M. C. W.; Cheung, K. K.; Peng, S. M.; Che, C. M. *Organometal.* **1999**, *18*, 3991-3997.

Chapter 3

Synthesis and Characterization

I. Introduction

In order to investigate self-quenching and cross-quenching reactions, the synthesis and characterization of the Pt(tmphen)(tdt) chromophore and quencher complexes were necessary. In this chapter, preparative details are described. In addition, the ^{1}H NMR spectra, UV-visible data, and electrochemical properties are reported, along with the crystal structures of several complexes. Unusual observations or modifications to literature procedures are included.

II. Experimental

A. Materials and Methods.

All reagents were obtained from Aldrich, Acros, Pressure Chemical, or Strem and used as received. Syntheses were performed using standard Schlenk line techniques.[1] Argon was predried using activated sieves, and trace oxygen was removed with activated R3-11 catalyst from Schweizerhall. Tetrahydrofuran was distilled under argon from sodium and benzophenone, and DMSO was distilled under vacuum and stored in a Strauss flask. Toluene and benzene were stored over molecular sieves and thoroughly degassed before use. All other solvents were used as received.

B. Instrumentation

^{1}H NMR spectra were recorded using a Bruker AC 250 MHz instrument and deuterated solvents purchased from Cambridge Isotope Laboratories. UV-visible absorption spectra were recorded using a HP8453 diode array spectrometer. Absorption data for Pt(tmphen)(tdt) and the Pt(diimine) quenchers are reported in Table 3.1. Elemental analyses were carried out by Atlantic Microlab, Inc (Table 3.2). Emission spectra were recorded using a SPEX-fluorolog-3

fluorimeter with a single excitation monochromator and a double emission monochromator. 77 K glassy solutions were prepared by inserting a quartz EPR tube containing a solution of the complex into a quartz-tipped finger dewar. Emission spectra were corrected for instrumental response.

C. Synthesis

1. *Synthesis of Pt(tmphen)(tdt).*

The procedure reported by Cummings and Eisenberg [2] did not result in the desired complex. Therefore, the complex was synthesized by modification of the method reported by Connick and Gray[3] for the preparation of Pt(bpy)(bdt). Two equivalents of $AgNO_3$ were added to $Pt(tmphen)Cl_2$ in dimethlyformamide (DMF) (approximately 10 ml per 100 mg of platinum starting material). After stirring for 1-2 hours, the precipitated AgCl was removed by filtration through celite resulting in a yellow filtrate. At low light level, the filtrate was added dropwise to a mixture of 0.1 M KOH and two equivalents of 1,2-toluenedithiolate (H_2tdt), and a red precipitate immediately began to form. The mixture was allowed to stir for another 30 minutes in the dark to ensure complete precipitation. The solid was collected by filtration and purified in the dark by Soxhlet extraction with CH_2Cl_2. It is imperative to minimize exposure to light because Pt(tmphen)(tdt) is light sensitive in solution. Violet solutions gradually fade to yellow during prolonged exposure to light. The ^1H NMR spectrum was in agreement with that reported by Cummings and Eisenberg.[2]

2. *Synthesis of Pt(dppe)($C_2H_4S_2$) and Pt(depe)($C_2H_4S_2$).*

The platinum starting material, $Pt(COD)(C_2H_4S_2)_2$, was prepared according to a literature procedure.[4] $Pt(dppe)(C_2H_4S_2)$ (dppe=diphenlyphosphinoethane) was prepared by modification of the literature procedure for similar dithiolate complexes (Pt(COD)(mnt) and Pt(COD)(ecda).[5]

In general, under an inert atmosphere, 1.1 equivalents of dppe were dissolved in acetone and added by cannula transfer to a solution of Pt(COD)($C_2H_4S_2$) in a mixture of acetone and THF. The platinum starting material was not completely soluble in acetone, so THF was added to increase solubility. The resulting yellow solution was stirred for 1.5 days at room temperature. The volume was reduced to 5-10 mL by rotary-evaporation and ether was added to induce crystallization. The resulting product was isolated as either yellow crystalline needles or a yellow solid. Pt(depe)($C_2H_4S_2$) (depe=diethylphosphinoethane) (65μL of depe per 0.1g of Pt(COD)($C_2H_4S_2$) was synthesized in a similar manner to Pt(dppe)($C_2H_4S_2$), however, the reaction mixture was prepared in the glove box due to the air sensitivity of the depe ligand.

3. Synthesis of Pt(diimine)Cl_2 complexes.

Pt(bpy)Cl_2, Pt(dmbpy)Cl_2, Pt(dbbpy)Cl_2, and Pt(dpbpy)Cl_2 were prepared as described by Morgan and Burstall[6] and later by Hodges and Rund.[7] In a typical procedure one equivalent of the diimine ligand was added to 0.5 g of K_2PtCl_4 in 66 ml of H_2O. After the addition of 4 drops of concentrated hydrochloric acid, the mixture was refluxed for 2.5 hours. Following filtration, the yellow solid was washed with H_2O and ether. Generally, the product was recrystallized for use in emission experiments. Typically, the solid was dissolved in a minimum amount of DMF with vigorous heating and allowed to cool to room temperature, usually resulting in crystalline material. If no precipitate formed, the solution was placed in the freezer. The Pt(dpbpy)Cl_2 complex was difficult to recrystallize from DMF because of its high solubility. Recrystallization was much more effective from a mixture of CH_2Cl_2/acetone solution layered with hexanes.

4. Synthesis of Pt(diimine)Ph_2 complexes.

The general synthetic procedure[8,9] involved the addition of the appropriate diimine to Pt(COD)Ph_2[10] or Pt(dmso)$_2Ph_2$[11] in degassed benzene or toluene under an argon atmosphere.

The solution was refluxed over a period ranging from four hours to three days depending on the diimine. Reactions using diimine ligands such as bpy and dmbpy were complete in approximately four hours, however, reactions using diimine ligands such as 2,9-dmphen and dmdpphen required longer time periods. In this procedure, it is important to monitor the reaction progress for products, platinum starting material and free diimine ligand using ^{1}H NMR spectroscopy. In particular, monitoring the reaction is extremely important when synthesizing Pt($(CF_3)_2$bpy)Ph_2.[12] During the initial synthesis, the reaction was allowed to reflux overnight. Evidently, the product decomposed as evidenced by the formation of a brown solid. Five to six hours of refluxing is sufficient for this complex.

In general, after completion of the reaction the resulting precipitate was isolated by filtration, or if no solid was present, the solvent was removed by rotary-evaporation. Before recrystallization, it is suggested that the solid be dissolved in CH_2Cl_2 and filtered by gravity to remove colloidal platinum. Recrystallization from either CH_2Cl_2/hexanes or CH_2Cl_2/pentane gave analytical grade material for use in subsequent experiments. ^{1}H NMR spectral data are given below and elemental analyses are listed in Table 3.2 for eleven previously unreported diphenyl complexes.

Pt(dmdpphen)Ph_2 from CH_2Cl_2/pentane,^{1}H NMR ($CDCl_3$, δ): 7.85 (2H, s, CH), 7.55-7.43 (12H, m, CH), 6.88 (4H, dd with platinum satellites, CH), 6.75 (2H, d, CH), 2.26 (6H, s, CH).

Pt(4,7-dmphen)Ph_2 from CH_2Cl_2/pentane, ^{1}H NMR ($CDCl_3$, δ): 8.79 (2H, d, CH), 8.12 (2H, s, CH), 7.55 (6H, m with platinum satellites, CH $J_{H\text{-}Pt}$=71 Hz), 7.07 (4H, dd, CH), 6.94 (2H, m, CH), 2.78 (6H, s, CH_3).

Pt(dpbpy)(Ph)$_2$ from CH_2Cl_2/pentane, ^{1}H NMR ($CDCl_3$, δ): 8.67 (2H, d, CH), 8.30 (2H, s, CH), 7.67 (4H, m, CH), 7.57 (12H, m with platinum satellites, CH $J_{H\text{-}Pt}$=70 Hz), 7.07 (4H, dd, CH), 6.93 (2H, m, CH).

Pt(5,5′-dmbpy)(Ph)$_2$ from CH_2Cl_2/pentane, ^{1}H NMR ($CDCl_3$, δ): 8.40 (2H, s, CH), 7.89 (2H, d, CH), 7.81 (2H, d, CH), 7.47 (4H, d with platinum satellites, CH $J_{H\text{-}Pt}$=70 Hz), 7.03 (4H, dd, CH), 6.89 (2H, m, CH), 2.32 (6H, s, CH_3).

Pt(dbbpy)(Ph)$_2$ from CH_2Cl_2/hexanes, ^{1}H NMR ($CDCl_3$, δ): 8.48 (2H, d, CH), 7.96 (2H, s, CH), 7.49 (2H, d with platinum satellites, CH $J_{H\text{-}P}$=70 Hz), 7.37 (4H, m, CH), 7.02 (4H, dd, CH), 6.89 (2H, m, CH), 1.39 (18H, s, CH_3).

Pt(tmphen)(Ph)$_2$ from CH_2Cl_2/hexanes, ^{1}H NMR ($CDCl_3$, δ): 8.65 (2H, d, CH), 8.10 (2H, s, CH), 7.56 (4H, d with platinum satellites, CH $J_{H\text{-}Pt}$=72 Hz), 7.06 (4H, dd, CH), 6.94 (2H, m, CH), 2.66 (6H, s, CH_3), 2.46 (6H, s, CH_3).

Pt(5-NO_2phen)Ph$_2$ from CH_2Cl_2/pentane, ^{1}H NMR ($CDCl_3$, δ): 9.40 (1H, d, CH), 9.12 (2H, m, CH), 8.94 (1H, s, CH), 8.76 (1H, d, CH), 7.91 (2H, m, CH), 7.54 (4H, d with platinum satellites, CH $J_{H\text{-}Pt}$=71 Hz), 7.10 (4H, dd, CH), 6.97 (2H, m, CH).

Several attempts also were made to synthesize Pt(6,6'-dmbpy)Ph_2 following the same procedure as for the other diphenyl complexes. In initial attempts, Pt(COD)Ph_2 was used as the starting material in degassed benzene. The desired product was not isolated. Pt(dmso)$_2Ph_2$ was subsequently used as a starting material because it was found that a mesityl analog with a similarly hindered diimine, 2,9-dmphen, was successfully synthesized using Pt(dmso)$_2$(Mes)$_2$ in toluene.[13] However, even with extensive refluxing of the 6,6'-dmbpy and Pt(dmso)$_2Ph_2$, the product was not isolated. According to ^{1}H NMR data, the reaction mixture using either starting material always consisted of starting platinum material and free 6,6'-dmbpy. Interestingly

Pt(2,9-dmphen)Ph_2 was successfully prepared using both Pt(COD)Ph_2 and Pt(dmso)$_2Ph_2$ as starting materials.

5. Synthesis of Pt(diimine)(3,5-dmPh)$_2$ complexes.

A procedure similar to that used for the synthesis of Pt(diimine)Ph_2 was adopted, except Pt(COD)(3,5-dmPh)$_2$ was used as the starting material. Both Pt(bpy)(3,5-dmPh)$_2$ and Pt(dppz)(3,5-dmPh)$_2$ have not been previously reported and their characterization data are given below.

Pt(bpy)(3,5-dmPh)$_2$ from CH_2Cl_2/pentane, ^{1}H NMR ($CDCl_3$, δ): 8.57 (2H, d, CH), 8.03 (4H, m, CH), 7.39 (2H, dd, CH), 7.15 (4H, s with platinum satellites, CH $J_{H\text{-}Pt}$=71 Hz), 6.54 (2H, s, CH).

Pt(dppz)(3,5-dmPh)$_2$ from CH_2Cl_2/pentane, ^{1}H NMR ($CDCl_3$, δ): 9.86 (2H, d, CH), 8.96(2H, d, CH), 8.44(2H, dd, CH), 8.02(2H, dd, CH), 7.87(2H, dd, CH), 7.26 (4H, s with platinum satellites, CH $J_{H\text{-}Pt}$=72 Hz), 6.60 (2H, s, CH), 2.27 (6H, s, CH_3). ^{1}H NMR (CD_2Cl_2, δ): 9.87 (2H, d, CH), 8.87(2H, d, CH), 8.45(2H, dd, CH), 8.04 (2H, dd, CH), 7.89 (2H, dd, CH), 7.19 (4H, s with platinum satellites, CH $J_{H\text{-}Pt}$=71 Hz), 6.57 (2H, s, CH), 2.27 (6H, s, CH_3).

6. Synthesis of Pt(diimine)(Mes)Cl and Pt(diimine)(Mes)$_2$ complexes.

Mesityl complexes were synthesized using reported procedures.[13-15] In a typical procedure, 1.16 equivalents of the diimine ligand were added to Pt(dmso)$_2$(Mes)$_2$[11] in toluene (~40 mL for ~0.15 g of starting material) under an argon atmosphere. Generally, an immediate color change was observed, although the solution was refluxed for up to three days. Progress of the reaction was monitored by ^{1}H NMR spectroscopy. If upon cooling, the product precipitated out of solution, the solid was isolated by filtration. If no solid formed, the solution was rotary-evaporated to dryness. In either case, the resulting residue was dissolved in hot 1,2-dichloroethane, and the solution was filtered to remove colloidal platinum. Cold hexanes

were added to the filtrate to induce crystallization. ^{1}H NMR spectra of the mesityl complexes were in agreement with literature data.[14-16]

Though the synthesis of Pt(bpy)(Mes)Cl has been previously reported,[15] in the present work it was prepared serendipitously by the same procedure as the dimesityl complexes. An orange crystalline material resulted and was characterized by UV-visible absorption spectroscopy in THF and toluene. The UV-visible spectra and ^{1}H NMR data were consistent with the reported literature data.[15] Several other methods were investigated for the preparation of Pt(bpy)(Mes)Cl. For example, Pt(COD)(Mes)Cl was used as a staring material. However, in agreement with results of other reactions using this starting material, ^{1}H NMR data indicated that the 1,5-cyclooctadiene ligand was not displaced by the diimine.

7. Synthesis of Pt(diimine)(C_6F_5)$_2$ and Pt(diimine)($C_6H_3F_2$)$_2$ complexes.

The fluorinated diimine complexes were synthesized following the same general procedure as the phenyl and 3,5-dmPh diimine derivatives with the exception of different platinum starting materials. Also, toluene was always used as solvent in place of benzene. The fluorinated dmso adducts, Pt(dmso)$_2$(C_6F_5)$_2$ and Pt(dmso)$_2$($C_6H_3F_2$)$_2$, were prepared from commercial Pt(C_6F_5)$_2$(Et_2S)$_2$ and Pt($C_6H_3F_2$)$_2$(Et_2S)$_2$ following a modification of the literature procedure.[17] The procedure for the dmso adducts suggests using THF as the solvent, however, the desired product was not isolated unless diethyl ether from a newly opened container was used as the solvent. Also, when recrystallizing, the product does not precipitate until placed in the freezer, resulting in white crystalline chunks.[18] Although, the synthesis of Pt(dmso)$_2$($C_6H_3F_2$)$_2$ has not been previously reported, the product was prepared in the same manner as Pt(dmso)$_2$(C_6F_5)$_2$ except 3,5-difluorobenzene was used as a reagent instead of

bromoperfluorobenzene. When recrystallizing, the literature procedure suggests using CH_2Cl_2 and petroleum ether. Large volumes of ether are necessary for the product to precipitate.

Synthesis of the diimine complexes was achieved by adding one equivalent of the appropriate diimine to $Pt(dmso)_2(C_6F_5)_2$ or $Pt(dmso)_2(C_6H_3F_2)_2$ in toluene.[17,19] The solution was refluxed, and the reaction progress was monitored by ^1H NMR spectroscopy. If upon cooling, the product precipitated, the solid was isolated by filtration. If not, the solution was rotary-evaporated to dryness. For example, $Pt(dppz)(C_6F_5)_2$ precipitated out of solution upon refluxing. Even after extensive washing with hexanes the solid still contained a small amount of the reaction solvent. Therefore, recrystallization is recommended to purify the solids. $Pt(bpy)(C_6F_5)_2$ is only somewhat soluble in CH_2Cl_2 and was not used as a quencher. However, quenching studies are probably feasible with this complex since $Pt(dppz)(C_6F_5)_2$ which has similar solubility, was successfully used as a quencher. It is necessary to recrystallize both compounds from large volumes of a CH_2Cl_2/acetone solution with a layer of hexanes for small amounts of product. The other fluorinated complexes may be recrystallized from CH_2Cl_2/hexanes or CH_2Cl_2/pentane. All four fluorinated complexes have not been previously reported, and the ^1H NMR data and elemental analyses are provided.

Pt(dmbpy)(C_6F_5)$_2$ from CH_2Cl_2/acetone/hexanes (yellow solid), ^1H NMR ($CDCl_3$, δ): 8.18 (2H, d, CH), 7.89 (2H, s, CH), 7.28 (2H, d, CH), 2.50 (6H, s, CH_3).

Pt(dbbpy)(C_6F_5)$_2$ from CH_2Cl_2/pentane (brownish crystalline material), ^1H NMR ($CDCl_3$, δ): 8.24 (2H, d, CH), 8.00 (2H, s, CH), 7.47 (2H, d, CH), 1.43 (18H, s, CH).

Pt(dppz)(C_6F_5)$_2$ from CH_2Cl_2/acetone/hexanes (yellow solid), ^1H NMR ($CDCl_3$, δ): 9.96 (2H, d, CH), 8.77 (2H, d, CH), 8.46 (2H, dd, CH), 8.08 (2H, dd, CH), 7.98 (2H, dd, CH).

Pt(dmbpy)($C_6H_3F_2$)$_2$ from CH_2Cl_2/pentane (yellow/green solid), ^{1}H NMR ($CDCl_3$, δ): 8.24 (2H, d, CH), 7.87 (2H, s, CH), 7.13 (2H, d, CH), 6.97 (4H, d with Pt satellites, CH), 6.37 (2H, m, CH), 2.46 (6H, s, CH_3).

8. Dipyrido[3,2-a:2′,3′-c]phenazine (dppz).

The dppz ligand was prepared according to a modified literature procedure.[20] 1,2-phenylene diamine (20% excess) was added to 1,10-phenanthroline-5,6-dione[20,21] in ethanol. The solution was refluxed for four hours. The resulting dark yellow solution was reduced in volume by rotary-evaporation to 2/3 of the original volume and then placed in a freezer to induce crystallization.

D. Electrochemistry

Cyclic voltammograms were recorded using a standard three-electrode cell and a CV50w potentiostat from Bioananalytical Systems. Samples were dissolved in CH_2Cl_2 solutions containing 0.1 M tetrabutylammonium hexafluorophosphate ($TBAPF_6$), which was recrystallized twice from methanol and dried in a vacuum oven prior to use. All scans were recorded using a platinum wire auxiliary electrode, Ag/AgCl reference electrode and a 7.07 mm^2 glassy carbon working electrode. The most common scan rate used for these experiments was 250 mV/s. Reported potentials for reversible and quasireversible couples were estimated as $(E_{pc}+E_{pa})/2$ and are referenced against Ag/AgCl. Potentials for irreversible couples were estimated at the current maximum of the observed wave. For most quenchers, oxidation did not occur at potentials <1.5 V, which was the solvent window. Four of the bipyridine and phenanthroline complexes undergo irreversible reduction, placing an upper limit on the thermodynamic reduction potentials. These compounds are Pt(tmphen)Ph_2, Pt(dmdpphen)Ph_2, Pt(5,5'-dmbpy)Ph_2, and Pt(bpy)(3,5-dmPh)$_2$.

E. X-ray Crystallography

General Parameters.

Intensity data were collected at 150K using a standard Siemens SMART[22] 1K CCD diffractometer with graphite-monochromated Mo Kα radiation (λ=0.71073 Å) for all complexes except Pt(dpphen)Ph_2. Intensity data for the latter complex were collected at 150K using a SMART6000 CCD diffractometer. Data frames were processed using the Siements SAINT program.[23] Intensities were corrected for decay, Lorentz and polarization effects. Absorption and beam correction based on the multi-scan technique were applied using SADABS.[24] The structure for Pt(dppe)$(C_2H_4S_2)_2$ was solved using a combination of the Patterson method using SHELXTL v5.03[25] and the difference Fourier technique. All other structures were solved using a combination of direct methods in SHELXTL v6.1[26] and the difference Fourier technique. All structures were refined by full-matrix least squares on F^2. Non-hydrogen atoms were refined with anisotropic displacement parameters. Hydrogen atoms were either located directly or calculated based on geometric criteria and treated with a riding model. The isotropic temperature factors were defined as *a* times U_{eq} of the adjacent atom where *a*=1.5 for methyl and 1.2 for all others. Weights were assigned as $w^{-1}=[\sigma^2(F_o^2)+ (0.0332P)^2 + 0.2810P]$ where $P=0.33333F_o^2+0.66667F_c^2$.

For the Pt(dppe)$(C_2H_4S_2)_2$ complex a final difference Fourier map was featureless, and the highest residual electron density peaks appear near the disordered acetone or Pt atom. No disorder model was developed for the acetone solvate. The final difference Fourier map for Pt(5,5'-dmbpy)Ph_2 showed the residual peak and hole are approximately 1 Å from H22 and C8, respectively. The highest residual peak for Pt(bpy)$(3,5\text{-}dmPh)_2$ is 1 Å from the Pt atom.

III. Results and Discussion

A. Synthesis and Characterization

All complexes were prepared by literature or modified literature procedures. Scheme 3.1 illustrates three general synthetic procedures for the preparation of the platinum(II) diimine complexes. Characterization of complexes included ^{1}H NMR spectroscopy, elemental analyses, and in some cases UV-visible absorption spectroscopy. In all cases, the complexes gave reasonable analytical data that was in agreement with available literature data.

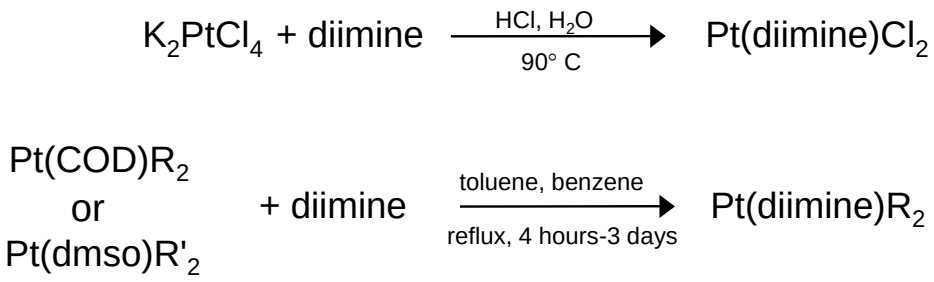

Scheme 3.1. General synthetic routes for platinum(II) diimine complexes.

B. Elemental Analyses

The elemental analysis data are provided in Table 3.2 for those complexes that have not been previously reported. Acceptable analyses were obtained for all complexes, except Pt(dpbby)Ph_2, Pt(dbbpy)Ph_2, and Pt(5-NO_2phen)Ph_2. Each of the latter gave unacceptably low analyses for carbon. For the Pt(dpbpy)Ph_2 complex, samples were recrystallized and submitted for analysis twice. Analysis of the Pt(dpbpy)Ph_2 complex was consistent for both trials. For the Pt(5-NO_2phen)Ph_2 complex, samples were submitted for analysis three times. The first and the third trials for the Pt(5-NO_2phen)Ph_2 complex were in agreement. The second trial was a

different batch of sample than either the first or third trial. The third trial was recrystallized material from the first trial. Pt(dbbpy)Ph_2 was only submitted once for analysis. In all cases, no reasonable formulae with co-crystallized solvent were found to be consistent with ^{1}H NMR data, and it seems probable that these compounds are not amenable to accurate analysis by combustion elemental analysis.

C. ^{1}H NMR Spectroscopy

The ^{1}H NMR data for the complexes agree with available literature data.[2,13-15,27] The ^{1}H NMR spectral data are provided in text for complexes not previously reported, and the observed chemical shifts, relative intensities, and splitting patterns are in keeping with expectations. For example, the diimine resonances for the complexes occur within expected ranges, 7.26-8.20 ppm for bipyridine, and 7.5-9.4 ppm for phenanthroline. Resonances for Pt(5-NO_2phen)Ph_2 and the dppz complexes (7.84-9.96 ppm) are shifted further downfield. The phenyl ligand resonances occur within 6.75-7.57 ppm with the ortho-proton resonances of the diphenyl complexes exhibiting ^{195}Pt. However, some of the ^{195}Pt satellites are not fully visible due to overlapping resonances. Finally, the aliphatic resonances for the methyl groups occur typically between 2.21-2.78 ppm, and the *t*-butyl resonances occur between 1.3-1.43 ppm.

D. UV-visible Absorption Spectroscopy

The absorption spectra of platinum(II) diimine complexes are characterized by intense π-π* transitions near 300 nm and MLCT transitions at longer wavelengths, 300-500 nm (2000-5000 $M^{-1}cm^{-1}$). For complexes with dithiolate ligands such s tdt^{2-}, an intense MMLLCT transition maximizes between 500-600 nm (6000-19000 $M^{-1}cm^{-1}$).[2,28] Pt(tmphen)(tdt) falls in this latter category with a maximum absorbance of 535 nm, consistent with data previously reported by Eisenberg and coworkers.[2] The quenchers in Table 3.1 exhibit well-resolved MLCT

absorption bands in most cases. The maximum wavelength for the lowest energy MLCT absorption and the molar absorptivity are reported for Pt(tmphen)(tdt) and the quencher complexes in Table 3.1. Quencher complexes exhibit higher energy absorptions than that of Pt(tmphen)(tdt), which allows for selective excitation of this complex. However, for some complexes, such as Pt(dpphen)$(Mes)_2$ with a lowest MLCT energy absorption maximum at 487 nm, excitation into the absorption tail is unavoidable.

The electronic properties of these platinum diimine complexes or similar complexes have been previously studied.[2,13,15,27,29-46] The observed relative changes in absorbances follow the general trends previously described based on the properties of the substituents on the diimine ligand as well as the anionic ancillary ligands. For example, complexes containing electron-donating substituents on the diimine ligand effectively destabilize the π^* level resulting in a shift of the MLCT band to shorter wavelength. This is exactly what we observe within a series of quenchers with the same anionic ligand. For example, within the bipyridine dichloride series, alkyl groups on the bipyridine ligand cause the absorption band shift to shorter wavelength (Pt(bpy)Cl_2, 394 nm; Pt(dmbpy)Cl_2, 389 nm; and Pt(dbbpy)Cl_2, 388 nm). These same relative shifts are observed in the phenanthroline series of quencher complexes (Pt(phen)Ph_2, 436 nm; Pt(dmphen)Ph_2, 412 nm; and Pt(tmphen)Ph_2, 404 nm). In the case of relatively electron-withdrawing phenyl groups, the π^* level is stabilized, and the MLCT band shifts to longer wavelengths (Pt(dbpby)Ph_2, 452 nm; compared to Pt(bpy)Ph_2, 436 nm; Pt(dpbpy)Cl_2, 404 nm; Pt(bpy)Cl_2, 394 nm).

When we consider the properties of the anionic ligands, similar trends emerge. As the electron-withdrawing character of the ligand increases, the absorption band shifts to lower energy due to decreasing electron-density on the metal center resulting in stabilization of the

metal d levels. The spectra of $Pt(bpy)Cl_2$ (394 nm) and $Pt(bpy)Ph_2$ (436 nm) are consistent with the view that phenyl is a more effective electron donor than chloride, as evidenced by its shift to lower energy MLCT absorption bands. This same pattern is observed as the electron-donating properties of the anionic ligand are increased ($Pt(bpy)(3,5\text{-}dmPh_2)$, 448 nm; $Pt(bpy)(Mes)_2$, 452 nm). Finally, it is interesting to note a few quencher complexes that involve a combination of both electron-donating and electron-withdrawing properties. For example, complexes with phenyl substituents on the diimine shift to lower energy due to the phenyl groups withdrawing capability independent of the anionic ligands, resulting in stabilization of the π^* level ($Pt(dbpby)Ph_2$, 452 nm compared to $Pt(bpy)Ph_2$, 436 nm and $Pt(dpbpy)Cl_2$, 404 nm compared to $Pt(bpy)Cl_2$, 394 nm). Figure 3.1 shows the maximum MLCT energy of the quenchers vs quencher reduction potential. No correlation is observed. In summary, the energies of the MLCT absorption maxima for these complexes are in accord with the relative electronic properties of the ligands.

E. Emission Spectroscopy

The 77 K glassy solution emission spectra of Pt(tmphen)(tdt) were collected using samples dissolved in butyronitrile solution and a combination of $EtOH/CH_2Cl_2/MeOH$ solution. Corrected spectra for both solutions are shown in Figure 3.2. The emission spectra are in agreement with that reported by Cummings and coworkers[2] in that an asymmetric emission is observed with shoulders separated from the emission maximum by approximately 1250-1300 cm^{-1}.[2]

Corrected 77 K emission spectra of select quencher complexes were measured in 4:1 EtOH/MeOH glassy solutions, and the corrected emission spectra are shown in Figures 3.3-3.6. The room-temperature emission spectra in CH_2Cl_2 also are shown for Pt(tmphen)(tdt) and two

mesityl complexes, Pt(dpphen)$(Mes)_2$ and Pt(dppz)$(Mes)_2$ (Figures 3.7-3.9). According to literature data, the emission from both mesityl complexes can be assigned to a lowest triplet MLCT state.[13,15] Some interesting observations arise from an emission study of these two complexes. For example, Pt(dpphen)$(Mes)_2$ (Figure 3.8) complex exhibits rigidochromism, characterized by a red shift of the room temperature fluid solution emission as compared to 77 K glassy solution. This behavior has been observed for other metal diimine complexes.[2,47] The emission spectra of the complexes in room temperature solution are generally broader than in 77 K glassy solution. For the Pt(dppz)$(Mes)_2$ complex, the observed emission appears to be concentration dependent, as the emission becomes broader and slightly shifts to lower energy at higher concentrations. This is suggestive of aggregation of the Pt(dppz)$(Mes)_2$ complex which is supported by observation of π-π^* stacking in a crystal structure of this molecule.[45] Finally, it is important to note that the emissions of all quencher complexes originate to the blue of the Pt(tmphen)(tdt) complex, which eliminates the possibility of energy-transfer.

F. Electrochemistry

To investigate the electron-transfer properties of Pt(tmphen)(tdt), its cyclic voltammogram was recorded in CH_2Cl_2/0.1 M $TBAPF_6$ (Figure 3.10). The complex exhibits an apparent one-electron reduction at -1.6 V vs Ag/AgCl. In analogy to earlier studies of this complex in DMF/0.1 M $TBAPF_6$, this process is attributed to the reduction of the tmphen diimine ligand.[2] The complex also undergoes two chemically irreversible oxidation steps at 0.3 and 0.5 V. The peak currents are approximately half that of the reduction, suggesting these correspond to half-electron oxidation steps. The mechanistic details of the half-electron oxidation processes are not fully understood, and full investigation was hampered by irreversible processes at higher potentials. Nevertheless, there is a qualitative resemblance between these

data and the cyclic voltammogram of Pt(bpy)(bdt) in CH_3CN/0.1 M $TBAPF_6$.[3] Pt(bpy)(bdt) exhibits chemically reversible half-electron oxidations (0.40 and 0.70 V) and a one-electron reduction (-1.31 V) vs Ag/AgCl (1.0 M KCl). It was suggested the approximate half-electron oxidation steps result from dimerization of Pt(bpy)(bdt).[3] A similar explanation may account for the cyclic voltammogram of Pt(tmphen)(tdt). In contrast, as reported by Cummings and Eisenberg, when DMF was used as the solvent, the half-electron oxidation waves were not observed, suggesting a shift in equilibrium toward the monomer.

From the potentials and optical zero-zero energies ($E_{0,0}$) estimated from the overlap of the absorption and room-temperature emission spectra, a Latimer diagram was constructed for Pt(tmphen)(tdt) (Figure 3.11). The first oxidation wave (0.3 V) was used as a lower limit for the oxidation potential. This diagram suggests that excited Pt(tmphen)(tdt) is a powerful reductant, but only a moderate oxidant.

Representative cyclic voltammagrams (Figures 3.12-3.16) from each general class of quenchers are shown for Pt(dmbpy)Cl_2, Pt(dbbpy)Ph_2, Pt(dbbpy)$(C_6F_5)_2$, Pt(dmbpy)$(C_6H_3F_2)_2$, and Pt(dppz)$(Mes)_2$. The electrochemical potentials for all investigated quenchers are listed in Table 3.3. Oxidation of the quenchers was not observed for most complexes up to 1.5 V vs. Ag/AgCl. In fact, it is well known that that platinum(II) diimine complexes typically undergo irreversible oxidations at relatively high potentials because of the instability of Pt(III) and the π-acidity of the diimine ligands. In contrast, all investigated complexes were reduced at potentials >-1.8 V, except Pt(tmphen)Ph_2. By analogy to electrochemical studies of related platinum(II) diimine complexes, these processes are assigned to ligand-centered reductions. The bipyridyl dichloride quenchers undergo a reversible one-electron reduction near -1.2 to -1.3 V attributed to bipyridine ligand reduction in analogy to studies of related compounds.[48,49]

Similarly, the phenanthrolinyl diphenyl quenchers undergo a phenanthroline-centered reduction near -1.2 to -1.3 V,[50] however the process is not as electrochemically or chemically reversible as observed for the bipyridine complexes. The fluorinated complexes, except Pt(dppz)$(C_6F_5)_2$ exhibit similar ligand-centered reduction processes, only slightly perturbed by the fluorine groups. However, the perfluorinated complexes exhibit more electrochemically reversible reactions than the difluorinated complex. Finally, the dppz quenchers undergo reversible one-electron reduction of the diimine ligand near -0.95 to -1.1 V, as noted for related compounds.[16,27] There also is evidence of a second, irreversible reduction at more negative potentials (-1.5 to -1.6V), near the CH_2Cl_2 solvent limit.

In general, the bipyridine dichloride quenchers are more easily reduced (-1.2 to -1.3 V) than the other complexes, with the exception of the dppz diimine quenchers (-0.95 to -1.1 V). Overall, the reduction potentials of the quenchers follow expected trends. For example, Pt(bpy)Cl_2 (-1.2 V) is more easily reduced than Pt(dbbpy)Cl_2 (-1.27 V). Pt(dmbpy)$(C_6F_5)_2$ (-1.37 V) and Pt(dbbpy)$(C_6F_5)_2$ (-1.42 V) also follow this pattern, namely, diimines with more electron-donating substituents are harder to reduce. On the other hand, Pt(5-NO_2phen)Ph_2 (-0.66 V) is significantly easier to reduce than Pt(phen)Ph_2 (-1.51 V). This result is probably not due to inductive effects, but rather a consequence of direct reduction of the nitro group as has been suggested for a similar platinum aryl acetylide complex.[46]

G. X-ray crystallography

Four compounds were structurally characterized in order to identify any unusual molecular geometries or intermolecular interactions. A summary of the crystallographic data for each compound is detailed in Table 3.4. ORTEP diagrams are shown in Figures 3.17-3.20 and distances and angles for each complex are shown in Tables 3.5-3.8. A comparison of the

complexes, particularly Pt(dpphen)$(Mes)_2$ and Pt(dppe)$(C_2H_4S_2)_2$ with available crystallographic data for similar complexes, reveals no unusual bond distances or angles.[5,14,16,27,45,51,52] The largest deviations are found when comparing Pt(dpphen)$(Mes)_2$ with Pt(2,9-dmphen)$(Mes)_2$. Pt(2,9-dmphen)$(Mes)_2$ has much longer Pt-N bonds (2.117(8) and 2.193(8) Å) than Pt(dpphen)$(Mes)_2$ (2.102(2) and 2.100(2)Å). It is known that the methyl groups of the 2,9-dmphen ligand cause the diimine ligand to tilt out of the coordination plane, resulting in long Pt-N distances. Also, the crystal structure of Pt(2,9-dmphen)Ph_2 indicates that steric demands of the methyl groups result in large distortions. The dihedral angle formed by the best fit plane for the diimine N=C-C=N atoms and the plane defined by the platinum center and two bonded carbon atoms is 31°,[27] as compared to 0° expected for a planar complex.

It is interesting to note that in crystals of Pt(5,5'-dmbpy)Ph_2 one of the phenyl rings was observed to be bent toward the diimine ligand. As a result, the distance between N1 of the diimine ligand and the C19 of the bent phenyl ring is slightly shorter (3.018 Å) than the distance between N7 and C13 (3.102 Å). Few of the diimine diphenyl complexes have been crystallized, and it is difficult at this point to comment whether this is typical or not. Nonetheless, in crystals of Pt(2,9-dmphen)Ph_2 complex, this bent geometry is not present. Kaim ***et. al.*** have suggested that a dihedral angle of approximately 70° between the pyridine and phenyl rings in Pt(diimine)$(Ph)_2$ provides optimal overlap between the phenyl rings and the π-system of the diimine ligand.[27] In the Pt(5,5'-dmbpy)Ph_2 complex, the dihedral angles between the bipyridine and phenyl rings are 72.58(2)° (C13-C18) and 79.52(2)° (C19-C24), the largest angle corresponding to the bent phenyl ring. Finally, it is interesting that the Pt(dpphen)$(Mes)_2$ complex crystallizes with two molecules of $C_2H_5Cl_2$ even though crystals were obtained from CH_2Cl_2/pentane solutions. Ethylene chloride is a common impurity reported for methylene

chloride, accounting for the presence of these solvate molecules. In summary, no special intermolecular interactions or differences were observed in any of these structures.

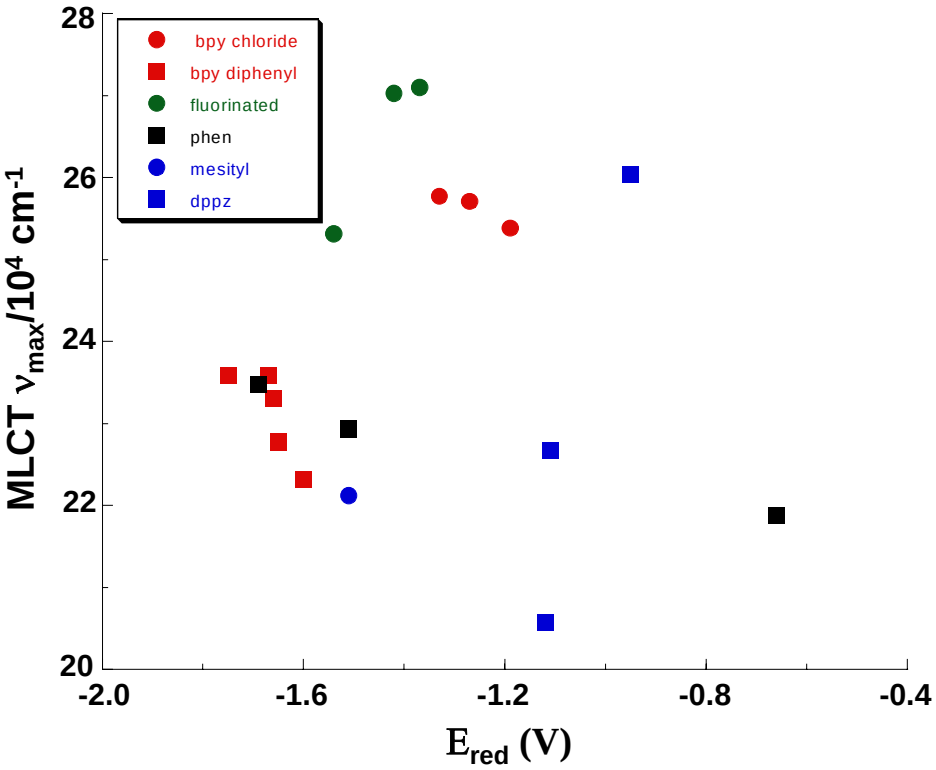

Figure 3.1 MCLT energy vs quencher reduction potential.

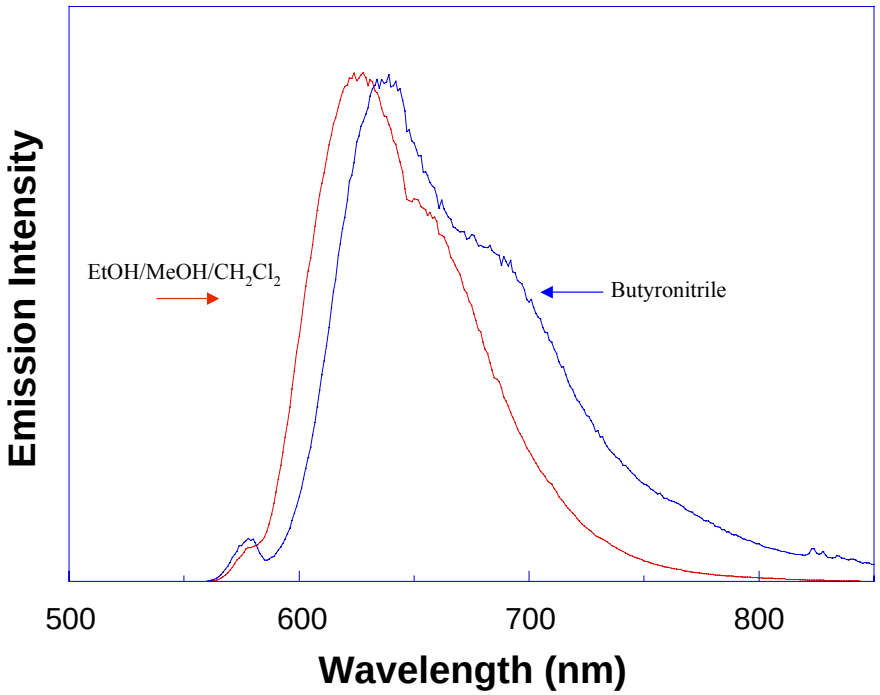

Figure 3.2. Corrected 77 K emission spectra of Pt(tmphen)(tdt). Spectra were arbitrarily scaled for purposes of comparison.

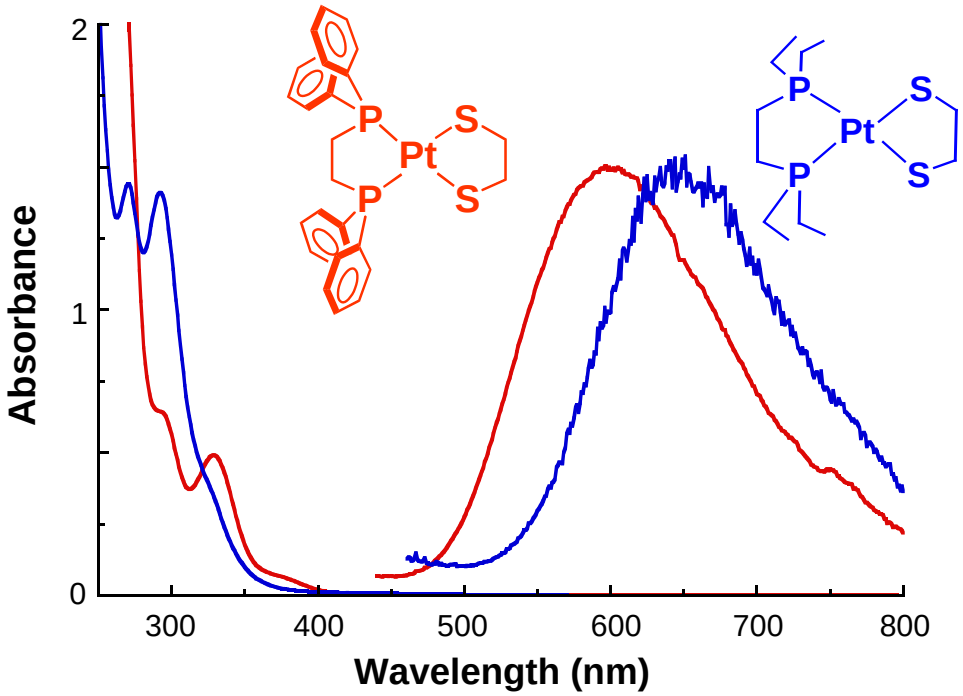

Figure 3.3. Room temperature absorption spectra of Pt(dppe)($C_2H_4S_2$) (red line) and Pt(depe)($C_2H_4S_2$) (blue line) in CH_2Cl_2, and respective corrected 77 K emisson spectra in EtOH/MeOH.

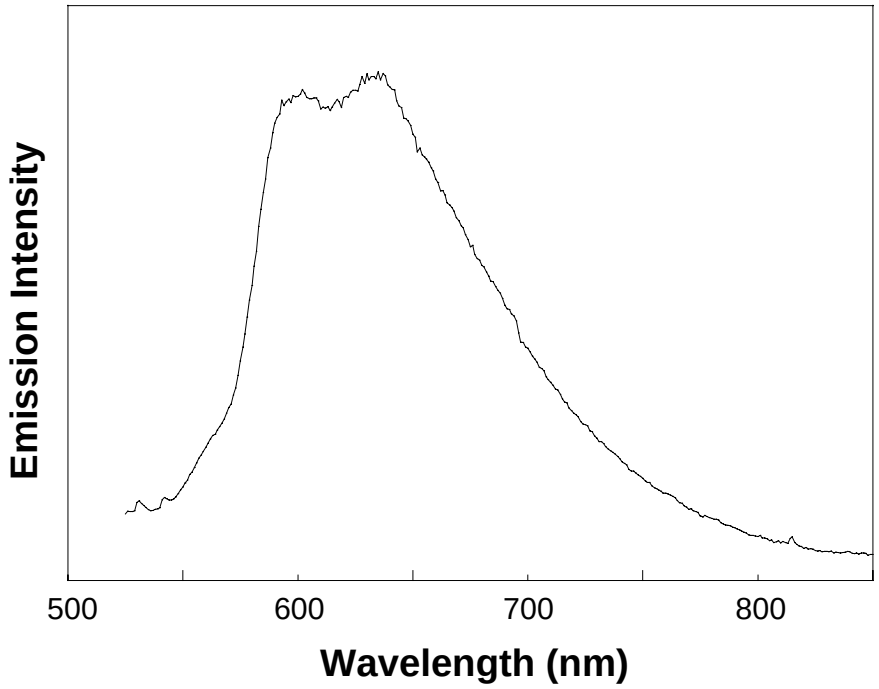

Figure 3.4. Corrected 77K emission spectrum of Pt(dpphen)Ph_2 in EtOH/MeOH.

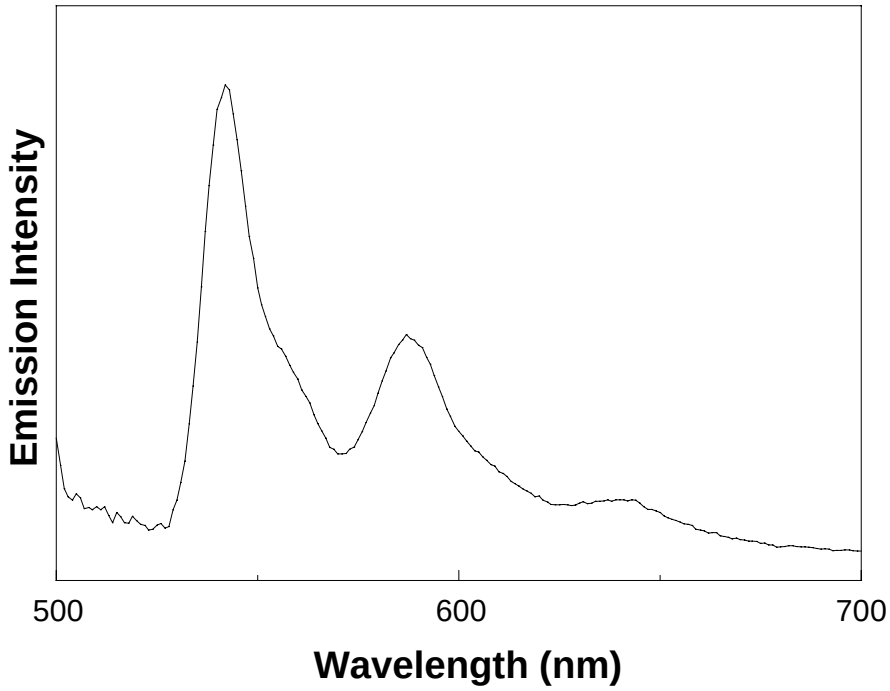

Figure 3.5. Corrected 77K emission spectrum of Pt(dppz)Ph_2 in EtOH/MeOH.

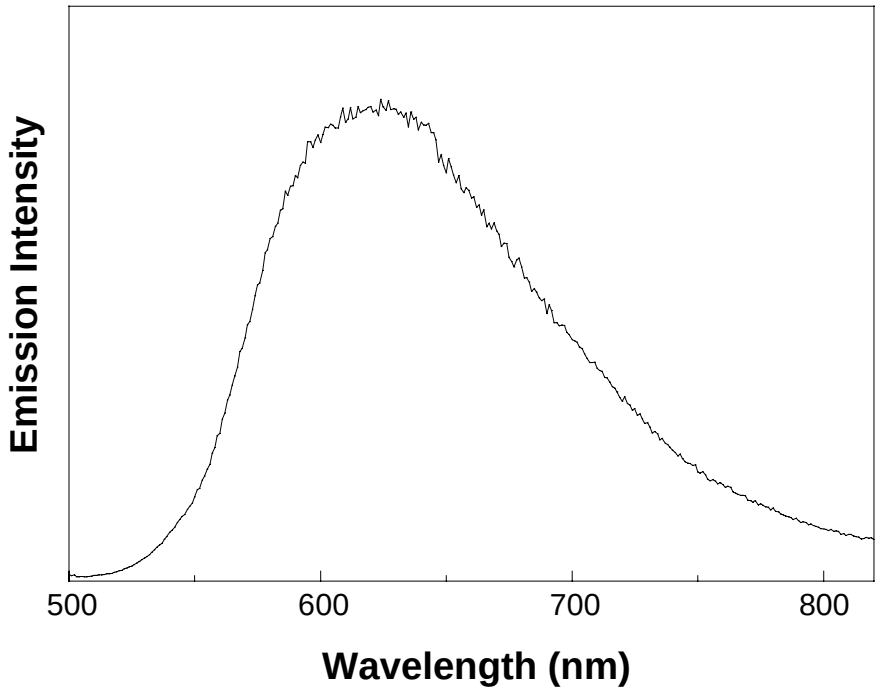

Figure 3.6. Corrected 77K emission spectrum of $Pt((CF_3)_2bpy)Ph_2$ in EtOH/MeOH.

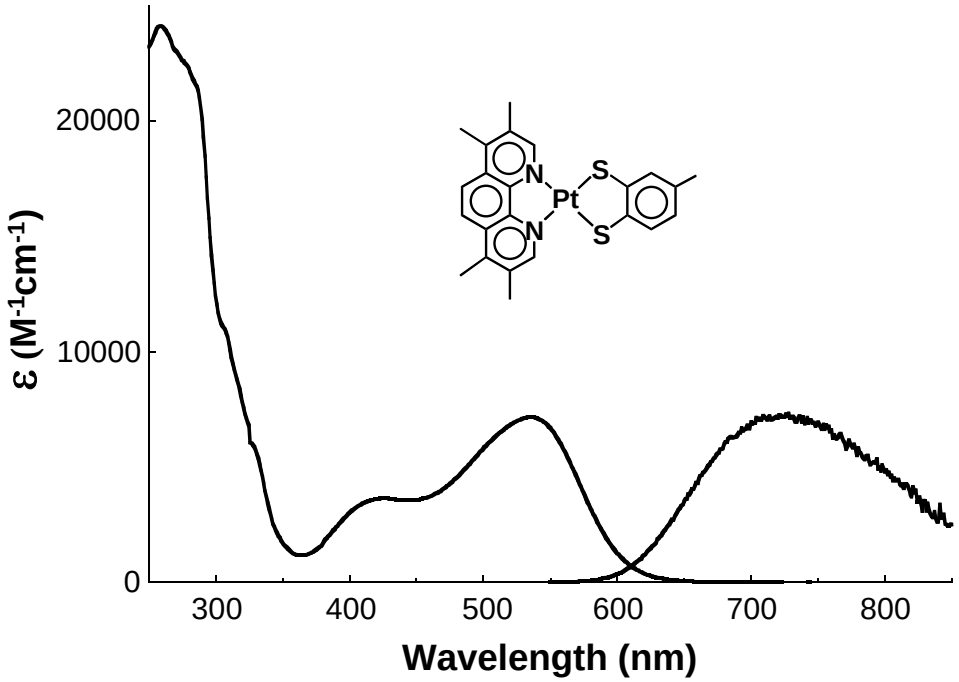

Figure 3.7. Room temperature absorbance spectrum of Pt(tmphen)(tdt) and emission spectrum in in CH_2Cl_2 solution.

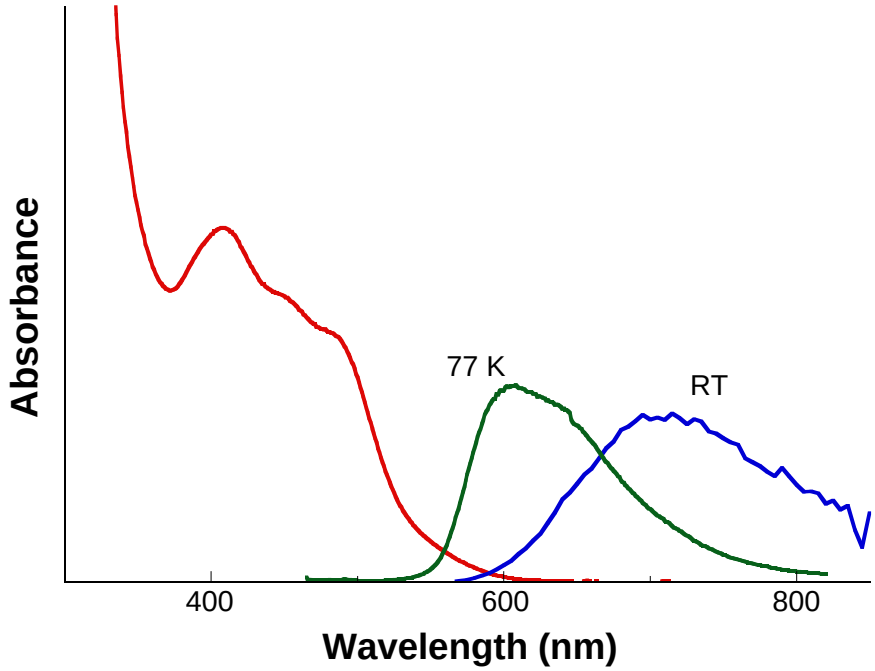

Figure 3.8. Room temperature absorption spectrum of Pt(dpphen)$(Mes)_2$ and room temperature and 77 K emission spectra in EtOH/MeOH.

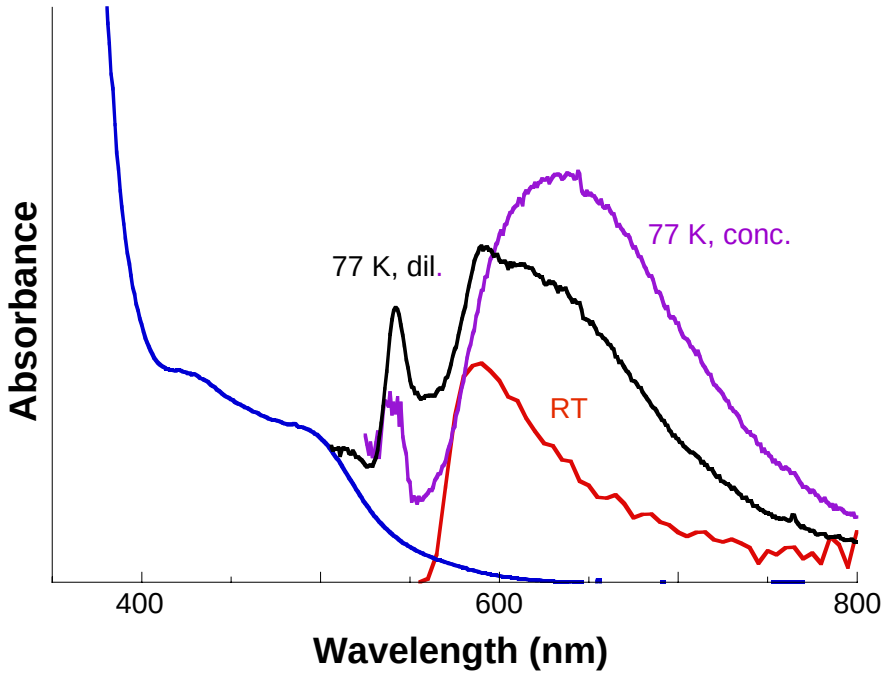

Figure 3.9. Room temperature absorption spectrum of Pt(dppz)$(Mes)_2$ and room temperature and 77 K emission spectra (concentrated and dilute solutions) in EtOH/MeOH.

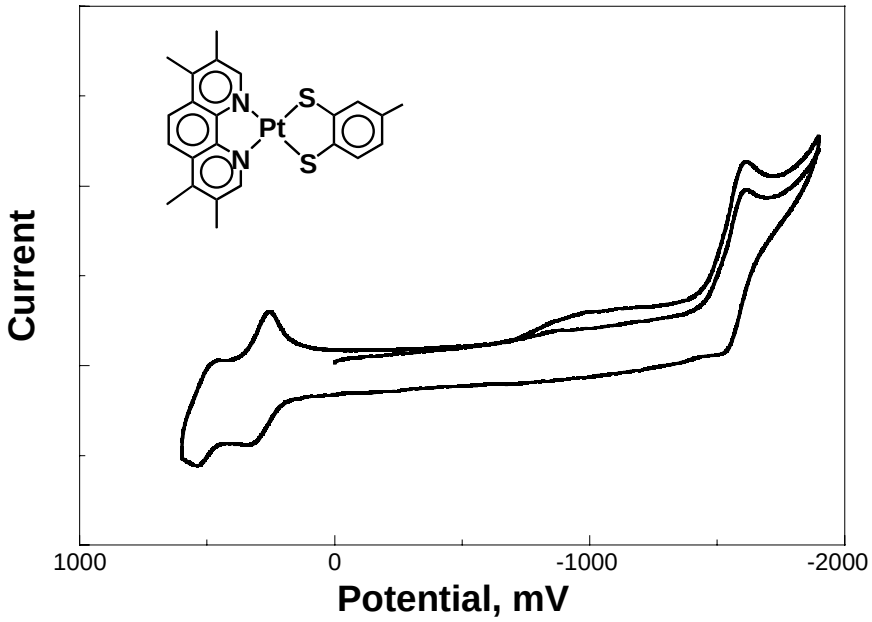

Figure 3.10. Cyclic voltammogram of Pt(tmphen)(tdt) in 0.1 M in CH_2Cl_2/$TBAPF_6$.

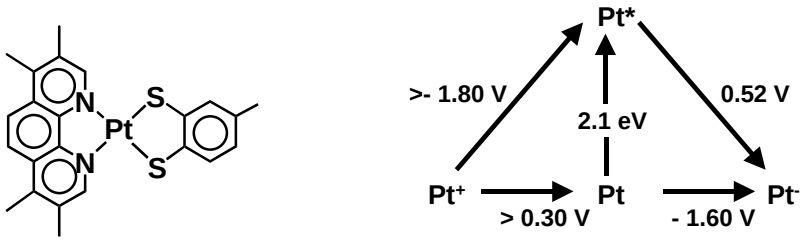

Figure 3.11. Latimer Diagram for Pt(tmphen)(tdt).

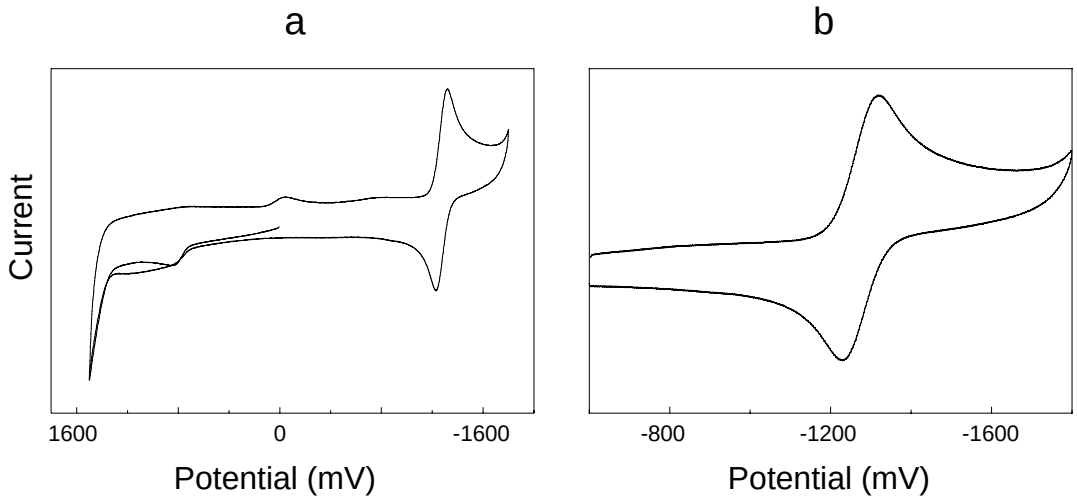

Figure 3.12. Cyclic Voltammograms of Pt(dmbpy)$(Cl)_2$ a) full scan b) short scan in CH_2Cl_2/TBAPF_6 (250 mV/s).

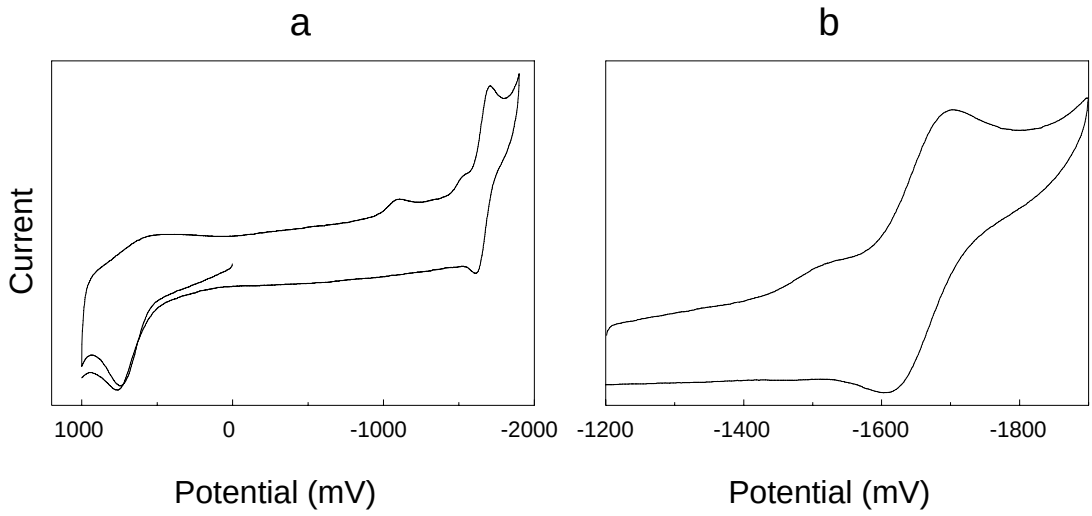

Figure 3.13. Cyclic Voltammograms of Pt(dbbpy)$(Ph)_2$ a) full scan b) short scan in CH_2Cl_2/$TBAPF_6$ (250 mV/s).

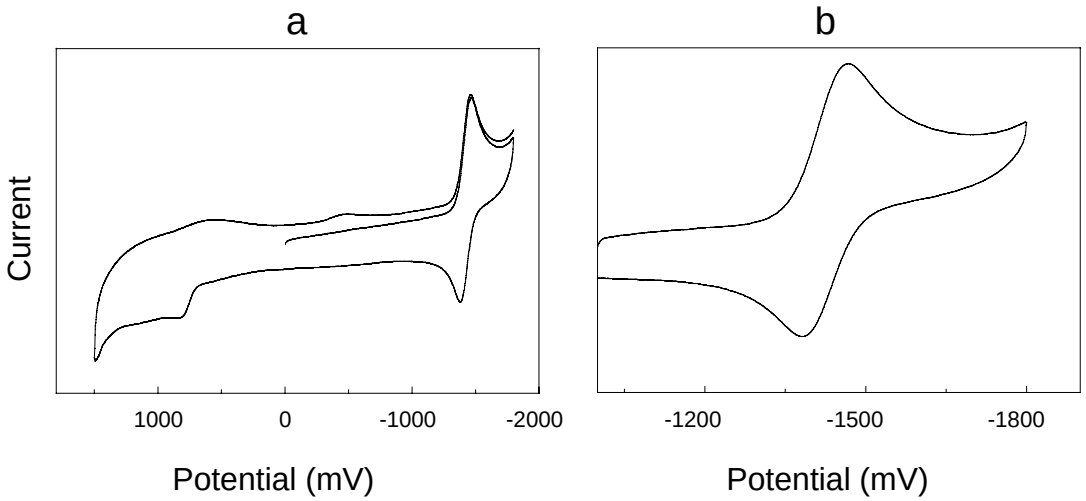

Figure 3.14. Cyclic Voltammograms of Pt(dbbpy)(C_6F_5)$_2$ a) full scan b) short scan in CH_2Cl_2/$TBAPF_6$ (250 mV/s).

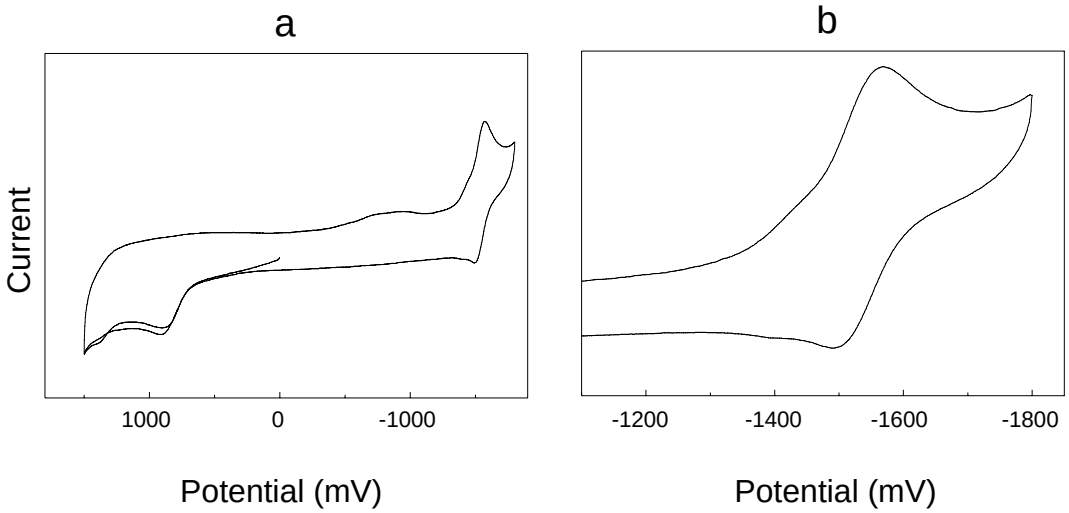

Figure 3.15. Cyclic Voltammograms of Pt(dmbpy)($C_6H_3F_2$)$_2$ a) full scan b) short scan in CH_2Cl_2/$TBAPF_6$ (250 mV/s).

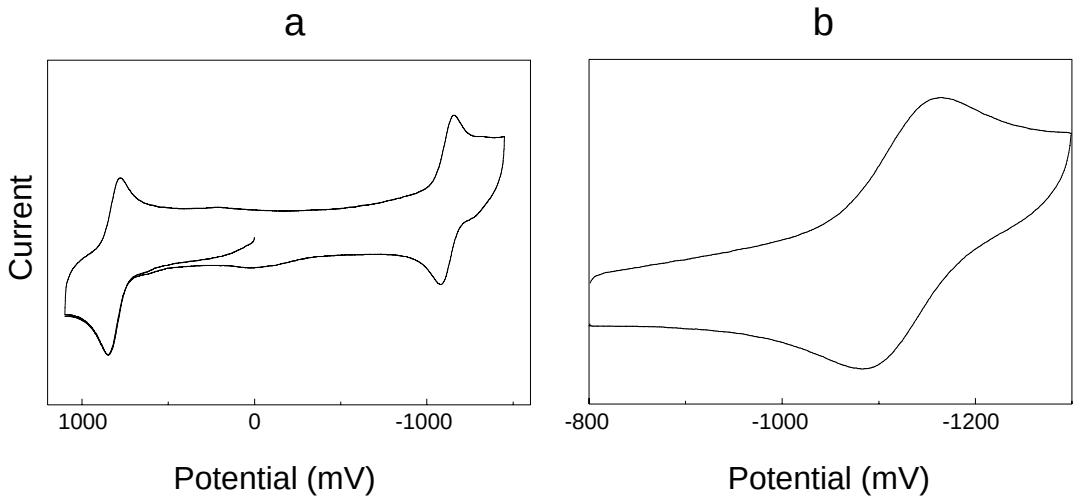

Figure 3.16. Cyclic Voltammograms of Pt(dppz)$(Mes)_2$ a) full scan b) short scan in CH_2Cl_2/$TBAPF_6$ (250 mV/s).

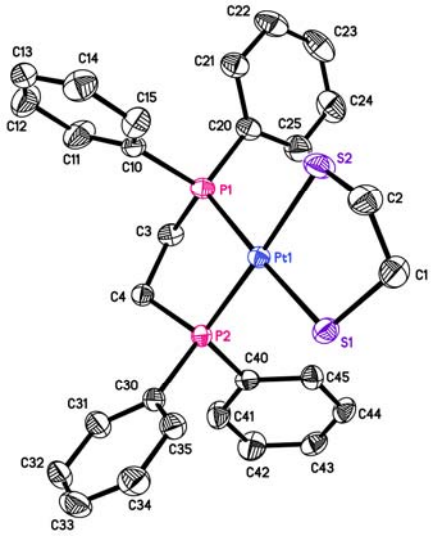

Figure 3.17. ORTEP diagram with 50% probability ellipsoids showing the geometry of the Pt(dppe)($C_2H_4S_2$) complex.

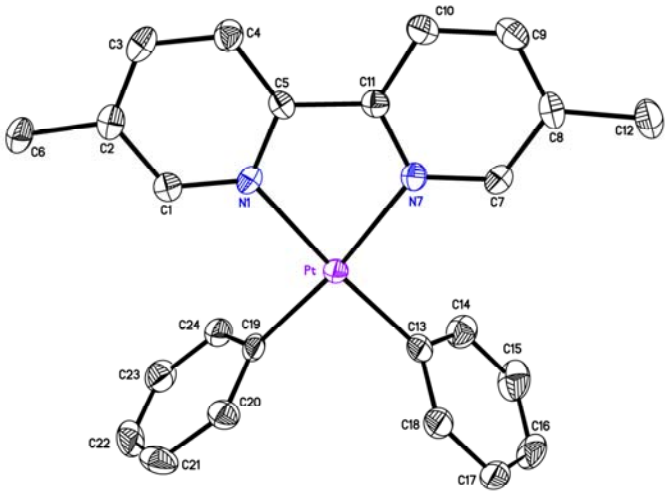

Figure 3.18. ORTEP diagram with 50% probability ellipsoids showing the geometry of the Pt(5,5'-dmbpy)Ph_2 complex.

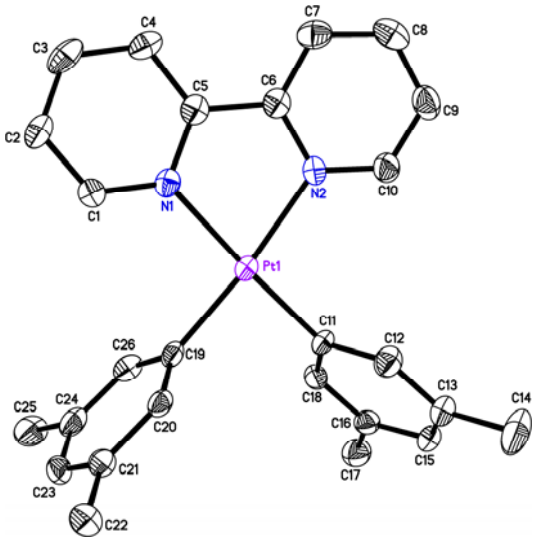

Figure 3.19. ORTEP diagram with 50% probability ellipsoids showing the geometry of the Pt(bpy)(3,5-dmPh)$_2$ complex.

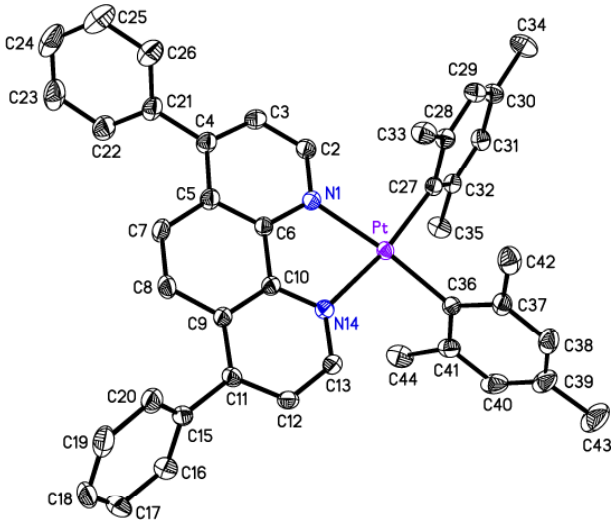

Figure 3.20. ORTEP diagram with 50% probability ellipsoids showing the geometry of the Pt(dpphen)$(Mes)_2$ complex.

Table 3.1. Absorption Data for Platinum(II) Diimine Complexes in CH_2Cl_2.		
Molecule	$\varepsilon(M^{-1}cm^{-1})$	$\lambda_{max}(nm)$[a]
Pt(tmphen)(tdt)	7160	535
Pt(bpy)Cl_2	3400	394
Pt(dmbpy)Cl_2	3585	389
Pt(dpbpy)Cl_2[b]	3674	404
Pt(dbbpy)Cl_2	3880	388
Pt(bpy)Ph_2	3190	439
Pt(dmbpy)Ph_2	3120	424
Pt(5,5'-dmbpy)Ph_2	3226	424
Pt(dbbpy)Ph_2	3275	429
Pt(dpbpy)Ph_2	4697	452
Pt(phen)Ph_2	3102	436
Pt(dmphen)Ph_2	4194	412
Pt(tmphen)Ph_2	4447	404
Pt(2,9-dmphen)Ph_2	2918	425
Pt(dpphen)Ph_2	4791	442
Pt(dmdpphen)Ph_2	4527	426
Pt(dppz)Ph_2	2654	441
Pt(bpy)MesCl	2527	420
Pt(bpy)$(Mes)_2$	2338	452
Pt(dpphen)$(Mes)_2$	3547	487
Pt(dppz)$(Mes)_2$	2972	486
Pt(bpy)$(3,5\text{-}dmPh)_2$	2779	448
Pt(dppz)$(3,5\text{-}dmPh)_2$	3982	452
Pt(dppz)$(C_6F_5)_2$	12613	384
Pt(dmbpy)$(C_6F_5)_2$	3044	369
Pt(dbbpy)$(C_6F_5)_2$	3665	370
Pt(dmbpy)$(C_6H_3F_2)_2$	3315	395
Pt(5-NO_2phen)Ph_2	3509	457

[a] λ_{max} = lowest energy absorption maximum (nm)
[b] The extinction measurement for the Pt(dpbpy)Cl_2 resulted in different values, therefore, a repeat measurement is necessary.

Table 3.2. Elemental analysis data for Pt(diimine)X_2 complexes.				
Compound	Molecular Formula	%C	%H	%N
Pt(dbbpy)Ph_2	$C_{34}H_{26}N_2Pt$	56.53(62.09)[a]	3.78(3.98)	3.89(4.26)
Pt(dpbpy)Ph_2	$C_{34}H_{26}N_2Pt$	57.33(62.09)	3.86(3.98)	3.83(4.26)
		56.53(62.09)	3.78(3.98)	3.89(4.26)
Pt(5-NO_2phen)Ph_2	$C_{24}H_{17}N_3O_2Pt$	48.12(50.18)	2.90(2.98)	6.88(7.31)
		53.12(50.18)	3.39(2.98)	6.74(7.31)
		48.50(50.18)	2.98(2.98)	6.91(7.31)
Pt(5,5′-dmbpy)Ph_2	$C_{24}H_{22}N_2Pt$	53.73 (54.03)	4.16 (4.16)	5.22 (5.25)
Pt(4,7-dmphen)Ph_2	$C_{38}H_{30}N_2Pt$	55.75 (56.01)	3.94 (4.01)	4.99 (5.02)
Pt(dmdpphen)Ph_2	$C_{38}H_{30}N_2Pt$	64.32 (64.31)	4.32 (4.26)	3.88 (3.95)
Pt(3,4,7,8-tmphen)Ph_2	$C_{28}H_{26}N_2Pt$	57.17 (57.43)	4.48 (4.48)	4.89 (4.78)
Pt(bpy)(3,5-dmPh)$_2$	$C_{24}H_{22}N_2Pt$	55.83 (55.60)	4.68 (4.67)	4.93 (4.99)
Pt(dppz)(3,5-dmPh)$_2$	$C_{18}H_{10}N_4Pt$	59.35 (59.40)	4.18 (4.08)	7.98 (8.15)
Pt(dmbpy)(C_6F_5)$_2$	$C_{27}H_{12}N_2F_{10}Pt$	40.46 (40.40)	1.76 (1.70)	3.78 (3.93)
Pt(dbbpy)(C_6F_5)$_2$	$C_{30}H_{24}N_2F_{10}Pt$	45.28 (45.18)	3.03 (3.03)	3.41 (3.51)
Pt(dppz)(C_6F_5)$_2$	$C_{30}H_{10}N_4F_{10}Pt$	44.41 (44.40)	1.36 (1.24)	6.64 (6.90)
Pt(dmbpy)($C_6H_3F_5$)$_2$	$C_{18}H_{10}N_2F_4Pt$	47.19 (47.60)	2.85 (3.00)	4.63 (4.63)

[a]Calculated values are found in parentheses.

Table 3.3. Electrochemical Data for Platinum(II) Diimine Complexes

(CH_2Cl_2/$TBAPF_6$, vs Ag/AgCl

Compound	$E_{1/2\ red.}$ (V)	$\Delta E_{red.}$ (mV)	$i_{pa}/i_{pc\ red.}$	$E_{1/2\ ox.}$ (V)	$\Delta E_{ox.}$ (V)	$i_{pa}/i_{pc\ ox.}$	ScanRate mV/s
Pt(tmphen)(tdt)	-1.58			>300			
$Pt(bpy)Cl_2$	-1.19	80	0.87	>0.8			250
$Pt(dmbpy)Cl_2$	-1.27	86	0.84	>0.8			250
$Pt(dbbpy)Cl_2$	-1.33	76	0.94				250
$Pt(bpy)Ph_2$[a]	-1.65						250
$Pt(dmbpy)Ph_2$[b]	-1.75						250
$Pt(5,5'\text{-}dmbpy)Ph_2$	-1.67 (irr)			>0.8			250
$Pt(dbbpy)Ph_2$	-1.66	72	0.86	788 (irr)			250
$Pt(dmbpy)(C_6F_5)_2$	-1.37	79	0.86	>0.8			250
$Pt(dbbpy)(C_6F_5)_2$	-1.42	83	0.73	>0.8			250
$Pt(dmbpy)(C_6H_3F_2)_2$	-1.54	64	0.56	>0.8			250
$Pt(phen)Ph_2$	-1.51			>0.8			250
$Pt(tmphen)Ph_2$	<-1.8(irr)			>0.8			250
$Pt(dmdpphen)Ph_2$	-1.69 (irr)			>0.8			250
$Pt(bpy)(3,5dmPh)_2$	-1.60 (irr)	79	0.56	1.0 (irr)			250
$Pt(5\text{-}NO_2phen)Ph_2$	-1.14	62	0.97				250
$Pt(bpy)(Mes)_2$	-1.51	58	0.84	891	54	2.81	250, 100, 50
$Pt(dppz)Ph_2$	-1.11	55	1.13	871 (irr)			250
$Pt(dppz)(3,5\text{-}dmPh)_2$	-1.09			1.1			250
$Pt(dppz)(Mes)_2$	-1.12	67	0.48	811	53	1.58	250, 100
$Pt(dppz)(C_6F_5)_2$	-0.95	68	0.72	>0.8			250

Table 3.4 Crystallographic Data for Compounds.

Formula	$C_{28}H_{28}P_2S_2Pt•C_3H_6O$	$C_{24}H_{22}N_2Pt$	$C_{26}H_{26}N_2Pt$	$C_{42}H_{38}N_2Pt•2C_2H_4Cl_2$
fw, g/mol	743.73	533.53	561.58	963.74
Color	Colorless	Yellow	Orange-yellow	Orange
Crystal Size (mm)	0.55 x 0.08 x 0.06	0.22 x 0.14 x 0.10	0.16x 0.10 x 0.06	0.45 x 0.10 x 0.05
Space group	$P2_1/n$	$P2_1/n$	$P2_1/n$	P-1
a, Å	8.9073(2)	7.0276(4)	8.0831(3)	12.3466(5)
b, Å	27.6168(4)	17.4239(9)	16.8616(7)	13.7792(5)
c, Å	12.2840(2)	16.2857(9)	15.6676(6)	14.7004(6)
α, °	90	90	90	109.613(1)
β, °	101.0830(10)	96.502(1)	93.4590(10)	106.767(1)
γ, °	90	90	90	105.082(1)
V, *Å*³	2965.401(9)	1981.33(19)	2131.51(14)	2071.41(14)
Z	4	4	4	2
T, K	1502)	150(2)	150(2)	150(2)
reflns collected	19130	11877	12300	28565
ind reflns	7225	4338	4330	10283
R_{int}	0.0422	0.0323	0.0428	0.0262
GOF on F^2	1.014	1.184	1.079	1.052
R1/wR2 [I>2σ(I)]	0.0331/0.0709	0.0342/0.0585	0.0327/0.0648	0.0247/0.0579
R1/wR2 (all data)	0.0497/0.0760	0.0430/0.0604	0.0519/0.0696	0.0315/0.0608

[a] $R_1 \Sigma \quad F_o \; - \; F_c \quad / \Sigma \quad F_o$, $wR_2 = [\Sigma w(F_o^2 - F_c^2)^2 / \Sigma w(F_o^2)^2]^{½}$.

Table 3.5. Bond lengths [Å] and angles [°] for Pt(dppe)($C_2H_4S_2$).

Pt(1)-P(1)	2.2588(10)	Pt(1)-P(2)	2.2732(10)
Pt(1)-S(2)	2.3206(11)	Pt(1)-S(1)	2.3424(10)
S(1)-C(1)	1.829(4)	C(1)-C(2)	1.491(6)
S(2)-C(2)	1.817(4)	P(2)-C(30)	1.825(4)
P(2)-C(40)	1.825(4)	P(2)-C(4)	1.837(4)
C(3)-C(4)	1.531(5)	C(3)-P(1)	1.821(4)
P(1)-C(10)	1.818(4)	P(1)-C(20)	1.819(4)
C(10)-C(11)	1.390(6)	C(10)-C(15)	1.397(6)
C(11)-C(12)	1.391(7)	C(12)-C(13)	1.381(7)
C(13)-C(14)	1.379(7)	C(14)-C(15)	1.389(6)
C(20)-C(21)	1.386(6)	C(20)-C(25)	1.390(6)
C(21)-C(22)	1.396(6)	C(22)-C(23)	1.382(7)
C(23)-C(24)	1.372(7)	C(24)-C(25)	1.391(6)
C(30)-C(35)	1.390(5)	C(30)-C(31)	1.402(6)
C(31)-C(32)	1.379(6)	C(32)-C(33)	1.379(7)
C(33)-C(34)	1.375(7)	C(34)-C(35)	1.402(6)
C(40)-C(45)	1.392(6)	C(40)-C(41)	1.398(6)
C(41)-C(42)	1.387(6)	C(42)-C(43)	1.400(7)
C(43)-C(44)	1.378(6)	C(44)-C(45)	1.388(6)
O(1)-C(51)	1.139(9)	C(50)-C(51)	1.523(14)
C(51)-C(52)	1.372(14)	P(1)-Pt(1)-P(2)	85.79(4)
P(1)-Pt(1)-S(2)	88.90(4)	P(2)-Pt(1)-S(2)	174.06(4)
P(1)-Pt(1)-S(1)	177.28(4)	P(2)-Pt(1)-S(1)	96.90(3)
S(2)-Pt(1)-S(1)	88.39(4)	C(1)-S(1)-Pt(1)	102.8(2)
C(2)-C(1)-S(1)	112.0(3)	C(2)-S(2)-Pt(1)	102.4(2)
C(1)-C(2)-S(2)	112.0(3)	C(30)-P(2)-C(40)	102.9(2)
C(30)-P(2)-C(4)	103.1(2)	C(40)-P(2)-C(4)	104.8(2)
C(30)-P(2)-Pt(1)	121.64(13)	C(40)-P(2)-Pt(1)	115.13(14)
C(4)-P(2)-Pt(1)	107.48(13)	C(4)-C(3)-P(1)	108.2(3)
C(3)-C(4)-P(2)	108.9(3)	C(10)-P(1)-C(20)	105.9(2)
C(10)-P(1)-C(3)	105.6(2)	C(20)-P(1)-C(3)	105.4(2)
C(10)-P(1)-Pt(1)	115.55(13)	C(20)-P(1)-Pt(1)	116.16(14)
C(3)-P(1)-Pt(1)	107.27(13)	C(11)-C(10)-C(15)	119.1(4)
C(11)-C(10)-P(1)	122.2(3)	C(15)-C(10)-P(1)	118.7(3)
C(10)-C(11)-C(12)	119.9(4)	C(13)-C(12)-C(11)	120.7(5)
C(14)-C(13)-C(12)	119.6(5)	C(13)-C(14)-C(15)	120.3(4)
C(14)-C(15)-C(10)	120.3(4)	C(21)-C(20)-C(25)	119.5(4)
C(21)-C(20)-P(1)	122.4(3)	C(25)-C(20)-P(1)	118.1(3)
C(20)-C(21)-C(22)	120.0(4)	C(23)-C(22)-C(21)	119.8(4)
C(24)-C(23)-C(22)	120.5(4)	C(23)-C(24)-C(25)	120.0(5)
C(20)-C(25)-C(24)	120.2(4)	C(35)-C(30)-C(31)	118.7(4)
C(35)-C(30)-P(2)	119.9(3)	C(31)-C(30)-P(2)	121.4(3)
C(32)-C(31)-C(30)	120.6(4)	C(33)-C(32)-C(31)	120.4(5)
C(34)-C(33)-C(32)	120.0(4)	C(33)-C(34)-C(35)	120.4(4)
C(30)-C(35)-C(34)	119.9(4)	C(45)-C(40)-C(41)	118.4(4)
C(45)-C(40)-P(2)	119.9(3)	C(41)-C(40)-P(2)	121.7(3)
C(42)-C(41)-C(40)	121.0(4)	C(41)-C(42)-C(43)	119.7(4)
C(44)-C(43)-C(42)	119.6(4)	C(43)-C(44)-C(45)	120.5(4)
C(44)-C(45)-C(40)	120.7(4)	O(1)-C(51)-C(52)	132.8(14)
O(1)-C(51)-C(50)	118.6(14)	C(52)-C(51)-C(50)	108.4(9)

Table 3.6. Bond lengths [Å] and angles [º] for Pt(5,5'-dmbpy)Ph_2.

Pt-C(19)	2.000(5)	Pt-C(13)	2.004(5)
Pt-N(7)	2.097(4)	Pt-N(1)	2.105(4)
N(1)-C(1)	1.334(6)	N(1)-C(5)	1.357(6)
C(1)-C(2)	1.382(7)	C(2)-C(3)	1.377(7)
C(2)-C(6)	1.512(7)	C(3)-C(4)	1.379(7)
C(4)-C(5)	1.376(7)	C(5)-C(11)	1.480(6)
N(7)-C(11)	1.347(6)	N(7)-C(7)	1.351(6)
C(7)-C(8)	1.391(7)	C(8)-C(9)	1.375(7)
C(8)-C(12)	1.505(7)	C(9)-C(10)	1.377(7)
C(10)-C(11)	1.393(6)	C(13)-C(18)	1.399(7)
C(13)-C(14)	1.411(7)	C(14)-C(15)	1.384(8)
C(15)-C(16)	1.390(8)	C(16)-C(17)	1.375(8)
C(17)-C(18)	1.407(7)	C(19)-C(20)	1.398(7)
C(19)-C(24)	1.412(7)	C(20)-C(21)	1.414(7)
C(21)-C(22)	1.354(8)	C(22)-C(23)	1.390(8)
C(23)-C(24)	1.387(7)		
C(19)-Pt-C(13)	89.02(18)	C(19)-Pt-N(7)	172.71(17)
C(13)-Pt-N(7)	98.27(17)	C(19)-Pt-N(1)	94.59(17)
C(13)-Pt-N(1)	176.15(17)	N(7)-Pt-N(1)	78.13(15)
C(1)-N(1)-C(5)	119.1(4)	C(1)-N(1)-Pt	125.6(3)
C(5)-N(1)-Pt	115.3(3)	N(1)-C(1)-C(2)	123.4(5)
C(3)-C(2)-C(1)	117.4(5)	C(3)-C(2)-C(6)	122.5(5)
C(1)-C(2)-C(6)	120.0(5)	C(2)-C(3)-C(4)	119.7(5)
C(5)-C(4)-C(3)	120.2(5)	N(1)-C(5)-C(4)	120.2(4)
N(1)-C(5)-C(11)	115.0(4)	C(4)-C(5)-C(11)	124.9(4)
C(11)-N(7)-C(7)	118.4(4)	C(11)-N(7)-Pt	115.2(3)
C(7)-N(7)-Pt	126.4(3)	N(7)-C(7)-C(8)	123.6(5)
C(9)-C(8)-C(7)	117.1(5)	C(9)-C(8)-C(12)	122.6(5)
C(7)-C(8)-C(12)	120.4(5)	C(8)-C(9)-C(10)	120.5(5)
C(9)-C(10)-C(11)	119.5(5)	N(7)-C(11)-C(10)	121.0(4)
N(7)-C(11)-C(5)	116.2(4)	C(10)-C(11)-C(5)	122.7(4)
C(18)-C(13)-C(14)	115.1(5)	C(18)-C(13)-Pt	123.1(4)
C(14)-C(13)-Pt	121.7(4)	C(15)-C(14)-C(13)	122.7(6)
C(14)-C(15)-C(16)	120.6(6)	C(17)-C(16)-C(15)	118.7(5)
C(16)-C(17)-C(18)	120.3(5)	C(13)-C(18)-C(17)	122.5(5)
C(20)-C(19)-C(24)	115.8(4)	C(20)-C(19)-Pt	122.1(4)
C(24)-C(19)-Pt	121.6(4)	C(19)-C(20)-C(21)	121.7(5)
C(22)-C(21)-C(20)	120.6(5)	C(21)-C(22)-C(23)	119.5(5)
C(24)-C(23)-C(22)	120.3(5)	C(23)-C(24)-C(19)	122.0(5)

Table 3.7. Bond lengths [Å] and angles [º] for Pt(bpy)(3,5-dmPh)$_2$.

Pt(1)-C(19)	1.993(5)	Pt(1)-C(11)	2.004(5)
Pt(1)-N(1)	2.095(4)	Pt(1)-N(2)	2.109(4)
N(1)-C(1)	1.342(7)	N(1)-C(5)	1.364(7)
N(2)-C(10)	1.328(7)	N(2)-C(6)	1.370(7)
C(1)-C(2)	1.380(8)	C(2)-C(3)	1.366(9)
C(3)-C(4)	1.399(9)	C(4)-C(5)	1.390(8)
C(5)-C(6)	1.470(8)	C(6)-C(7)	1.379(8)
C(7)-C(8)	1.390(9)	C(8)-C(9)	1.367(9)
C(9)-C(10)	1.372(8)	C(11)-C(18)	1.392(8)
C(11)-C(12)	1.404(7)	C(12)-C(13)	1.410(8)
C(13)-C(15)	1.386(8)	C(13)-C(14)	1.501(8)
C(15)-C(16)	1.383(8)	C(16)-C(18)	1.403(7)
C(16)-C(17)	1.511(8)	C(19)-C(26)	1.390(8)
C(19)-C(20)	1.406(8)	C(20)-C(21)	1.395(8)
C(21)-C(23)	1.389(8)	C(21)-C(22)	1.522(8)
C(23)-C(24)	1.402(9)	C(24)-C(26)	1.396(8)
C(24)-C(25)	1.502(9)		

C(19)-Pt(1)-C(11)	87.5(2)	C(19)-Pt(1)-N(1)	95.76(19)
C(11)-Pt(1)-N(1)	176.5(2)	C(19)-Pt(1)-N(2)	173.84(19)
C(11)-Pt(1)-N(2)	98.6(2)	N(1)-Pt(1)-N(2)	78.12(17)
C(1)-N(1)-C(5)	118.2(5)	C(1)-N(1)-Pt(1)	126.4(4)
C(5)-N(1)-Pt(1)	115.4(4)	N(1)-C(1)-C(2)	123.4(6)
C(10)-N(2)-C(6)	117.9(5)	C(10)-N(2)-Pt(1)	127.1(4)
C(6)-N(2)-Pt(1)	114.9(3)	C(3)-C(2)-C(1)	119.1(6)
C(2)-C(3)-C(4)	118.7(6)	C(5)-C(4)-C(3)	119.7(6)
N(1)-C(5)-C(4)	120.8(5)	N(1)-C(5)-C(6)	115.7(5)
C(4)-C(5)-C(6)	123.5(5)	N(2)-C(6)-C(7)	120.5(5)
N(2)-C(6)-C(5)	115.4(5)	C(7)-C(6)-C(5)	124.1(5)
C(6)-C(7)-C(8)	120.4(6)	C(9)-C(8)-C(7)	118.2(6)
C(8)-C(9)-C(10)	119.1(6)	N(2)-C(10)-C(9)	123.8(6)
C(18)-C(11)-C(12)	115.9(5)	C(18)-C(11)-Pt(1)	123.3(4)
C(12)-C(11)-Pt(1)	120.8(4)	C(11)-C(12)-C(13)	122.5(5)
C(15)-C(13)-C(12)	118.7(5)	C(15)-C(13)-C(14)	121.2(5)
C(12)-C(13)-C(14)	120.1(6)	C(16)-C(15)-C(13)	121.0(5)
C(15)-C(16)-C(18)	118.7(5)	C(15)-C(16)-C(17)	119.5(5)
C(18)-C(16)-C(17)	121.8(5)	C(11)-C(18)-C(16)	123.1(5)
C(26)-C(19)-C(20)	115.8(5)	C(26)-C(19)-Pt(1)	122.8(4)
C(20)-C(19)-Pt(1)	121.2(4)	C(21)-C(20)-C(19)	123.3(5)
C(23)-C(21)-C(20)	118.4(6)	C(23)-C(21)-C(22)	121.0(5)
C(20)-C(21)-C(22)	120.6(5)	C(21)-C(23)-C(24)	120.7(5)
C(26)-C(24)-C(23)	118.5(6)	C(26)-C(24)-C(25)	121.2(6)
C(23)-C(24)-C(25)	120.3(6)	C(19)-C(26)-C(24)	123.3(6)

Table 3.8. Bond lengths [Å] and angles [º] for Pt(dpphen)$(Mes)_2$.

Pt-C(27)	2.019(3)	Pt-C(36)	2.031(3)
Pt-N(1)	2.100(2)	Pt-N(14)	2.102(2)
N(1)-C(2)	1.334(3)	N(1)-C(6)	1.366(3)
C(2)-C(3)	1.391(4)	C(3)-C(4)	1.382(4)
C(4)-C(5)	1.425(4)	C(4)-C(21)	1.486(4)
C(5)-C(6)	1.401(4)	C(5)-C(7)	1.429(4)
C(6)-C(10)	1.440(4)	C(7)-C(8)	1.357(4)
C(8)-C(9)	1.432(4)	C(9)-C(10)	1.411(4)
C(9)-C(11)	1.427(4)	C(10)-N(14)	1.363(4)
C(11)-C(12)	1.382(4)	C(11)-C(15)	1.482(4)
C(12)-C(13)	1.392(4)	C(13)-N(14)	1.334(3)
C(15)-C(16)	1.394(4)	C(15)-C(20)	1.395(4)
C(16)-C(17)	1.394(5)	C(17)-C(18)	1.380(6)
C(18)-C(19)	1.374(6)	C(19)-C(20)	1.395(4)
C(21)-C(22)	1.389(5)	C(21)-C(26)	1.396(5)
C(22)-C(23)	1.389(5)	C(23)-C(24)	1.382(6)
C(24)-C(25)	1.376(6)	C(25)-C(26)	1.380(5)
C(27)-C(32)	1.417(4)	C(27)-C(28)	1.421(4)
C(28)-C(29)	1.397(4)	C(28)-C(33)	1.516(4)
C(29)-C(30)	1.391(4)	C(30)-C(31)	1.395(4)
C(30)-C(34)	1.509(4)	C(31)-C(32)	1.397(4)
C(32)-C(35)	1.506(4)	C(36)-C(37)	1.413(4)
C(36)-C(41)	1.415(4)	C(37)-C(38)	1.396(4)
C(37)-C(42)	1.509(4)	C(38)-C(39)	1.396(5)
C(39)-C(40)	1.379(5)	C(39)-C(43)	1.511(5)
C(40)-C(41)	1.406(4)	C(41)-C(44)	1.507(5)
Cl(50)-C(51)	1.791(4)	C(51)-C(52)	1.493(6)
C(52)-Cl(53)	1.791(4)	Cl(54)-C(55A)	1.675(15)
Cl(54)-C(55B)	1.842(12)	C(55A)-C(56A)	1.61(2)
C(56A)-Cl(57)	1.609(13)	C(55B)-C(56B)	1.51(2)
C(56B)-Cl(58)	1.79(2)		

C(27)-Pt-C(36)	92.13(11)	C(27)-Pt-N(1)	93.21(10)
C(36)-Pt-N(1)	174.23(10)	C(27)-Pt-N(14)	170.83(10)
C(36)-Pt-N(14)	96.35(10)	N(1)-Pt-N(14)	78.46(9)
C(2)-N(1)-C(6)	117.5(2)	C(2)-N(1)-Pt	128.00(19)
C(6)-N(1)-Pt	114.45(18)	N(1)-C(2)-C(3)	122.6(3)
C(4)-C(3)-C(2)	121.1(3)	C(3)-C(4)-C(5)	117.3(3)
C(3)-C(4)-C(21)	120.3(3)	C(5)-C(4)-C(21)	122.4(3)
C(6)-C(5)-C(4)	117.9(3)	C(6)-C(5)-C(7)	118.3(3)
C(4)-C(5)-C(7)	123.7(3)	N(1)-C(6)-C(5)	123.4(2)
N(1)-C(6)-C(10)	115.9(2)	C(5)-C(6)-C(10)	120.6(2)
C(8)-C(7)-C(5)	121.3(3)	C(7)-C(8)-C(9)	121.9(3)
C(10)-C(9)-C(11)	117.9(2)	C(10)-C(9)-C(8)	118.0(2)
C(11)-C(9)-C(8)	124.1(2)	N(14)-C(10)-C(9)	123.2(2)
N(14)-C(10)-C(6)	117.0(2)	C(9)-C(10)-C(6)	119.8(2)
C(12)-C(11)-C(9)	117.3(2)	C(12)-C(11)-C(15)	120.8(2)
C(9)-C(11)-C(15)	121.8(2)	C(11)-C(12)-C(13)	121.1(3)
N(14)-C(13)-C(12)	122.7(3)	C(13)-N(14)-C(10)	117.7(2)
C(13)-N(14)-Pt	128.14(19)	C(10)-N(14)-Pt	113.86(17)
C(16)-C(15)-C(20)	119.1(3)	C(16)-C(15)-C(11)	120.4(3)
C(20)-C(15)-C(11)	120.5(3)	C(17)-C(16)-C(15)	119.8(3)
C(18)-C(17)-C(16)	120.8(4)	C(19)-C(18)-C(17)	119.7(3)
C(18)-C(19)-C(20)	120.4(3)	C(19)-C(20)-C(15)	120.2(3)

C(22)-C(21)-C(26)	118.4(3)	C(22)-C(21)-C(4)	122.5(3)
C(26)-C(21)-C(4)	119.1(3)	C(23)-C(22)-C(21)	120.8(3)
C(24)-C(23)-C(22)	119.8(4)	C(25)-C(24)-C(23)	119.9(3)
C(24)-C(25)-C(26)	120.4(4)	C(25)-C(26)-C(21)	120.6(4)
C(32)-C(27)-C(28)	116.4(2)	C(32)-C(27)-Pt	123.7(2)
C(28)-C(27)-Pt	119.59(19)	C(29)-C(28)-C(27)	120.8(2)
C(29)-C(28)-C(33)	117.3(2)	C(27)-C(28)-C(33)	121.9(2)
C(30)-C(29)-C(28)	122.5(3)	C(29)-C(30)-C(31)	117.0(3)
C(29)-C(30)-C(34)	121.7(3)	C(31)-C(30)-C(34)	121.3(3)
C(30)-C(31)-C(32)	122.0(3)	C(31)-C(32)-C(27)	121.3(2)
C(31)-C(32)-C(35)	118.4(2)	C(27)-C(32)-C(35)	120.3(2)
C(37)-C(36)-C(41)	116.3(3)	C(37)-C(36)-Pt	124.3(2)
C(41)-C(36)-Pt	119.4(2)	C(38)-C(37)-C(36)	121.6(3)
C(38)-C(37)-C(42)	116.9(3)	C(36)-C(37)-C(42)	121.6(3)
C(37)-C(38)-C(39)	121.8(3)	C(40)-C(39)-C(38)	116.9(3)
C(40)-C(39)-C(43)	122.0(4)	C(38)-C(39)-C(43)	121.1(4)
C(39)-C(40)-C(41)	122.8(3)	C(40)-C(41)-C(36)	120.4(3)
C(40)-C(41)-C(44)	117.2(3)	C(36)-C(41)-C(44)	122.3(3)
C(52)-C(51)-Cl(50)	111.8(3)	C(51)-C(52)-Cl(53)	111.3(3)
C(56A)-C(55A)-Cl(54)	111.0(10)	Cl(57)-C(56A)-C(55A)	121.2(12)
C(56B)-C(55B)-Cl(54)	98.9(11)	C(55B)-C(56B)-Cl(58)	113.4(17)

References

1. Shriver, D. F.; Drezdzon, M. A. *The Manipulation of Air-Sensitive Compounds*; 2nd ed.; John Wiley & Sons: New York, 1986.
2. Cummings, S. D.; Eisenberg, R. *J. Am. Chem. Soc.* **1996**, *118*, 1949-1960.
3. Connick, W. B.; Gray, H. B. *J. Am. Chem. Soc.* **1997**, *119*, 11620-11627.
4. Keefer, C. E.; Bereman, R. D.; Purrington, S. T.; Knight, B. W.; Boyle, P. D. *Inorg. Chem.* **1999**, *38*, 2294-2302.
5. Bevilacqua, J. M.; Zuleta, J. A.; Eisenber, R. *Inorg. Chem.* **1994**, *33*, 258-266.
6. Morgan, G. T.; burstall, F. H. *J. Chem. Soc.* **1934**, 965.
7. Hodges, K. D.; Rund, J. V. *Inorg. Chem.* **1975**, *14*, 525-528.
8. Chaudhury, N.; Puddephatt, R. C. *J. Organomet. Chem.* **1975**, *84*, 105-115.
9. Ghedini, M.; Longeri, M.; Neve, F. *Inorg. Chim. Acta* **1987**, *132*, 223-228.
10. Eaborn, C.; Odell, K. J.; Pidcock, A. *J. Chem. Soc., Dalton Trans.* **1978**, 357-368.
11. Eaborn, C.; Kundu, K.; Pidcock, A. *J. C.S. Dalton* **1981**, 933-938.
12. The ligand ($(CF_3)_2$bpy) was prepared by Rachel Lieberman following a literature procedure, Chan, C. W., Tse, A. K. S. Synthetic Comm., 1993, 1929-1934.
13. Dungey, K. E.; Thompson, B. D.; Kane-Magiore, N. A. P.; Wright, L. L. *Inorg. Chem.* **2000**, *39*, 5192-5196.
14. Klein, A.; Hausen, H. D.; Kaim, W. *J. Organomet. Chem.* **1992**, *440*, 207-217.
15. Klein, A.; Kaim, W. *Organometallics* **1995**, *14*, 1176-1186.
16. Klein, A.; Kaim, W.; Waldhor, E.; Hausen, H.-D. *J. Chem. Soc. Perkin Trans.* **1995**, *2*, 2121-2126.
17. Minniti, D. *J. Chem. Soc. Dalton Trans.* **1993**, 1343-1345.

18. (Pt (COD)(C_6F_5)$_2$[Deacon, G. B.; Nelson-Reed, K. T., *J. Organomet. Chem.* **1987**, 322, 257-268] was originally investigated as a starting material, but once again, the diimine did not displace the COD. Similarly, Pt (COD)(C_6F_5)$_2$ was isolated only by using fresh ether and not THF).
19. When recrystallizing, the procedure suggests using CH_2Cl_2 and petroleum ether. Large volumes of ether are necessary for the product to precipitate.
20. Dickeson, J. E.; Summers, L. A. *Aust. J. Chem.* **1970**, *23*, 1023-1027.
21. A modified procedure of Dickeson (ref. 20) adopted in our lab by Nathan Eckert.
22. SMART v5.054 was used for data collection (Bruker Analytical X-ray Instruments, Inc. or Siemens Analytical X-ray Instruments, Inc, Madison, WI).
23. Saint v5.A06 (Siemens Analytical X-ray Instruments, Inc, Madison, WI) or v6.22A (Bruker Analytical X-ray Instruments, Inc., Madison, WI) were used for data processing.
24. SADABS v.2.03 was used for the application of semi-empirical absorption and beam corrections. G.M. Sheldrick, University of Goettingen, Germany.
25. SHELXTL v5.03 was used for the structure solution and generation of figures and tables. G. M. Sheldrick, University of Goettingen, Germany and Siemens Analytical X-ray Instruments, Inc., Madison, WI.26).
26. SHELXTL v6.1 was used for the structure solution and generation of figures and tables. G. M. Sheldrick, Univeristy of Goettingen, Germany and Bruker Analytical X-ray Instruments, Madison, WI.
27. Klein, A.; McInnes, E. J. L.; Kaim, W. *J. Chem. Soc., Dalton Trans.* **2002**, 2371-2378.
28. Huertas, S.; Hissler, M.; McGarrah, J. E.; Lachicotte, R. J.; Eisenberg, R. *Inorg. Chem.* **2001**, *40*, 1183-1188.

29. Miskowski, V. M.; Houlding, V. H. *Inorg. Chem.* **1989**, *28*, 1529-1533.

30. Miskowski, V. M.; Houlding, V. H. *Inorg. Chem.* **1991**, *30*, 4446-4452.

31. Miskowski, V. M.; Houlding, V. H.; Che, C.-M.; Wang, Y. *Inorg, Chem.* **1993**, *32*, 2518-2524.

32. Houlding, V. H.; Miskowski, V. M. *Coord. Chem. Rev.* **1991**, *111*, 145-152.

33. Biedermann, J.; Wallfahrer, M.; Gliemann, G. *J. Luminesc.* **1987**, *37*, 323-329.

34. Weiser-Wallfahrer, M.; Gliemann, G. *Z. Naturforsch.* **1990**, *45b*, 652-657.

35. Biedermann, J.; Gliemann, G.; Klement, U.; Range, K.-J.; Zabel, M. *Inorg. Chem.* **1990**, *29*, 1884-1888.

36. Biedermann, J.; Gliemann, G.; Klement, U.; Range, K.-J.; Zabel, M. *Inorg. Chim. Acta* **1990**, *171*, 35-40.

37. Biedermann, J.; Gliemann, G.; Klement, U.; Range, K.-J.; Zabel, M. *Inorg. Chim. Acta* **1990**, *169*, 63-70.

38. Kato, M.; Sasano, K.; Kosuge, C.; Yamazaki, M.; Yano, S.; Kimura, M. *Inorg. Chem.* **1996**, *35*, 116-123.

39. Kato, M.; Kozakai, M.; Fukagawa, C.; Funayama, T.; Yamauchi, S. *Mol. Cryst. Liq. Cryst.* **2000**, *343*, 353-358.

40. Connick, W. B.; Miskowski, V. M.; Houlding, V. H.; Gray, H. B. *Inorg. Chem.* **2000**, *39*, 2585-2592.

41. Connick, W. B.; Henling, L. M.; Marsh, R. E.; Gray, H. B. *Inorg. Chem.* **1996**, *35*, 6261-6265.

42. Che, C.-M.; Wan, K.-T.; He, L.-Y.; Poon, C.-K.; Yam, V. W.-W. *J. Chem. Soc., Chem. Commun.* **1989**, 943-945.

43. Wan, K.-T.; Che, C.-M.; Cho, K.-C. *J. Chem. Soc., Dalton Trans.* **1991**, 1077-1080.

44. Vogler, C.; Schwederski, B.; Klein, A.; Kaim, W. *J. Organomet. Chem.* **1992**, *436*, 367-378.

45. Klein, A.; Scheiring, T.; Kaim, W. *Z. Anorg. Allg. Chem.* **1999**, *625*, 1177-1180.

46. Hissler, M.; Connick, W. B.; Geiger, D. K.; McGarrah, J. E.; Lipa, D.; Lachicotte, R. J.; Eisenberg, R. *Inorg. Chem.* **2000**, *39*, 447-457.

47. Juris, A.; Balzani, V.; Barigeletti, F.; Campagna, S.; Belser, P.; von Zelewsky, A. *Coord. Chem. Rev.* **1988**, *84*, 85-277.

48. McInnes, E. J. L.; Farley, R. D.; Rowlands, C. C.; Welch, A. J.; Rovatti, L.; Yellowlees, L. J. *J. Chem. Soc., Dalton Trans.* **1999**, 4203-4208.

49. Yang, L.; Wimmer, F. L.; Wimmer, S.; Zhao, J.; Braterman, P. S. *J. Organomet. Chem.* **1996**, *525*, 1-8.

50. Braterman, P. S.; Song, J.-I. *Inorg. Chim. Acta* **1991**, *183*, 131-132.

51. Landis, K. G.; Hunter, A. D.; Wagner, T. R.; Curtin, L. S.; Filler, F. L.; Jansen-Vamum, S. A. *Inorg. Chim. Acta* **1998**, *282*, 155.

52. Vicente, R.; Ribas, J.; Solans, X.; Font-Altaba, M.; Mari, A.; de Loth, P.; Cassoux, P. *Inorg. Chim. Acta* **1987**, *132*.

Chapter 4

Cross-Quenching Reactions

I. Introduction

There is considerable interest in understanding, learning to control, and exploiting the self-quenching behavior of platinum(II) diimine complexes. A major obstacle is that the exact nature of the intermolecular interactions stabilizing the excimers is uncertain. Three modes of association have been suggested: (i) diimine-diimine interactions, (ii) metal-metal interactions, or (iii) a combination of these (Scheme 4.1).

Scheme 4.1. Proposed modes of association of a ground-state and an excited-state molecule.

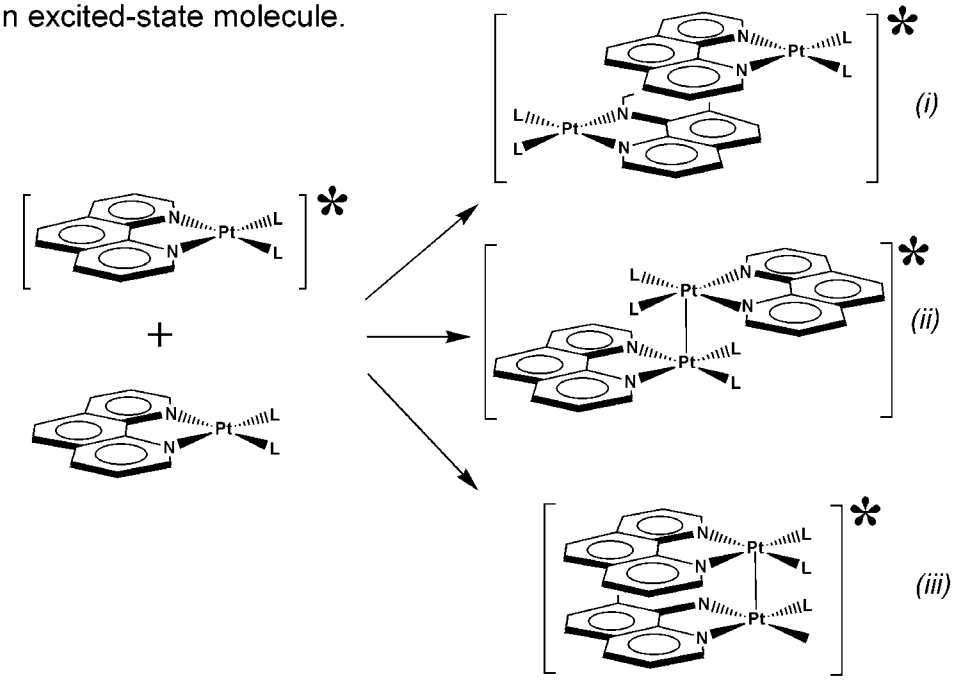

Direct characterization of the excimer is often hampered by the apparent short lifetimes and low emission quantum yields of the excimers as compared to those of the monomers. Additional complications include poor solubility of the monomers and possible ground-state aggregation at high concentrations. These considerations have led to investigations of cross-

quenching reactions as an indirect means of elucidating the interactions that play a role in association of an excited complex with a ground-state complex.

A cross-quenching reaction is similar to its self-quenching counterpart with the distinction that the excited monomer, M*, reacts with a *different* ground-state complex, Q, presumably to form an exciplex, MQ*:

$$M^* + Q \rightarrow MQ^* \rightarrow M + Q$$

Employing this strategy the photophysical behavior of a *single* chromophore (M) can be investigated in the presence of a wide variety of individual quenchers (Q). As discussed in Chapter 2, the results of analogous self-quenching studies are decidedly more difficult to interpret because changing the properties of the quencher necessarily changes the properties of the chromophore, including the photophysics of the monomer. In the present study, the emission properties of one chromophore were investigated in the presence of a series of quenchers. Pt(tmphen)(tdt) was selected as the chromophore because it possesses several attractive photophysical properties, which include a fairly long excited-state lifetime ($\tau=1/k_i=1911$ ns). Quenchers were selected according to strict criteria, discussed in detail in the chromophore and quencher requirement section later in this chapter.

By varying the steric and electronic properties of the quenchers, it is possible to investigate the influence of these parameters on the efficiency of the cross-quenching reaction. Taken together, the accumulated data can help to elucidate the interactions favoring exciplex formation, which can then be extended to self-quenching by inference. Selected quenchers are initially divided into three main groups: organic aromatic molecules and nitrogen-based nucleophiles (Figure 4.1), platinum(II) complexes lacking a diimine ligand (Figure 4.1), and

platinum(II) complexes with a diimine ligand (Figure 4.5-4.8). The latter group can be subdivided into three more categories that will be discussed in Chapters 5 and 6.

II. Experimental

For a typical cross-quenching experiment, stock solutions of the Pt(tmphen)(tdt) chromophore (1.4-2.3 mM) and quencher (0.4-2.8 mM) were prepared in distilled methylene chloride. The chromophore is not readily soluble in methylene chloride, and as a result, sonication was necessary to achieve a concentrated sample. A 2.28×10^{-4} M solution was the highest concentration obtained with confidence that no undissolved material was present. Depending on the quencher, solubility was similar to that of the chromophore or significantly greater.[1] The concentration of the Pt(tmphen)(tdt) stock solution was adjusted, so that upon dilution to give samples for photophysical studies (*vide infra*), the absorbance at 535 nm was approximately 0.4 (60-70 μM). Nearly the maximum possible concentration of quencher solution was used in order to probe as wide a range of quencher concentrations as possible. Due to the high concentration of quencher, the absorbance of the stock solutions was recorded in 1 cm and 1 mm cells.

Using these stock solutions and distilled methylene chloride, up to six solutions with identical volumes (8-12 mL) were prepared using volumetric pipettes. The solutions contained identical concentrations of Pt(tmphen)(tdt) (60-70 μM, usually 3-4 mL stock solution), and varying concentrations of quencher (0-1.8×10^{-3} M, 0-8 mL stock solution). One sample served as the control, containing only the chromophore. Each sample was placed in a custom-designed quartz cell (Figure 4.2) equipped with an attached 25 ml solution reservoir bulb, and subsequently freeze-pump-thaw (FPT) degassed (3-4) cycles under high vacuum ($<10^{-5}$ torr).[2] Throughout sample preparation and measurements, the samples were protected from light using

dark cloth and aluminum foil and by working in dim light. Absorption spectra of each sample were recorded before the steady-state and time-resolved emission experiments, as well as at the conclusion of all measurements. In some instances ($Pt(acac)_2$, $Pt(dppe)(C_2H_4S_2)$, nitrogen-based nucleophiles, and anthracene), the quencher was added to the chromophore solution as a solid. The solution was freeze-pump-thaw degassed 3-4 times, and subsequently a weighed sample of solid quencher was added to the quartz portion of the cell through the top valve opening. The other valve separating the quartz portion of the cell from the bulb, was kept closed to avoid possible exposure of the solution to air. After addition of solid, the top valve was replaced and the quartz portion of the cell was evacuated. Once the cell was removed from the line, the solid and solution were mixed, and the typical experimental procedure described below was followed.

Quenching of the emission from Pt(tmphen)(tdt) was investigated by steady-state and time-resolved emission spectroscopies. Cross-quenching rates (k_{cq}) were obtained by monitoring the decrease in integrated emission intensity (650-700 nm) of Pt(tmphen)(tdt) in distilled CH_2Cl_2 with increasing quencher concentration. The uncorrected emission maximum occurred at 675 nm, and data were not corrected prior to integration since this had no impact on the calculation of I_0/I where I_0 is the integrated emission intensity in the absence of quencher and I is the integrated emission intensity in the presence of quencher. The ratio of the emission quantum yield in the absence (Φ_0) to that in presence (Φ) of quencher is given by I_0/I and found to depend linearly on the concentration of added quencher, [Q], according to:

$$I_0/I = \Phi_0/\Phi = 1 + k_{cq}^{ss}/k'[Q] \quad (1)$$

where k_{cq}^{ss} is the bimolecular cross-quenching rate constant as determined by steady-state emission spectroscopy. The value of k_{cq}^{ss} was determined from the slope of a line fitted to a Stern-Volmer plot of Φ_0/Φ vs. quencher concentration. In nearly all cases, the plots were linear

within the scatter of the data. Values of the rate of emission decay in the absence of quencher (k)′ were calculated using equation 2, obtained from self-quenching experiments:

$$k' = k_i + k_{sq}[Pt] \quad (2)$$

For Pt(tmphen)(tdt), values of k_i (5.23 x 10^5 s^{-1}) and k_{sq} (4.2 x 10^9 $M^{-1}s^{-1}$) have been previously reported.[3]

To ensure that the correct value for k_{sq} of Pt(tmphen)(tdt) was used in the data analysis, this value was remeasured in CH_2Cl_2. Six samples with varying concentrations of chromophore ranging from 60-230 μM were prepared and freeze-pump-thaw-degassed. The lifetime of each sample was measured. These six measurements were combined with previous measurements[3] to determine the self-quenching rate of Pt(tmphen)(tdt) according to equation (2) (Figure 4.3). Error analysis was performed by estimating the standard deviation for the rate of emission decay (k'). The data were fit according to equation (2) by the least squares method with individual squares weights given by σ^{-1}. Values of σ were estimated as 2.5% of k'. This estimate comes from an investigation of the rate of emission decay of Pt(tmphen)(bdt) as a function of concentration performed by Ms. P.J. Ball. For this complex, 36 emission decay rates were measured for different chromophore concentrations over the course of one year. All values were plotted vs chromophore concentration and fit by uniformly weighted linear least squares according to equation (2). Error bars defined as plus-and-minus a percentage of k' were arbitrarily varied. For 34 of the points (94% of data), it was found that error bars of ±5% of k' overlapped with the fitted line. Therefore, ±5% of k' was taken as the 95% confidence limit for k'. The results of this analysis for Pt(tmphen)(tdt) are shown in Figure 4.3. The values of k_{sq} and k_i obtained from this analysis were 4.15(9) x 10^9 $M^{-1}s^{-1}$ and 5.33(7) x 10^5 s^{-1}, where the numbers

in parentheses represent estimated standard deviations (σ). These values were used in all subsequent calculations of cross-quenching rates.

In most instances, the results of the steady-state measurements were corroborated by time-resolved experiments in which the emission lifetime (τ_{obs}) of the chromophore was determined in the absence and presence of quencher. The rate of Pt(tmphen)(tdt) emission decay ($k''=1/\tau_{obs}$) was found to depend linearly on the concentration of added quencher according to:

$$\frac{k''}{k'} = \frac{k_{cq}^{tr}}{k'}[Q] + 1 \quad (3)$$

where k' is given by equation 2.

Steady-state emission spectra were obtained using a SPEX Fluorolog-3 flourimeter with a single excitation monochromator and a double emission monochromator in a right-angle configuration. To ensure the observed emission originates only from the excitation of the Pt(tmphen)(tdt) chromophore, samples were excited at 535 nm, where most quenchers do not absorb. For quenchers with weak, long wavelength absorption, even longer excitation wavelengths were necessary: Pt(bpy)Ph_2, 545 nm; Pt(dppz)Ph_2, 560 nm; Pt(bpy)(3,5-dm$Ph)_2$, 565 nm; Pt(5-NO_2phen)Ph_2, 570 nm; Pt(bpy)$(Mes)_2$, 570 nm; Pt(dpphen)$(Mes)_2$, 570 nm; and Pt(dppz)$(Mes)_2$, 570 nm. The emission maximum and bandshape were independent of excitation wavelength and quencher. A 570 nm cut-off filter was used to minimize scattered light. Before collecting the emission, it is important to ensure that the cell is perfectly vertical and not tilted in order to minimize scattered light and to obtain reproducible emission scans. Due to some decomposition of the chromophore a short emission scan (650-700 nm) was always collected first. The integrated intensity from the first scan of each sample was used to determine the cross-quenching rate. Subsequent scans (normally repeated runs of 650-700 and one to two runs of

540-850 nm) were typically taken to monitor any possible changes in the sample associated with decomposition. During these multiple emission scans, the sample was not moved from its original position. After completion of steady-state emission measurements for all samples, lifetime data were collected.

Emission samples for lifetime measurements were excited using 4-6 ns pulses from a Continuum Panther Optical Parametric Oscillator (535-570 nm), pumped with the third harmonic (355 nm) of a Surelite II Nd:YAG laser. Emission transients were detected at 675 nm with a modified PMT connected to a Tektronix TD5580D oscilloscope (sometimes via a Phillips DC-300 MHz bipolar amplifier, model number 695, fixed gain =10), and data were modeled as single-exponential decays using in-house software on a Microsoft Excel platform. In all cases, the emission decays were well-modeled with a single-exponential function. Once again, exposure to light was minimized during this experiment. Also, just as in the steady-state experiment it was important to have the sample positioned correctly in the path of the laser beam, to avoid unnecessary laser shots, which are likely to decompose samples. Generally, several test shots were collected to make certain the sample was appropriately positioned and to ensure suitable signal intensity (< 5 mV single-shot intensity maximum without amplifier and < 50 mV maximum with amplifier). Data sets consisted of averages of emission decay traces resulting from ten to twenty laser shots. Usually 6-8 data sets were collected per sample. The resulting fitted decay rates were averaged to obtain an estimate of k'. Another series of absorption spectra were collected after the laser experiment. Typically, no changes in the absorbance were evident.

For time-resolved measurements, standard deviations (σ) for k' were estimated as 2.5% of k' for reasons previously described. The data were fit by the least squares method to equation (3)

with weights given by σ^{-1}. For steady-state measurements, the ratio of I_0/I was fit by the least squares method with weights given by σ^{-1}. Standard deviations for I_0/I were propagated from the estimated standard deviations for the individual intensity measurements, namely 1% of the integrated emission intensity. This estimate for σ came from two analyses, which yield similar results. The first analysis involved analyzing multiple emission intensity measurements for six samples in a quenching study with $Pt(dbbpy)Cl_2$. The emission intensity was recorded three times for each sample. All measurements for a given sample fell within 1% of the average intensity. The second analysis involved ten measurements of the integrated emission intensity of a concentrated and a dilute solution of Pt(tmphen)(bdt). Again, all measurements fell within 1% of the average intensity. Though repeated emission runs resulted in decomposition, the first run for each sample was always used in data analysis and the estimated standard deviation for this measurement was taken as 1% of the intensity. Estimated standard deviations for values of the cross-quenching rate as determined by the steady-state (k_{cq}^{ss}) and time-resolved (k_{cq}^{tr}) methods are reported in parentheses with the rate.

III. Chromophore and Quencher Requirements.

Selection of the Pt(tmphen)(tdt) chromophore for cross-quenching studies represents a balancing of desirable attributes. The complex is acceptably soluble and reasonably stable in methylene chloride solution. The relatively high emission quantum yield (~0.6% at 298K in CH_2Cl_2),[3,4] and a long lifetime ($\tau=1/k_i$=1911 ns; λ_{max}=720 nm) provide good dynamic range for steady-state and time-resolved experiments. In addition, this chromophore possesses a broad, low-energy intense absorption band (λ_{max}=535 nm, 7160 M^{-1} cm^{-1}, CH_2Cl_2)[3] allowing for selective excitation. The relatively low energy of the lowest triplet state ($E_{0,0}$=2.1eV) also

provides a moderately wide window of potential quenchers that are unable to quench effectively by energy transfer.

Stringent criteria restricted the selection of possible quenchers. Suitable compounds were soluble in methylene chloride and thermally stable in the presence of Pt(tmphen)(tdt). In fact, several complexes were excluded as possible quenchers due to thermal reaction with the chromophore (Pt(phen)$(CH_3)_2$, Pt(dpphen)Cl_2, and Pt(bpy)(pyrazolate)$_2$), insolubility in CH_2Cl_2 (Pt(phen)Cl_2), and the probability of quenching by energy transfer (Pt(5,5′-(CF_3)bpy)Ph_2). Neutral quenchers were preferred in order to avoid complications associated with variations in ionic strength. The energetics of each candidate also was considered in order to avoid the possibility of quenching by energy or outer-sphere electron transfer. In order to avoid energy transfer, only compounds with lowest triplet states > 2.1 eV were considered. Representative complexes of each type of quencher were used to assess the possibility of energy transfer by comparison to literature or experimental data. The $E_{0,0}$ for the quencher complexes was estimated from the overlap of the absorption and 77 K or room-temperature emission bands of the quencher. For example, the emission of one of the most efficient quenchers, Pt(bpy)Cl_2, originates from a ^{3}LF excited state with an onset of emission approximately λ=530 nm ($E_{0,0} \geq 2.4$ eV). Also, the emission of one of the least effective quenchers, Pt(dppe)$(C_2H_4S_2)$, originates at approximately λ=540 nm ($E_{0,0} \geq 2.3$ eV). To eliminate the possibility of energy transfer to the mesityl complexes, the emission of Pt(dpphen)$(Mes)_2$ (λ=560 nm, ($E_{0,0} \geq 2.2$ eV) was measured. Though endergonic energy transfer is conceivable for some of the investigated quenchers, we will show in Chapter 6 that the observed relative rates are not consistent with this mechanism of quenching. Likewise, when selecting quenchers, those with unfavorable driving forces for electron transfer were chosen. Although, it was not practical to completely exclude

compounds that could participate in electron-transfer reactions, in most instances the electron-transfer driving forces are only weakly favorable (Chapter 5).

IV. Photodecomposition During Cross-quenching Experiments

Platinum diimine dithiolates in solution are known to undergo photodecomposition in the presence of oxygen[5] and in halogenated solvents most likely through a radical-type reaction.[6] An estimate of the extent of photodecomposition is necessary in order to assess the significance of the rate measurements. In our studies, photodecomposition as estimated from changes in the Pt(tmphen)(tdt) absorption band near 535 nm during the course of the experiments for all samples (over 2-6 runs for each sample), with or without quencher, typically ranged from 4-8%. In some instances, however, the decomposition was as little as 0.8% and as much as 18% (unusual case). Apparent decomposition in the absorbance of Sample A, which contains only the chromophore, during any set of measurements for the first and second emission scans ranged from -1.7 to 2.3% as estimated from changes in absorbance of the chromophores at 535 nm. It is interesting to note that decomposition of samples containing the chromophore and quencher was greater for quenchers with chloride ligands. In contrast, quenchers with ancillary ligands such as phenyl and mesityl ligands suppressed decomposition, suggesting interference with the previously mentioned radical reaction.

V. Inefficient Quenchers.

The emission intensity of the chromophore was monitored in the presence of varying concentrations of organic aromatics and nitrogen-based nucleophiles. Previously, Eisenberg and coworkers[7] measured the rate of Pt(tmphen)(tdt) in the presence of high concentrations ($< 10^{-2}$ M) of 1,10-phenanthroline and naphthalene. These aromatic molecules had no significant effect on the emission lifetime of the chromophores. Subsequently, we investigated the effect of

solutions of neutral nitrogen-based nucleophiles ($<10^{-2}$ M) such as 2,2′-bipyridine and 4,4′-bipyridine, as well as another aromatic molecule, anthracene ($<10^{-2}$ M) on the chromophore. We also observed negligible effect on the emission intensity of the chromophore with the nitrogen-based nucleophiles. These results suggest that organic aromatics and nitrogen-based nucleophiles are inefficient quenchers. In contrast, when using a steady-state analysis, the addition of anthracene to a solution of Pt(tmphen)(tdt) resulted in a decrease in the emission intensity, corresponding to a cross-quenching rate of 3.5×10^8 $M^{-1}s^{-1}$, which is somewhat slower than the self-quenching rate of Pt(tmphen)(tdt) ($4.15(9) \times 10^9$ $M^{-1}s^{-1}$). The energy of the lowest triplet state of anthracene ($E_{0,0}$=1.85 eV) is consistent with quenching by energy transfer.

Platinum complexes lacking a diimine ligand also were investigated as quenchers (Figure 4.1). Analysis of the steady-state data indicated no quenching ($<10^6$ $M^{-1}s^{-1}$) (Figure 4.4) of Pt(tmphen)(tdt) emission upon addition of Pt(dppe)($C_2H_4S_2$) up to concentrations of 10^{-2} M. Addition of a large excess of $Pt(acac)_2$ (1.5×10^{-2} M) to a solution of Pt(tmphen)(tdt) resulted in a slight, but discernible decrease in emission intensity, not attributable to irreversible photochemistry. Although the metal center of $Pt(acac)_2$ is relatively exposed, the corresponding cross-quenching rate ($<10^7$ $M^{-1}s^{-1}$) (Figure 4.4) is slow compared to self-quenching rates. Taken together, these data suggest the platinum center and diimine ligand play an important role in the self-quenching reactions of platinum(II) diimine complexes.

VI. Efficient Quenchers

In the cross-quenching investigations discussed thus far, only inefficient quenching of the chromophore emission was observed. In an earlier study by Eisenberg and coworkers,[7] emission lifetime data suggested that other platinum(II) diimine complexes, such as Pt(dbbpy)Cl_2, noticeably affect the rate of emission decay of the chromophore. In fact, a cross-quenching rate

of 2.1 x 10^9 $M^{-1}s^{-1}$ was observed for Pt(dbbpy)Cl_2, establishing that cross-quenching reactions of platinum(II) diimine complexes occur at rates comparable to self-quenching. To establish the validity of assessing quenching using steady-state emission spectroscopy, emission spectra of Pt(tmphen)(tdt) solutions in CH_2Cl_2 were measured in the presence of varying concentrations of Pt(dbbpy)Cl_2. The observed cross-quenching rate (2.23(4) x 10^9 $M^{-1}s^{-1}$) was in agreement with the value obtained from emission decay measurements (2.1 x 10^9 $M^{-1}s^{-1}$). These results are our first indication that cross-quenching rates obtained using the steady-state method (k_{cq}^{ss}) are in good agreement with those obtained using the time-resolved methods (k_{cq}^{tr}), *i.e.*, $k_{cq}^{ss} \approx k_{cq}^{tr}$. Thus, either method can be used to measure k_{cq}. Moreover, these results confirm that cross-quenching is dominated by diffusional quenching rather than ground-state aggregation (static quenching). In the case of static quenching, we expect $k_{cq}^{ss} > k_{cq}^{tr}$. More significantly, these results suggest rapid quenching (10^9-10^{10} $M^{-1}s^{-1}$) is observed for complexes containing both a *diimine ligand and a platinum center.*

As a result, a series (Figures 4.5-4.8) of neutral Pt(II) diimine complexes with varying steric and electronic properties were synthesized and characterized (Chapter 3). The diimine was either a substituted 2,2′-bipyridine, a substituted 1,10-phenanthroline, or dipyrido[3,2-*a*:2′,3′-*c*]phenazine (dppz). The results of cross-quenching studies using these complexes are discussed in Chapter 5.

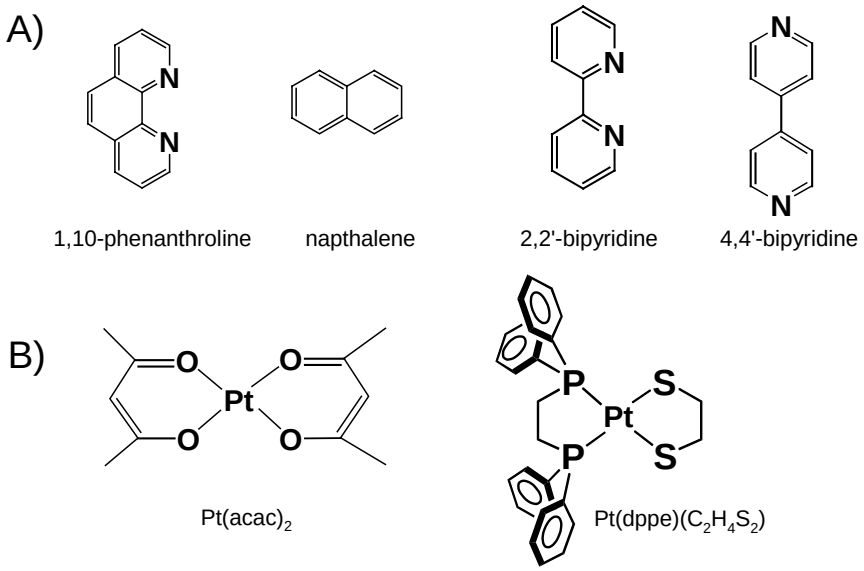

Figure 4.1. A) Organic aromatic and nitrogen-based nucleophile quenchers. B) Platinum(II) quencher complexes lacking a diimine ligand.

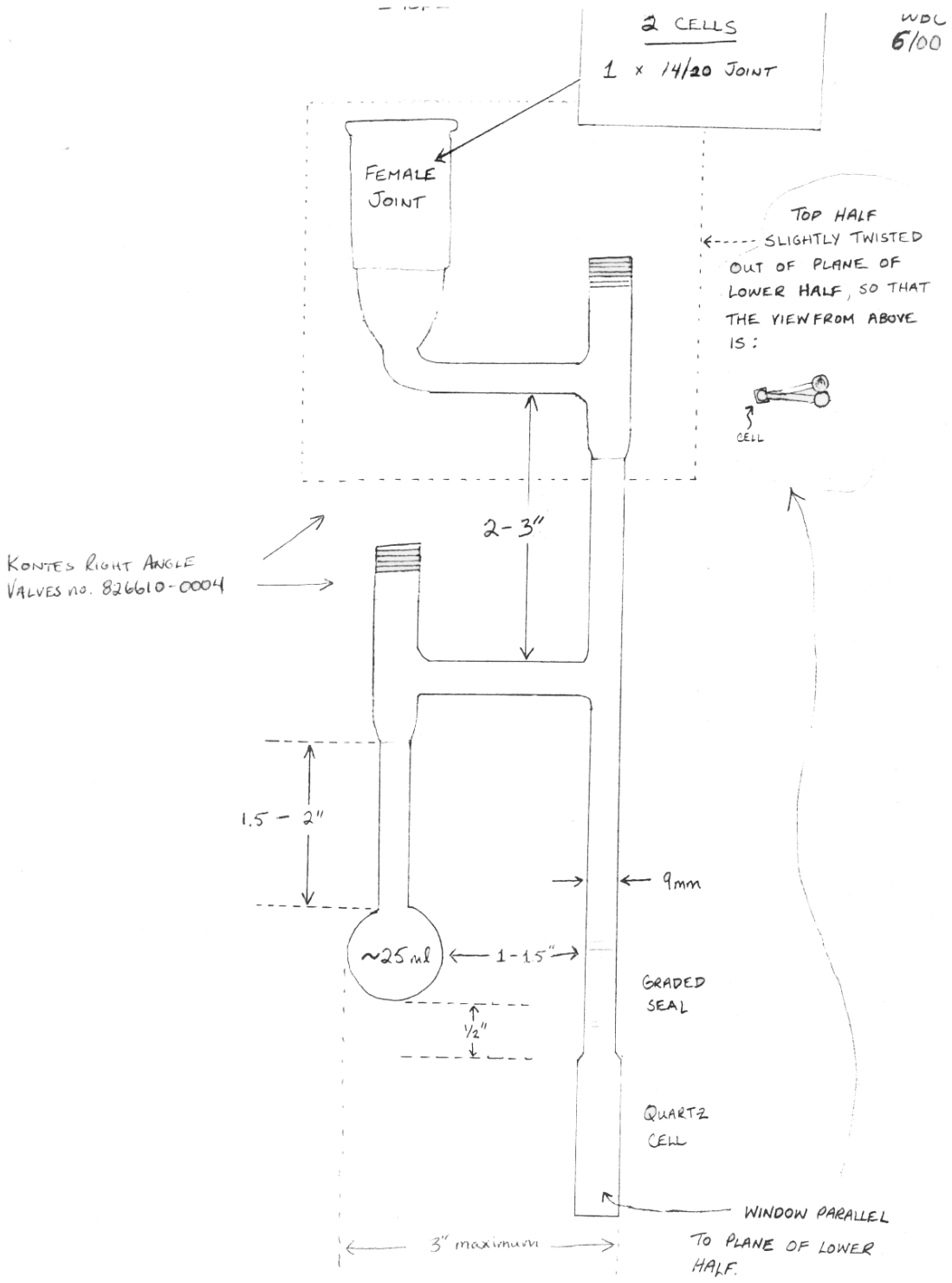

Figure 4.2. Custom-designed quartz cell.

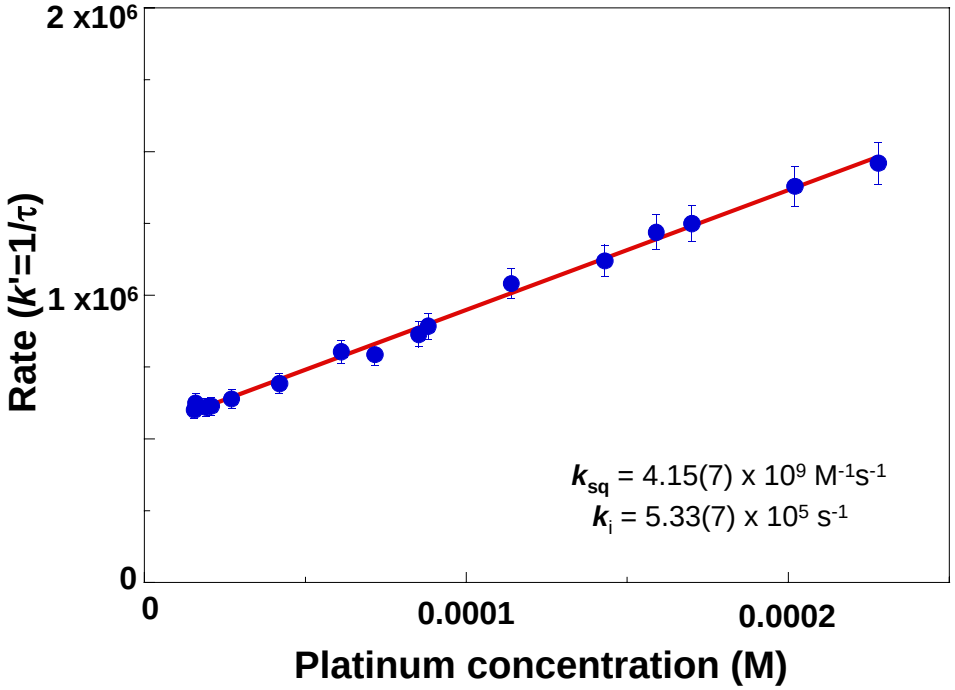

Figure 4.3. Plot of self-quenching rate of Pt(tmphen)(tdt) with error analysis. Error bars represented ± 2σ. For some points, the error bars are hidden by larger size of data points.

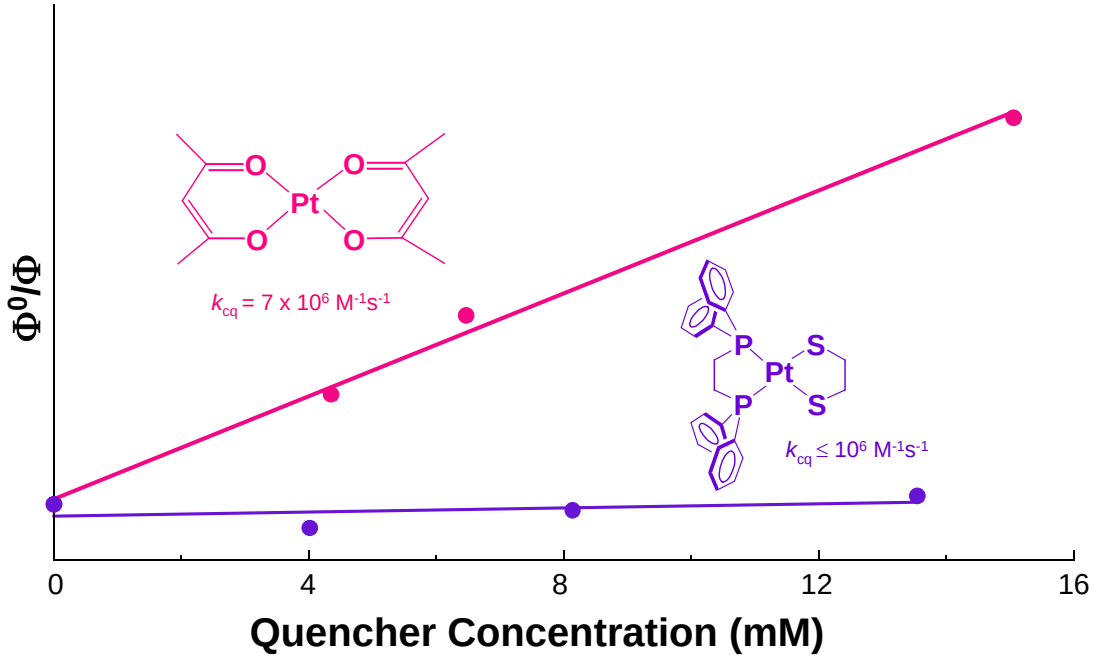

Figure 4.4. Stern-Volmer plot of steady-state emission data for inefficient quenchers lacking a diimine ligand: the ratio of the quantum yields in the absence of quencher (Φ_0) and presence of quencher (Φ) vs. quencher concentration.

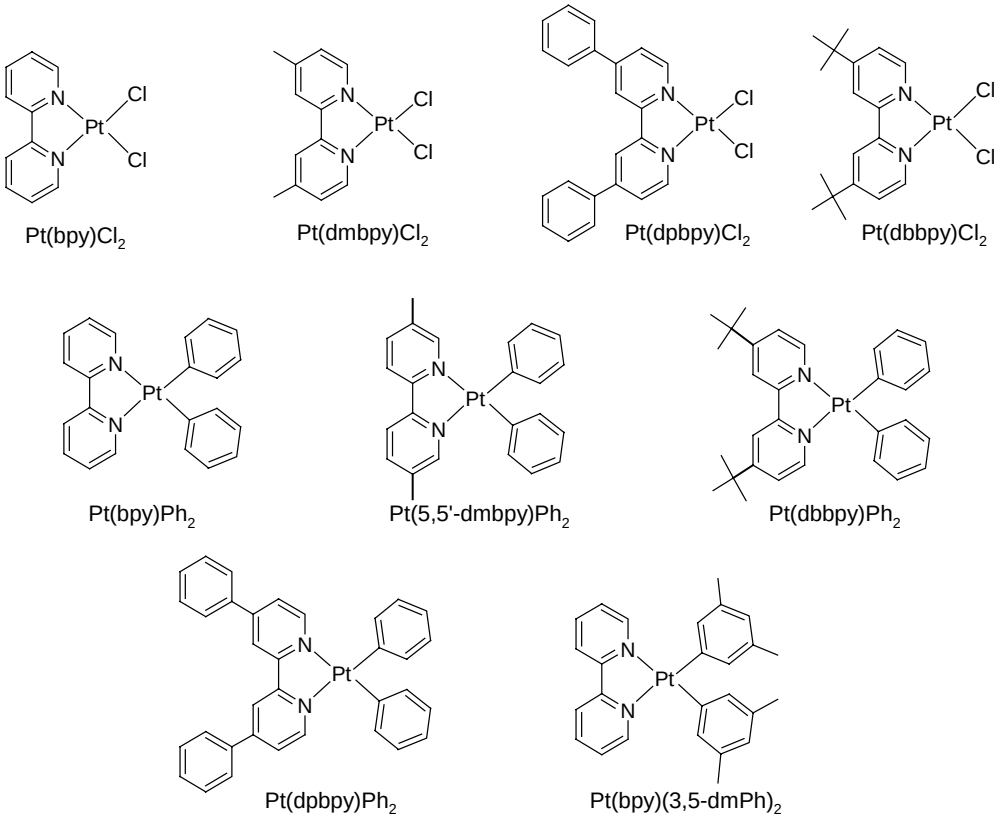

Figure 4.5. Platinum(II) bipyridine quencher complexes.

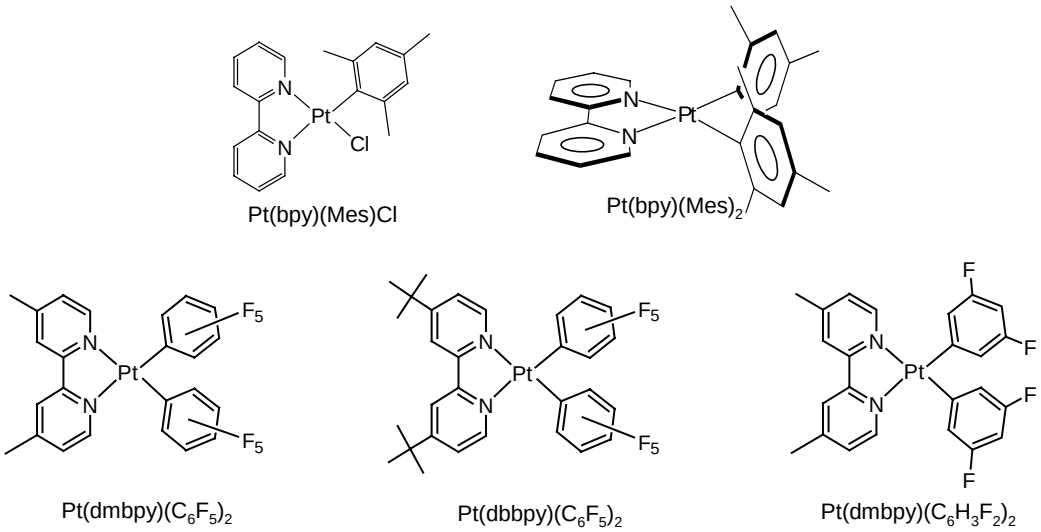

Figure 4.6. Platinum(II) bipyridine quencher complexes with substituted mesityl and flourinated anionic ligands.

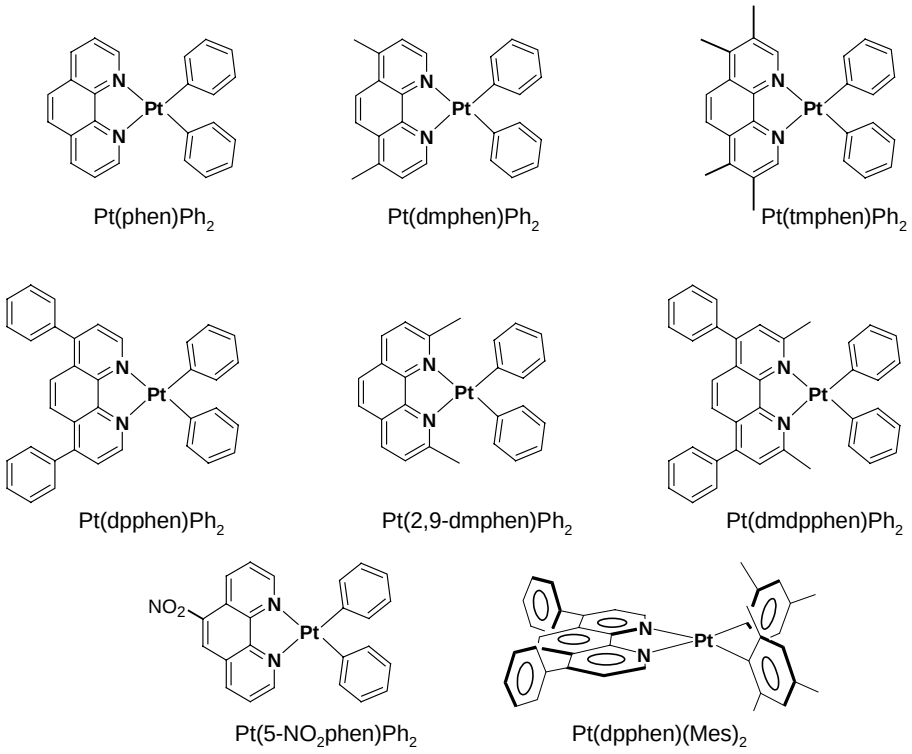

Figure 4.7. Platinum(II) phenanthroline quencher complexes.

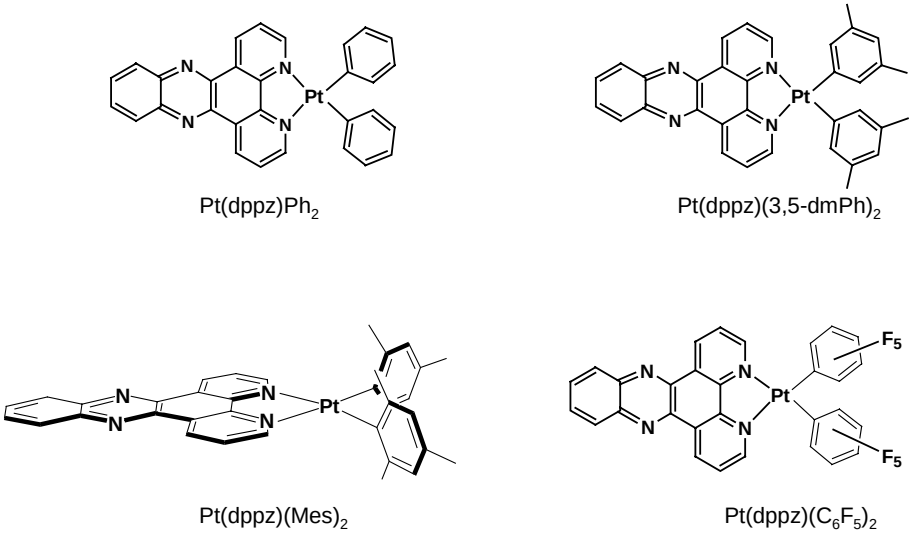

Figure 4.8. Platinum(II) dppz quencher complexes.

References

1. For example, most of the chloride quenchers are much less soluble than the phenyl quencher complexes. Also, unsubstituted bipyridine or phenanthroline complexes are much less soluble than those with substituents.
2. It should be noted that samples were FPT degassed in sets of three because the pump performs better with only three samples even though four is feasible. Also, the double-bulb cell was placed in the far left position, where it is less likely to get bumped. To avoid breaking cells when freezing the samples it is best to use the lab jacks for holding the dewars instead of depending on clamps to hold up the weight of the dewar.
3. Cummings, S. D.; Eisenberg, R. *J. Am. Chem. Soc.* **1996**, *118*, 1949-1960.
4. The quantum yield measurement was repeated for Pt(tmphen)(tdt). Cresyl violet red was used as the reference in an ethanol solution. Samples of both complexes were prepared with similar absorbances and exited at 535 nm to obtain the emission spectrum of each. The quantum yield was calculated using the following standard equation also used by Cummings and Eisenberg: $\Phi=\Phi_s[(1-10^{A_r l})\eta^2_s I_s/(1-10^{A_s l})\eta^2_r I_r]$ where A=absorbance, I=intensity of emission, η=viscosity of the solvent, and l=pathlength of the cell. The quantum yield value obtained for the repeated measurement was 1.2%
5. Connick, W. B.; Gray, H. B. *J. Am. Chem. Soc.* **1997**, *119*, 11620-11627.
6. Chaudhury, N.; Puddephatt, R. C. *J. Organomet. Chem.* **1975**, *84*, 105-115.
7. Connick, W. B.; Geiger, D.; Eisenberg, R. *Inorg. Chem.* **1999**, *38*, 3264-3265.

Chapter 5

Platinum(II) Diimine Quenchers

I. Introduction

In the previous chapter, we found that of the investigated cross-quenchers, only platinum(II) diimine complexes quenched the emission from Pt(tmphen)(tdt) at rates comparable to those observed in self-quenching reactions. In the present chapter, we report the quenching rates for all investigated platinum(II) diimine quenchers. We begin with an analysis of the kinetics of cross-quenching and the corresponding implications for exciplex formation. Next, we examine the accumulated data in the context of the steric and electronic properties of the ligands surrounding the metal center. The quenchers are divided into three classes based on the types of ligands. For the bipyridine and phenanthroline quenchers, the cross-quenching rate decreases as the steric bulk around the diimine, as well as around the metal center, increases. However, little dependence on electronic factors is evident. In particular, the rates showed no correlation with driving forces, Hammett substituents constants, or orbital character of the lowest excited states of the quencher. In fact, the extremely slow rates of quenching for fluorinated phenyl ancillary ligands were the only evidence of significant electronic effects. Finally, the dppz quenchers showed negligible changes in rates with both steric and electronic properties.

II. Experimental

Pt(II) diimine quenchers were synthesized and characterized as described in Chapter 3. The experimental procedure for cross-quenching experiments is detailed in Chapter 4. Similarly, cross-quenching rates (k_{cq}^{ss} and k_{cq}^{tr}) were obtained by methods described in Chapter 4. Rates are reported as determined from time-resolved measurements when available, otherwise steady-state rates are reported.

III. Cross-Quenching Reactions With Pt(II) Diimine Complexes

The accumulated data from cross-quenching experiments with Pt(II) diimine quenchers are consistent with the mechanism described by equation (1) in Chapter 4. Steady-state (k_{cq}^{ss}) and time-resolved (k_{cq}^{tr}) cross-quenching rates were obtained using the following steady-state and time-resolved expressions introduced in Chapter 4:

$$I_0/I = \Phi_0/\Phi = 1 + k_{cq}/k'[Q] \quad (1)$$

$$\frac{k''}{k'} = \frac{k_{cq}}{k'}[Q] + 1 \quad (2)$$

Representative Stern-Volmer quenching plots for diimine quencher complexes are shown in Figures 5.3-5.6, and 5.12, along with the respective cross-quenching rates, ranging from 10^7 $M^{-1}s^{-1}$ to 10^9 $M^{-1}s^{-1}$ (Table 5.1). In these studies, 10^7 $M^{-1}s^{-1}$ represents the detection limit under typical experimental conditions. Error bars are shown for all Stern-Volmer plots. However, in most cases, the associated errors are not visible due to the larger size of the data points.

Generally, for the platinum(II) diimine complexes we have found the rates determined from steady-state data are faster than those determined from time-resolved data. This observation is consistent with a small amount of ground-state aggregation of the chromophore with quencher resulting in static quenching. For twelve (75%) of the sixteen cases where both k_{cq}^{ss} and k_{cq}^{tr} were determined, these values were significantly different. For eleven measurements with rates greater than 10^9 $M^{-1}s^{-1}$, k_{cq}^{ss} ranges from being 6% ($Pt(5\text{-}NO_2phen)Ph_2$) to 75% ($Pt(dppz)(Mes)_2$) greater than k_{cq}^{tr}, with a an average of 24(19)%. The average for the four dppz complexes is 33(28)%. The average for the remaining seven quenchers is 18(11)%. Crude modeling shows that for a dynamic cross-quenching rate of 4 x 10^9 $M^{-1}s^{-1}$, and an equilibrium constant of 300 M^{-1} for formation of a quencher-chromophore aggregate, k_{cq}^{ss} is

predicted to be 25% (5 x 10^9 $M^{-1}s^{-1}$) larger than k_{cq}^{tr}. These results establish the validity of both methods of experimentation as well as establish that the observed quenching is dynamic (dominated by diffusional quenching) and not ground-state aggregation.[1] Generally speaking, the values of k_{cq}^{tr} and k_{cq}^{ss} track one another. Though neither parameter is a precise predictor of the other, these results indicate both provide a measure of the efficiency of dynamic cross-quenching with k_{cq}^{tr} being the more accurate measure of the rate constant for this process.

To determine the dependence of the cross-quenching rate on the concentration of the Pt(tmphen)(tdt) solution, a quenching study using $Pt(bpy)Ph_2$, was undertaken. Poor solubility of the chromophore prevented extensive investigation over a wide range of concentrations. Nevertheless, two extreme concentrations, 1.1 x 10^{-4} M and 3 x 10^{-5} M were examined. Three solutions (12 mL each) of each Pt(tmphen)(tdt) solution were prepared with 3 x 10^{-5} M and 1.1 x 10^{-4} M quencher, respectively. The cross-quenching rates were determined from steady-state and time-resolved experiments as previously described (Chapter 4). The data are summarized in Table 5.1 along with the rates for an intermediate concentration (6 x 10^{-5} M) determined from six samples (Figures 5.1 and 5.2). It was determined that as the concentration of the chromophore increased, the cross-quenching rate measured by steady-state emission spectroscopy became slightly faster (3.69(7), 4.36(7), and 4.3(1) x 10^9 $M^{-1}s^{-1}$, respectively). A comparison of the rates measured by time-resolved emission spectroscopy for the same three solutions were in excellent agreement (3.9(1), 3.9(1) and 3.9(2) x 10^9 $M^{-1}s^{-1}$). At present, the reason for the relatively slow rate (3.69(6) x 10^9 $M^{-1}s^{-1}$) obtained from steady-state measurements on the dilute sample of Pt(tmphen)(tdt) (3 x 10^{-5} M) is not known.

It is noteworthy that exciplex emission has not been observed in these or any other quenching experiments. Perhaps this is not surprising since excimer emission has not been

observed in fluid solution for any platinum(II) diimine dithiolate complexes. In fact, excimer emission has only been observed for a few platinum diimine complexes with lowest $^3(\pi\text{-}\pi^*)$ or ^{3}MLCT monomer excited states. Direct characterization has been hindered by short lifetimes as compared to those of the excited monomer. Although, excimer emission quantum yields are unavailable based upon the relative intensities of monomer and excimer emissions, it appears that complexes with $^3(\pi\text{-}\pi^*)$ monomer states have higher quantum yields than those with lowest ^{3}MLCT monomer states. This trend is qualitatively consistent with energy gap law considerations, which also could account for the absence of excimer or exciplex emission from platinum diimine dithiolate complexes.

IV. Cross-quenching Reaction Kinetics

In this section, we present a mathematical analysis of the kinetics of emission decay following a short laser pulse. As discussed previously, in all cross-quenching cases, single-exponential decay is observed. However, the model in Scheme 5.1 predicts triexponential decay of monomer emission, according to the solutions to three simultaneous differential equations describing the concentrations of excited monomer, excimer and exciplex.

Scheme 5.1. Cross-quenching Kinetics.

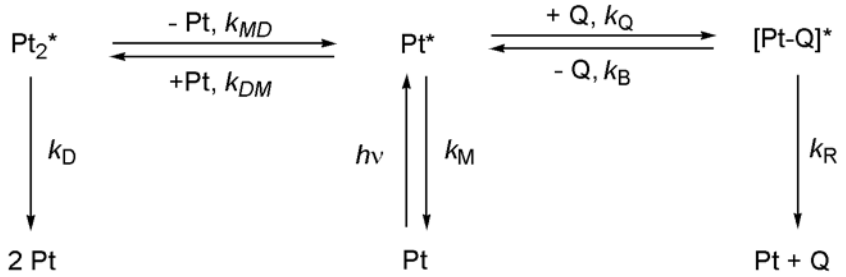

To help resolve this apparent discrepancy, we consider the conclusion from Chapter 2, that the excimer (Pt_2*) is tightly bound and/or short-lived. In other words, the back reaction represented by k_{MD} is considered to be insignificant. This reduces the analytical solution to two differential equations, suggesting biexponential decay. We next examine the conditions that cause this solution to behave as a single exponential function, namely that the exciplex is tightly bound and/or short-lived. Together these assumptions lead to the prediction that $k_{cq}^{ss} \approx k_{cq}^{tr} \approx k_Q$, in agreement with the results of time-resolved and steady-state measurements. This analysis provides important insight into exciplex formation.

A scheme showing all available relaxation pathways for an excited Pt(II) complex (Pt*) in the presence of quencher (Q) is illustrated in Scheme 5.1. Three new rate constants are introduced, k_Q, k_B, and k_R, with respect to the scheme for self-quenching (Chapter 2). k_Q and k_B are the rate constants for exciplex formation (Pt-Q*) and dissociation, respectively. k_R is the rate constant for unimolecular exciplex relaxation to give two ground state molecules.

We first we turn our attention to the predicted results for the steady-state quenching experiment. Under steady-state conditions and with the assumption that the excimer is tightly bound and/or short-lived ($k_D >> k_{MD}$), the total quantum yield of monomer emission intensity is given by:

$$\Phi = \frac{k_{PM}(k_B + k_R)}{k_M(k_B + k_R) + k_{DM}(k_B + k_R)[\mathrm{Pt}] + k_R k_Q [Q]} \qquad (3)$$

where k_{PM} is the phosphorescence radiative constant. The ratio of the quantum yield in the absence of quencher (Φ_0) to that in the presence of quencher, is given by (4)

$$\frac{\Phi_0}{\Phi} = 1 + \frac{k_R k_Q}{(k_B + k_R)(k_M + k_{DM}[\mathrm{Pt}])}[Q] \quad (4)$$

Making the following definitions:

$$k' = k_M + k_{DM}[Pt] \qquad (5)$$

$$k_{cq}^{ss} = \frac{k_Q k_R}{(k_B + k_R)} \qquad (6)$$

allows us to rewrite equation (4) as the following:

$$1 + \frac{k_{cq}^{ss}}{k'}[Q] \quad (7)$$

which is the cross-quenching equation used to fit steady-state data.

In the case that k_B is small relative to k_R (*vide infra*), the cross-quenching rate becomes:

$$k_{cq}^{ss} = \frac{k_Q k_R}{(k_B + k_R)} \approx \frac{k_Q k_R}{k_R} = k_Q$$

In other words, measurement of k_{cq}^{ss} provides a good estimate of k_Q.

Returning to Scheme 5.1, this model results in three simultaneous differential equations describing the concentration of excited monomer, excimer and exciplex. The function d[Pt*]/dt is the derivative of the function describing excited monomer concentration with respect to time.

$$\frac{d[Pt^*]}{dt} = k_{MD}[Pt_2^*] + k_B[Pt\text{-}Q^*] - (k_M + k_{DM}[Pt] + k_Q[Q])[Pt^*]$$

$$\frac{d[Pt_2^*]}{dt} = k_{DM}[Pt^*]Pt] - (k_D + k_{MD})[Pt_2^*]$$

$$\frac{d[Pt\text{-}Q^*]}{dt} = k_Q[Pt^*][Q] - (k_R + k_B)[Pt\text{-}Q^*]$$

Analytical solutions, obtained for example using Laplace transformations, are composed of sums of three terms, each containing a time-dependent factor of e^{-at}, e^{-bt}, or e^{-ct}, where a, b, and c are algebraic functions of k_M, k_{DM}, k_{MD}, k_D, k_Q, k_B, k_R, [Pt], and [Q]. Therefore, the concentrations of

these excited complexes are expected to exhibit triexponential decay as a function of time. The emission intensity (i_M) is linearly proportional to [Pt*] according to:

$$i_M(t) = \frac{k_{PM}[Pt^*]}{[Pt^*]_0} \qquad (8)$$

$[Pt^*]_0$ is the concentration of platinum at time zero after the arrival of the excitation pulse. Therefore, the transient emission signal also is predicted to exhibit triexponential decay kinetics. This prediction is not borne out by experimental observations, which are consistent with single exponential decay. One explanation for the observed self-quenching behavior of Pt(tmphen)(tdt) is $k_{MD} << k_{DM}[Pt]$, and $k_{MD} << k_D$ as discussed in Chapter 2. Applying this condition reduces the problem to two simultaneous differential equations:

$$\frac{d[Pt^*]}{dt} = k_B[Pt\text{-}Q^*] - (k_{DM}[Pt] + k_Q[Q])[Pt^*]$$

$$\frac{d[Pt\text{-}Q^*]}{dt} = k_Q[Pt^*][Q] - (k_R + k_B)[Pt\text{-}Q^*]$$

Analytical solutions, obtained for example by Laplace transformations are composed of sums of two exponential terms. Inserting the expression for [Pt*] into equation (8) gives

$$i_M(t) = \frac{k_{PM}(\lambda_2 - X)}{\lambda_2 - \lambda_1}(e^{-\lambda_1 t} + \frac{X - \lambda_1}{\lambda_2 - X}e^{-\lambda_2 t}) \qquad (9)$$

where

$$\lambda_{1,2} = \frac{1}{2}\left[X + Y \mu \sqrt{(Y - X)^2 + 4k_B k_Q[Q]}\right]$$

and $\quad X = k_M + k_{DM}[Pt] + k_Q[Q]$ and $Y = k_R + k_B$

This predicted triexponential decay is at odds with the results of the time-resolved studies. To account for the observed single exponential decay, we consider the three conditions under which

equation (8) reduces to a single exponential function. Three cases span the possible relative values of X and Y.

In the fortuitous case that the two terms in equation 8 decay at the same rate, λ_1 and λ_2 must be approximately equal. This condition is satisfied when

$$X \approx Y >> \sqrt{4k_B k_Q[Q]}$$

Values of k_M ($k_i = 5.33 \times 10^5\ s^{-1}$) and k_{DM} ($k_{SQ} = 4.15 \times 10^9\ M^{-1}s^{-1}$) are known from self-quenching experiments, establishing a minimum value for X of $\sim 10^6\ s^{-1}$, and therefore, a minimum value for Y from the first condition. In a typical cross-quenching experiment, $k_Q \sim 10^9\ M^{-1}s^{-1}$, and therefore $k_Q[Q]$ can approach values of $10^6\ s^{-1}$ as [Q] is increased to $\sim 10^{-3}$. Together, these considerations suggest $X \sim 10^6$, establishing an approximate value for Y from the first condition. Therefore, it is evident that the second condition requires:

$$10^6 >> \sqrt{4k_B k_Q[Q]} \approx 2 \times 10^3 \sqrt{k_B}$$

or:

$$k_B << 10^6$$

This result is consistent with a tightly bound exciplex ($k_Q[Q] >> k_B$) that decays rapidly relative to dissociation ($k_R >> k_B$).

The second case in which we would observe single exponential decay is if

$$\lambda_2 - X \approx 0 << X - \lambda_1.$$

In this case,

$$(Y - X) << (X - Y)$$

or:

$$X >> Y$$

$$k_M + k_{DM}[Pt] + k_Q[Q] >> k_R + k_B$$

If $X >> \sqrt{4k_B k_Q[Q]}$, which is satisfied when:

$$k_B << X \approx 10^6 \qquad (10)$$

then:

$$\lambda_2 = \frac{1}{2}\left[(X+Y) + \sqrt{(Y-X)^2 + 4k_B k_Q[Q]}\right] = \frac{1}{2}\left[X + Y + \sqrt{(Y-X)^2}\right] = X$$

In that case, the observed decay will be according to λ_2=X. The condition specified by equation (10) is consistent with a tightly bound exciplex. However, in order for X >> Y, $k_R << 10^6\ s^{-1}$. This is consistent with a long-lived exciplex relative to the monomer and the back reaction. Finally, to reconcile the approximate agreement between steady-state and time-resolved measurements,

$$k_B << k_R << 10^6 \text{ (assuming that } k_{MD} \text{ is small)}$$

The third case assumes that $X-\lambda_1 >> \lambda_2-X$ and Y>>X, so we expect to observe decay as λ_1. If if $Y >> \sqrt{4k_B k_Q[Q]}$, which is satisfied when:

$$k_B + k_R >> k_Q[Q] \approx 10^6 s^{-1},$$

then:

$$\lambda_1 = \frac{1}{2}\left[(X+Y) - \sqrt{(Y-X)^2 + 4k_B k_Q[Q]}\right] = \frac{1}{2}\left[X + Y - \sqrt{(Y-X)^2}\right] = X$$

The following three conditions satisfy this conclusion.

a) If $k_B \approx k_Q[Q]$ then $k_R >> k_B$.

b) If $k_B < k_Q[Q]$ then $k_R >> k_B$.

Both a and b satisfy our steady-state equation and yield the same result, namely that the exciplex rapidly decays relative to back reaction. Finally, if we examine the last solution:

c) If $k_B >> k_Q[Q]$, then the equation is always satisfied and as a result, there are no restrictions on k_R. However, the apparent rate of quenching will be given by $k_{cq}^{tr} \approx k_Q$. To

satisfy approximate agreement between this rate and that obtained from steady-state measurements (equation 6), $k_R >> k_B$. In other words, the exciplex is short-lived.

In summary, from examining the kinetics of cross-quenching it has been determined that three possible solutions may account for the single-exponential decay of the time-resolved analysis. However, in order to satisfy the steady-state experiment and to reconcile observed rates from both types of cross-quenching experiments, we must conclude that $k_R >> k_B$. As a result, $k_{cq}^{ss} \approx k_{cq}^{tr} \approx k_Q$. This condition strictly holds for nearly all investigated cross-quenching reactions

V. Steric Effects of Bipyridine and Phenanthroline Quenchers

The observed cross-quenching rates (k_{cq}) can be largely understood in terms of the steric properties of the quencher complexes. Quenchers with bulky substituents are less effective quenchers than unsubstituted derivatives, suggesting steric interactions interfere with exciplex formation. For example, investigations of a series of platinum bipyridyl quenchers with chloride ancillary ligands show that the rate decreases as the steric bulk of the substituents on the diimine increase (Figure 5.3). $Pt(bpy)Cl_2$, the least sterically-hindered quencher, exhibits the fastest rate ($8.1(1) \times 10^9$ $M^{-1}s^{-1}$), indicating it is the most effective quencher of the series. Upon substitution of the diimine as in $Pt(dmbpy)Cl_2$ ($5.8(1) \times 10^9$ $M^{-1}s^{-1}$) and $Pt(dbbpy)Cl_2$ ($2.23(4) \times 10^9$ $M^{-1}s^{-1}$, steady-state), the rate decreases with the complex having the most bulky substituents, $Pt(dbbpy)Cl_2$, being the least efficient quencher.

Similarly, variations in cross-quenching rates of a series of diphenyl platinum quencher complexes with unsubstituted and substituted phenanthroline ligands also can be understood in terms of the steric demands of the diimine ligand (Figure 5.4). However, the changes in rates are less pronounced. For example, the rates of quenching for $Pt(bpy)Ph_2$ and $Pt(dmbpy)Ph_2$ are

3.9(1) x 10^9 $M^{-1}s^{-1}$ and 2.6(1) x 10^9 $M^{-1}s^{-1}$, respectively. The rates observed for the phenanthroline counterparts of these bipyridine quenchers are almost indistinguishable, 4.48(9) x 10^9 $M^{-1}s^{-1}$ ($Pt(phen)Ph_2$) and 4.39(9) x 10^9 $M^{-1}s^{-1}$ ($Pt(dmphen)Ph_2$). Further, substitution of methyl groups in positions 3-8 on the phenanthroline ligand has little or no effect on the cross-quenching rate. Nevertheless, a significant change in rate was observed for $Pt(dpphen)Ph_2$ (2.65(6) x 10^9 $M^{-1}s^{-1}$). Much slower rates also are observed with methyl groups at the 2 and 9 positions. In fact, the observed rate of quenching for $Pt(2,9\text{-}dmphen)Ph_2$ (2.42(5) x 10^9 $M^{-1}s^{-1}$) is slower than that of $Pt(dpphen)Ph_2$.

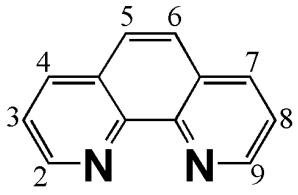

1,10-phenanthroline

A series of quenchers was examined to address the question of how increasing the steric bulk of the ancillary anionic ligands in the vicinity of the metal center influences the cross-quenching rate (Figures 5.5-5.6). More significant changes in cross-quenching rates were observed as the ancillary ligands increased in size. For example, replacing two chloride ligands with two phenyl ligands resulted in a nearly two-fold decrease in the rate of observed quenching. The effect is illustrated by comparing a series of bipyridyl quenchers with various anionic ligands shown in Figure 5.5. The most efficient quencher, $Pt(bpy)Cl_2$, has the least bulky ligands surrounding the metal center. However, the slowest rates observed are associated with quenchers having one or two mesityl ancillary ligands ($Pt(bpy)(Mes)Cl$, 0.01(4) x 10^9 $M^{-1}s^{-1}$; $Pt(bpy)(Mes)_2$, 0.14(6) x 10^9 $M^{-1}s^{-1}$; $Pt(dpphen)(Mes)_2$, 0.02(3) x 10^9 $M^{-1}s^{-1}$. In general, all of the mesityl complexes were poor quenchers of the chromophore.

VI. Electronic Effects of Bipryidine and Phenanthroline Quenchers

In its lowest excited state, Pt(tmphen)(tdt) chromophore is a powerful reductant ($E°'(Pt^{+/}*)$ =-1.6 V) and a moderate oxidant ($E°'(Pt\ *^{/-})$= 0.3 V). Consequently, electron transfer might be expected to play a dominant role in quenching. Using the collected electrochemical data for twenty of the platinum diimine quenchers (Chapter 3), the driving forces (ΔG_{ET}=-E_{ET}) for photoinduced quencher reduction and oxidation were estimated from the corresponding half-reactions of Pt(tmphen)(tdt) and the quenchers utilizing the following equations.

$$Pt^* + e^- \longrightarrow Pt^- \qquad E^{0'}(Pt^{*/-})$$

$$Q \longrightarrow Q^+ + e^- \qquad E^{0'}(Q^{+/0})$$

$$Pt^* + Q \longrightarrow Pt^- + Q^+ \qquad \mathbf{E_{ET}^{ox}} = (E^{0'}(Pt^{*/-}) + E^{0'}(Q^{+/0})$$

$$Pt^* \longrightarrow Pt^+ + e^- \qquad -E^{0'}(Pt^{*/-})$$

$$Q + e^- \longrightarrow Q^- \qquad E^{0'}(Q^{0/-})$$

$$Pt^* + Q \longrightarrow Pt^+ + Q^- \qquad \mathbf{E_{ET}^{red}} = (-E^{0'}(Pt^{*/-}) + E^{0'}(Q^{0/-})$$

Due to the weak oxidizing power of the chromophore, the driving forces for photoinduced quencher oxidation are unfavorable ($\Delta G_{ET}^{ox} \geq$ 0.2 eV), precluding the possibility of quenching by this mechanism. In contrast, photoinduced quencher reduction is favorable in most cases. To analyze the collected data, RTln(k_{cq}) was plotted as a function of ΔG_{ET}^{red} (eV) for quencher of reduction in Figure 5.7. In this analysis, RTln(k_{cq}) should exhibit a quadratic dependence on the driving force for an electron-transfer mechanism. However, for all twenty quenching rates for which driving force data is available, there is no evidence of a quadratic dependence that would be diagnostic of an outer-sphere electron-transfer quenching mechanism. At first glance, it

might appear that the series of platinum bipyridyl quenchers ((Pt(bpy)Cl_2, Pt(dmbpy)Cl_2, Pt(dbbpy)Cl_2, and Pt(bpy)$(Mes)_2$) follow expected electron-transfer behavior. However, upon further inspection, electron transfer cannot account for quenchers such as Pt(5,5'-dmbpy)Ph_2, which has a faster rate than Pt(dbbpy)Cl_2, but considerably less driving force. On the other hand, Pt(5-NO_2phen)Ph_2, with the electron-withdrawing nitro group exhibits a much faster rate (9.4(2) x 10^9 $M^{-1}s^{-1}$) than that of the unsubstituted Pt(phen)Ph_2 (4.48(9) x 10^9 $M^{-1}s^{-1}$). In fact, of all the diimine quenchers this is the fastest cross-quenching rate observed.

The dependence of k_{cq} on the electronic properties of the diimine ligand on cross-quenching was also investigated for two series of quencher complexes, Pt(bipyridyl)Cl_2 and Pt(phenanthrolinyl)Ph_2, with varying substituents on the diimine ligand (H, Me, Ph, and *t*-butyl). Though admittedly spanning a narrow range of Hammett σ values, there is no obvious correlation with this parameter (Figures 5.8-5.10). It is also notable that the rate of quenching seems to be independent of the orbital character of the lowest excited-state of the platinum diimine quencher. For example, Pt(dbbpy)Cl_2 (2.23(4) x 10^9 $M^{-1}s^{-1}$; ^{3}LF), Pt(dbbpy)$(Ph)_2$ (1.57 x 10^9 $M^{-1}s^{-1}$; ^{3}MLCT), and Pt(dbbpy)$(CN)_2$2 (2.1 x 10^9 $M^{-1}s^{-1}$; $^3\pi$-π *) (Figure 5.11) quench the emission from Pt(tmphen)(tdt) at comparable rates despite having very different lowest excited-states**.**

VII. DPPZ and Fluorinated Quenchers

The quenchers with the dppz ligand and those with the fluorinated phenyl ligands behave differently than the previously discussed quenchers. In the case of dppz, the observed rates are insensitive to the steric properties of the ancillary anionic ligands. Four quenchers were investigated: Pt(dppz)$(Ph)_2$, Pt(dppz)(3,5-dm$Ph)_2$, Pt(dppz)$(Mes)_2$, and Pt(dppz)$(C_6F_5)_2$. Surprisingly, all of these complexes show comparable cross-quenching rates

(4.3(2)-7.5(3) x 10^9 $M^{-1}s^{-1}$) that appear to be almost insensitive to the nature of the anionic ligands. Specifically, Pt(dppz)$(Ph)_2$ exhibits the slowest rate of quenching, whereas Pt(dppz)$(C_6F_5)_2$ is the most efficient quencher of this class.

In contrast, for the bipyridine and phenanthroline quenchers, those with fluorinated phenyl ligands were less effective than their non-fluorinated counterparts. Four of these complexes were investigated. The perflouro-phenyl complexes, Pt(dmpby)$(C_6F_5)_2$ and Pt(dbbpy)$(C_6F_5)_2$, had little effect (k_{cq}^{tr} ~10^7 $M^{-1}s^{-1}$) on the emission lifetime of the chromophore (Figure 5.12). In fact, these fluorinated complexes proved to be the least efficient quenchers of all the platinum(II) diimine complexes. On the other hand, Pt(dmpby)$(C_6H_3F_2)_2$ is a significantly more effective quencher (1.28(6) x 10^9 $M^{-1}s^{-1}$) (Figure 5.12), though still less effective than Pt(dmbpy)Ph_2 with the unsubstituted phenyl groups (2.6(1) x 10^9 $M^{-1}s^{-1}$).

Table 5.1. Cross-quenching rates of Pt(tmphen)(tdt) in CH_2Cl_2.

Molecule	$k_{cq}^{ss}(\sigma)$,[a] $10^9\ M^{-1}s^{-1}$	$k_{cq}^{tr}(\sigma)$,[b] $10^9\ M^{-1}s^{-1}$
$Pt(bpy)Cl_2$	8.1(1)	
$Pt(dmbpy)Cl_2$	5.8(1)	
$Pt(dpbpy)Cl_2$[c]	3.7(1)	
$Pt(dbbpy)Cl_2$	2.23(4)	2.1[c]
$Pt(dbbpy)(CN)_2$	2.2[c]	
$Pt(bpy)Ph_2$	4.36(7)	3.9(1)
$Pt(dmbpy)Ph_2$	3.36(6)	2.6(1)
$Pt(5,5'\text{-}dmbpy)Ph_2$	4.25(7)	3.5(1)
$Pt(dbbpy)Ph_2$	1.57(8)	
$Pt(dpbpy)Ph_2$	3.5(1)	
$Pt(dmbpy)(C_6F_5)_2$	0.052(9)	0.01(4)
$Pt(dbbpy)(C_6F_5)_2$	0.15(2)	0.01(4)
$Pt(dmbpy)(C_6H_3F_2)_2$	1.76(4)	1.28(6)
$Pt(phen)Ph_2$	4.48(9)	
$Pt(dmphen)Ph_2$	4.39(9)	
$Pt(tmphen)Ph_2$	4.48(8)	
$Pt(2,9\text{-}dmphen)Ph_2$	2.42(5)	
$Pt(dpphen)Ph_2$	2.65(6)	
$Pt(2,9\text{-}dmdpphen)Ph_2$	1.10(2)	1.01(4)
$Pt(bpy)(3,5dmPh)_2$	3.5(1)	3.0(2)
$Pt(5\text{-}NO_2phen)Ph_2$	10.0(1)	9.4(2)
Pt(bpy)MesCl	0.10(2)	0.01(4)
$Pt(bpy)(Mes)_2$	0.40(3)	0.14(6)
$Pt(dpphen)(Mes)_2$	0.26(2)	0.02(3)
$Pt(dppz)Ph_2$	5.5(1)	4.3(2)
$Pt(dppz)(Mes)_2$	9.3(1)	5.3(2)
$Pt(dppz)(3,5dmPh)_2$	7.6(1)	6.7(2)
$Pt(dppz)(C_6F_5)_2$	8.8(1)	7.5(3)

[a] Steady-state emission measurements. [b]Time-resolved emission measurements.
[c]Ref. 2.

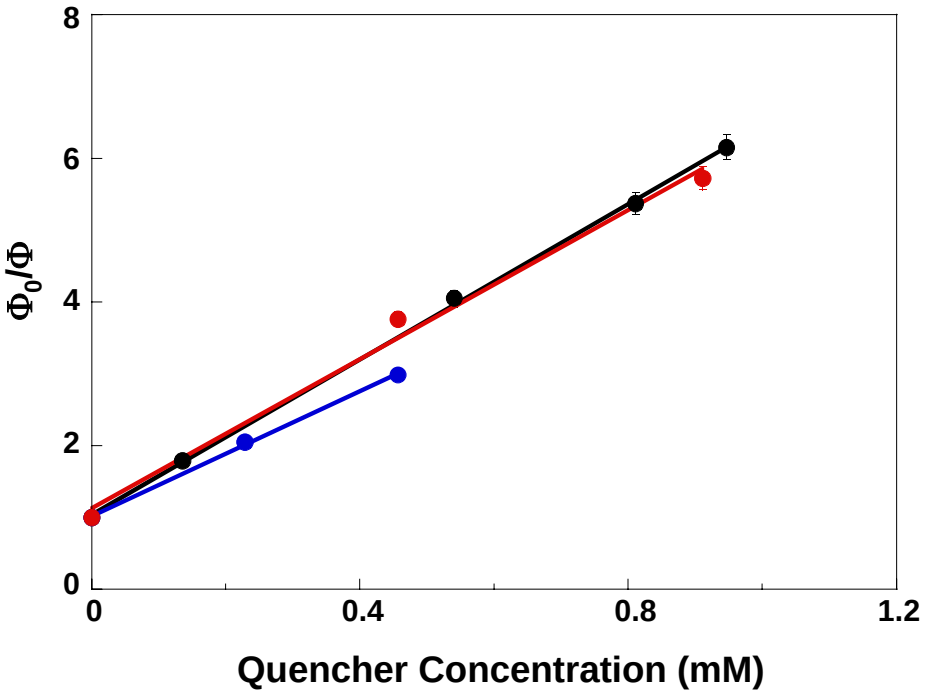

Figure 5.1. Stern-Volmer plots showing steady-state data of three different concentrations of Pt(tmphen)(tdt) with Pt(bpy)Ph_2: 30μM (red), 60 μM (black), and 110 μM (blue). Error bars represented as ± 2σ. For some points, the error bars are hidden by larger size of data points.

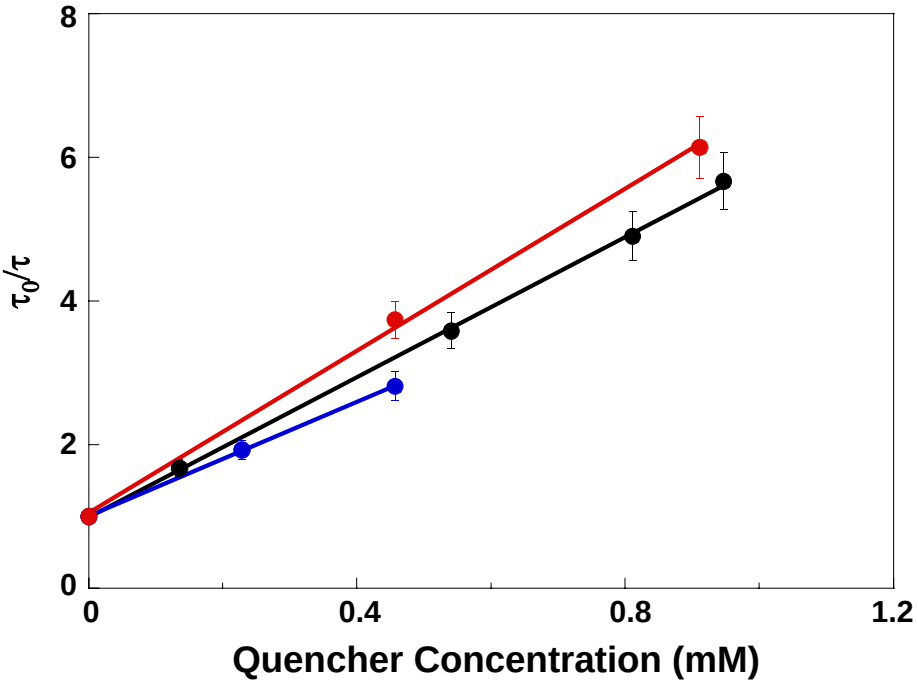

Figure 5.2. Stern-Volmer plots showing time-resolved data of three different concentrations of Pt(tmphen)(tdt) with $Pt(bpy)Ph_2$: 30μM (red), 60 μM (black), and 110 μM (blue). Error bars represented as ± 2σ. For some points, the error bars are hidden by larger size of data points.

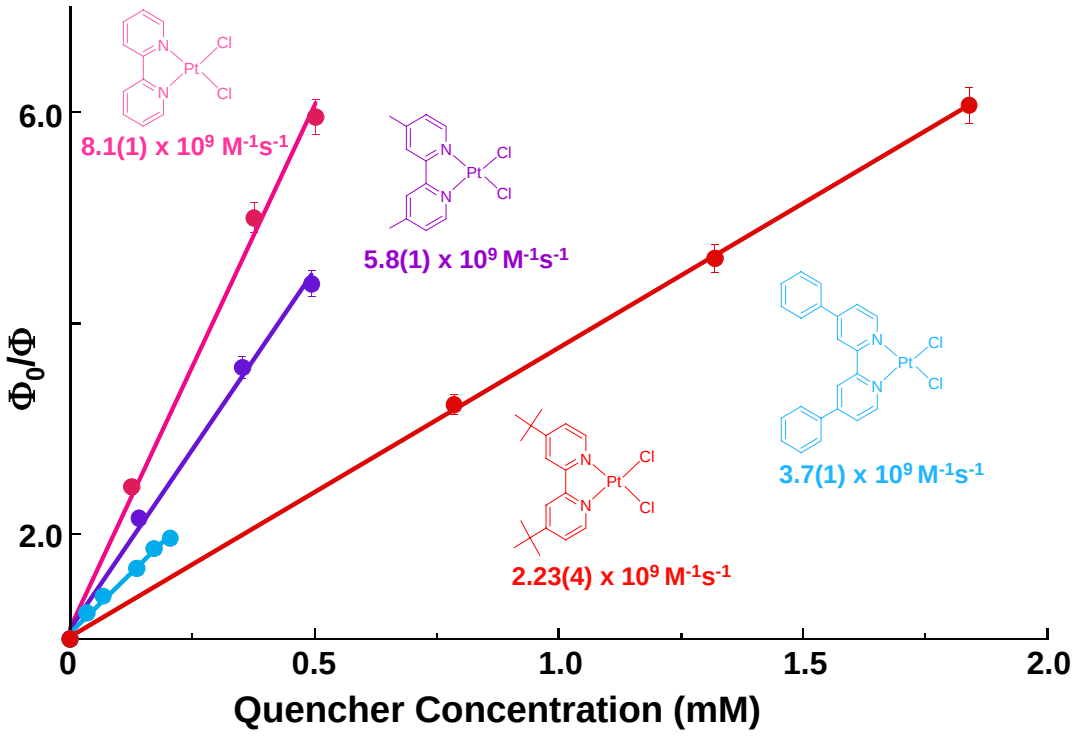

Figure 5.3. Stern-Volmer plots showing the influence of substituents on the bipyridine ligand. Error bars represented as $\pm 2\sigma$. For some points, the error bars are hidden by larger size of data points.

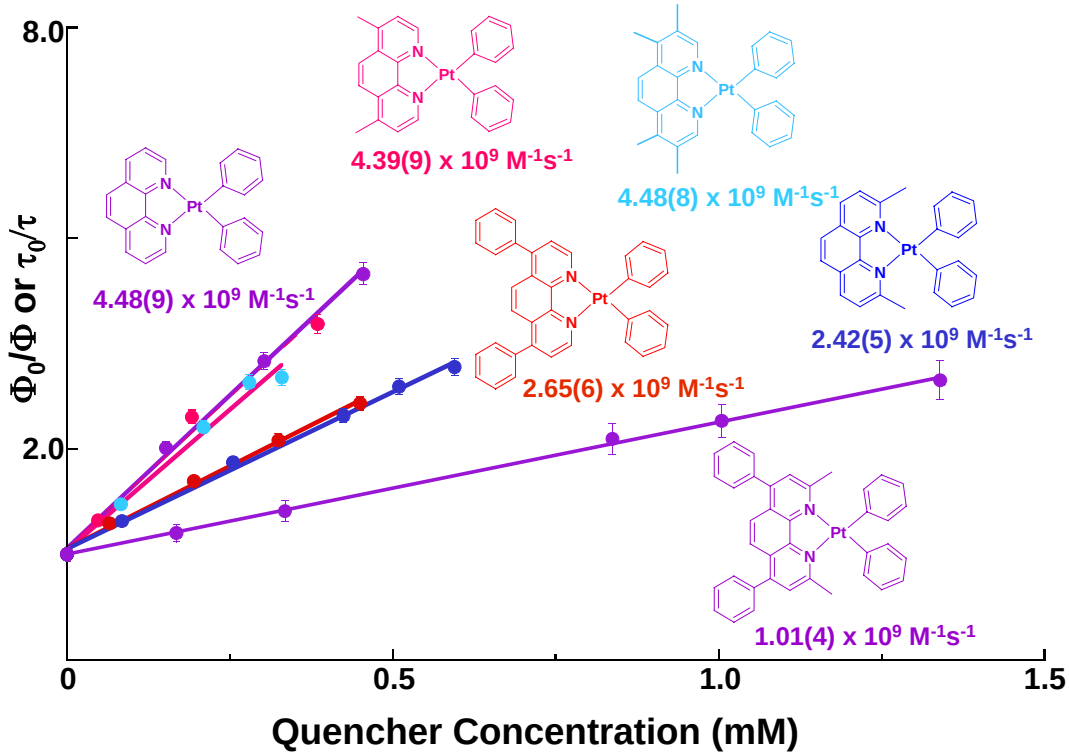

Figure 5.4. Stern-Volmer plots showing the influence of substituents on the 1,10-phenanthroline ligand. Error bars represented as ± 2σ. For some points, the error bars are hidden by larger size of data points.

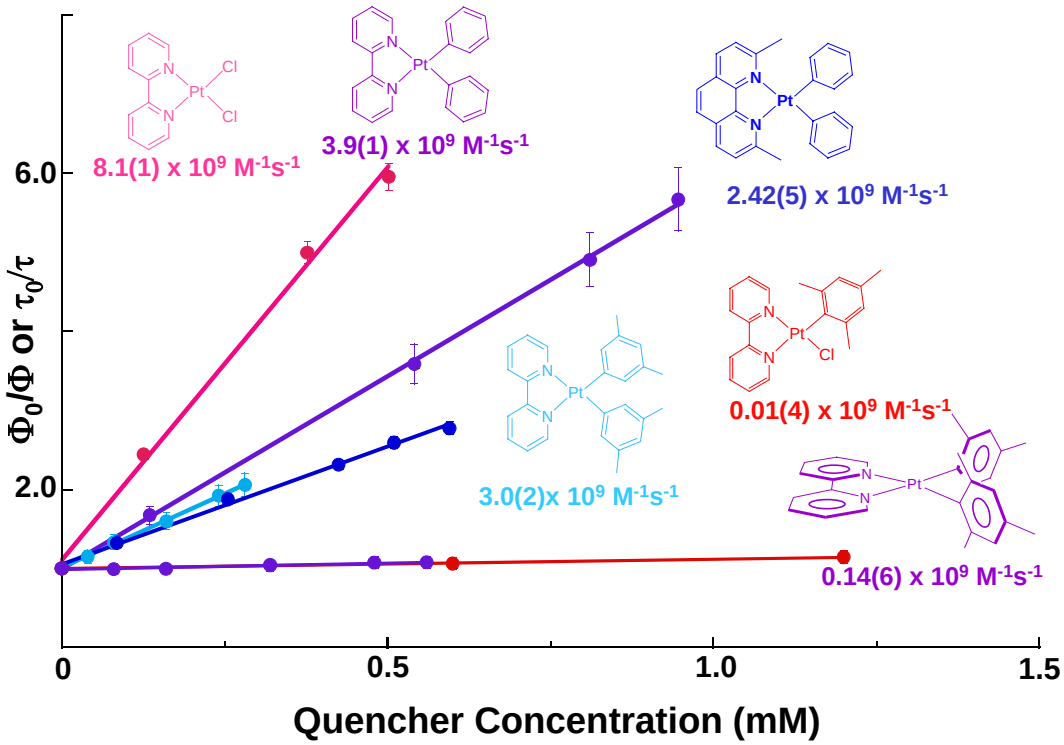

Figure 5.5. Stern-Volmer plots showing the influence of steric bulk near the Pt center. Error bars represented as ± 2σ. For some points, the error bars are hidden by larger size of data points.

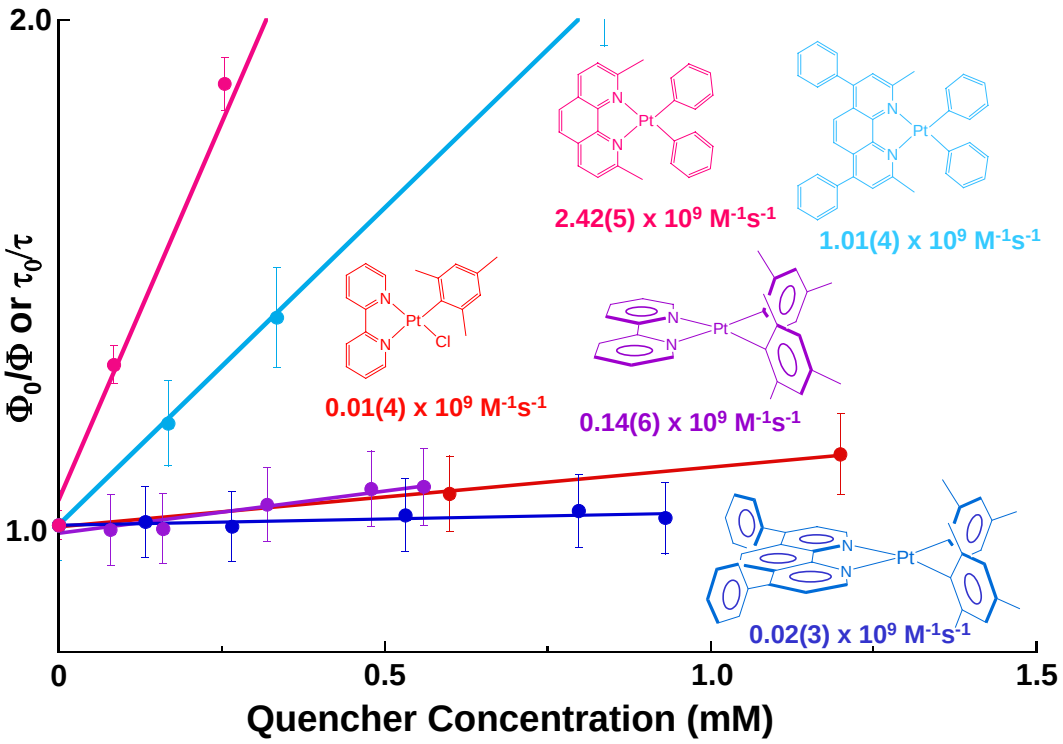

Figure 5.6. Expanded view of the influence of steric bulk near the Pt center. Error bars represented as ± 2σ.

Table 5.2. Electron-Transfer Driving Forces for Platinum(II) Diimine Quencher Complexes

Compound	**ΔG (eV)**
$Pt(bpy)Cl_2$	-0.61
$Pt(dmbpy)Cl_2$	-0.53
$Pt(dbbpy)Cl_2$	-0.47
$Pt(bpy)Ph_2$	-0.15
$Pt(dmbpy)Ph_2$	-0.05
$Pt(dbbpy)Ph_2$	-0.14
$Pt(5,5'\text{-}dmbpy)Ph_2$	-0.13
$Pt(bpy)(3,5\text{-}dmPh)_2$	-0.20
$Pt(phen)Ph_2$	-0.29
$Pt(tmphen)Ph_2$	>0
$Pt(dmdpphen)Ph_2$	-0.11
$Pt(5\text{-}NO_2phen)Ph_2$	1.14
$Pt(bpy)(Mes)_2$	-0.29
$Pt(dmbpy)(C_6F_5)_2$	-0.43
$Pt(dbbpy)\ )(C_6F_5)_2$	-0.38
$Pt(dmbpy)(C_6H_3F_2)_2$	-0.26
$Pt(dppz)(C_6F_5)_2$	-0.85
$Pt(dppz)Ph_2$	-0.68
$Pt(dppz)(Mes)_2$	0.67
$Pt(dppz)(3,5\text{-}dmPh)_2$	-0.71

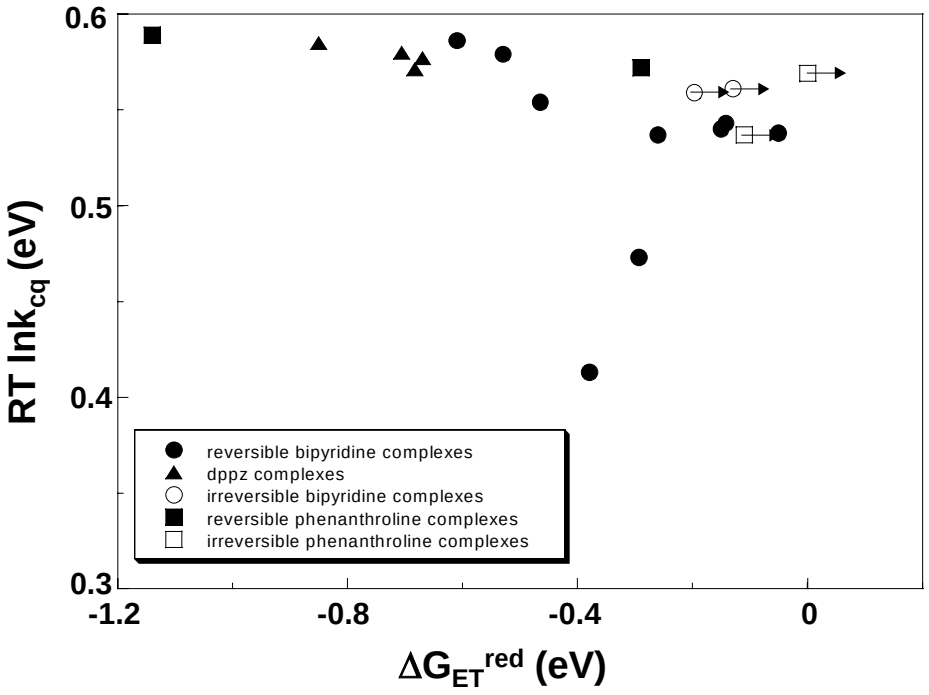

Figure 5.7. Cross-quenching rate dependence on electron-transfer driving force ΔG_{ET}^{red} for photoinduced reduction of the quencher. Arrows indicate irreversible complexes.

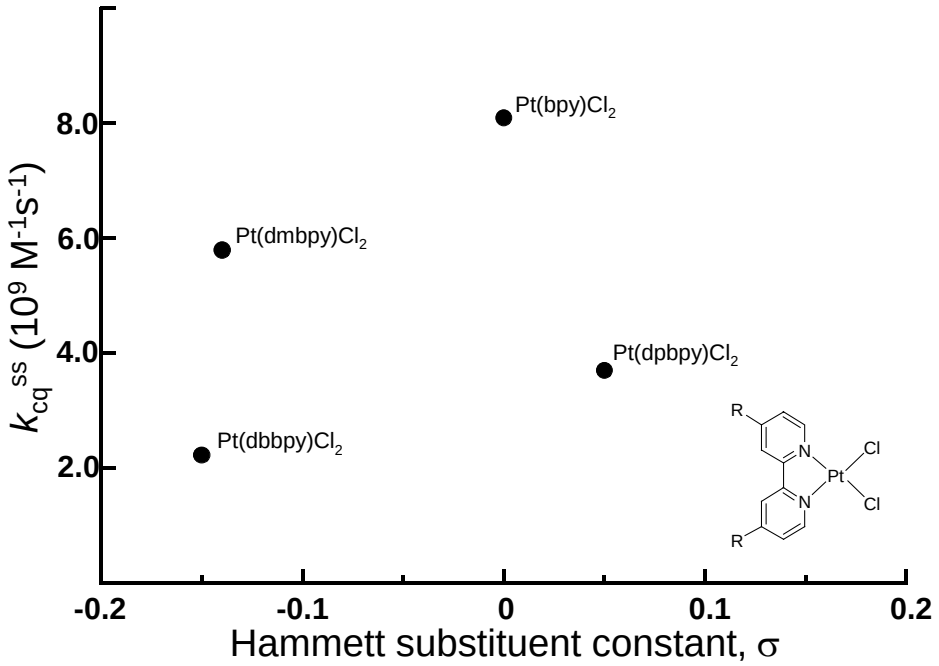

Figure 5.8. Plot illustrating the effect of various bipyridine for Pt(bipyridine)Cl_2 complexes on the cross-quenching rate. The x-axis is the Hammett substituent constants for the diimine substituents.

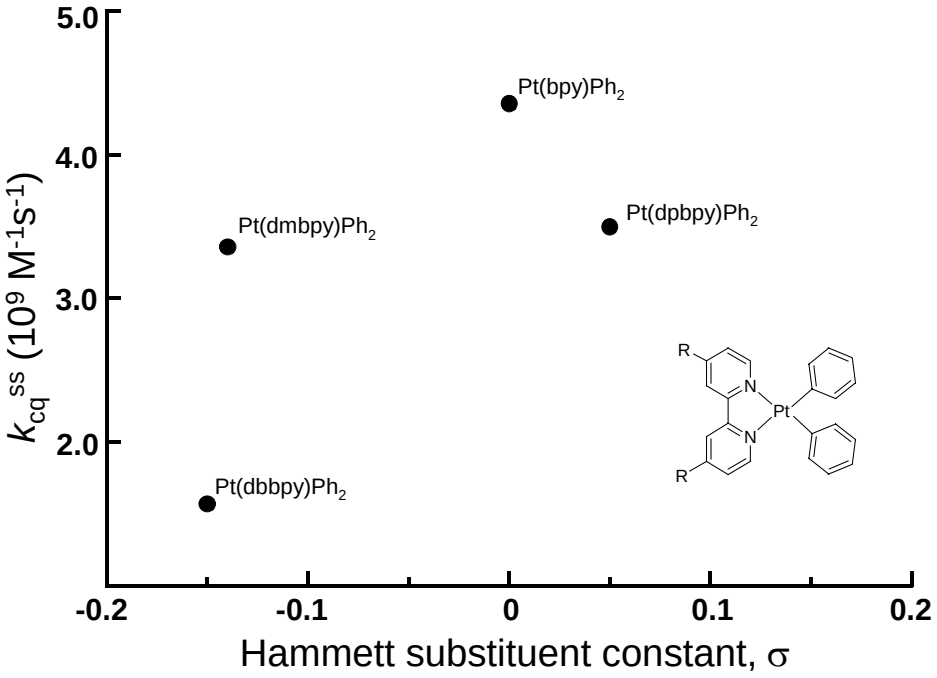

Figure 5.9. Plot illustrating the effect of various bipyridine substituents for Pt(bipyridine)Ph_2 complexes on the cross-quenching rate. The x-axis is the Hammett substituent constants for the diimine substituents.

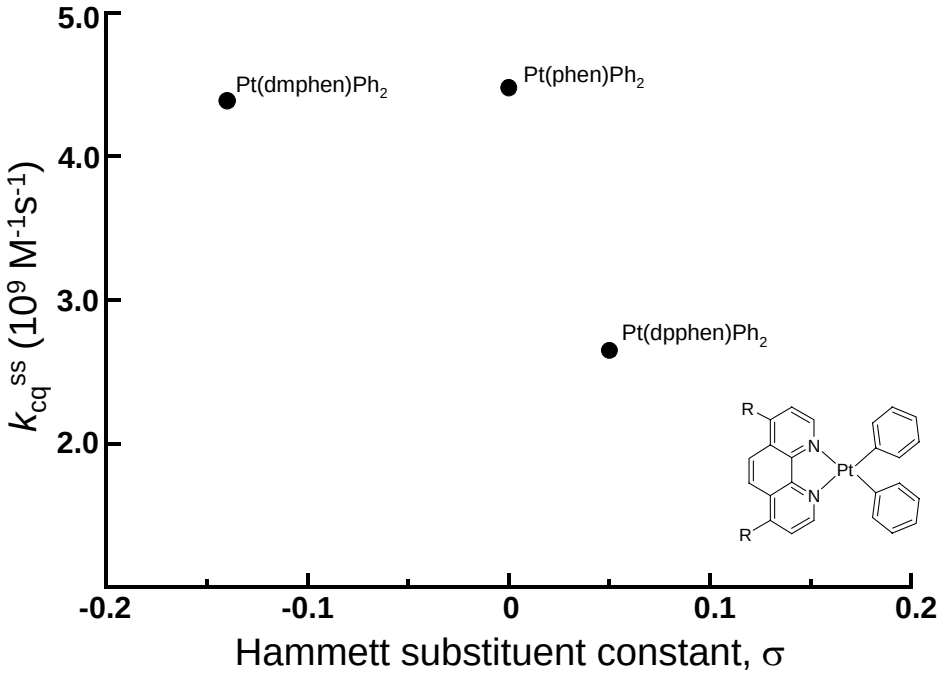

Figure 5.10. Plot illustrating the effect of various phenanthroline substituents for Pt(phenanthroline)Ph_2 complexes on the cross-quenching rate. The x-axis is the Hammett substituent constants for the diimine substituents.

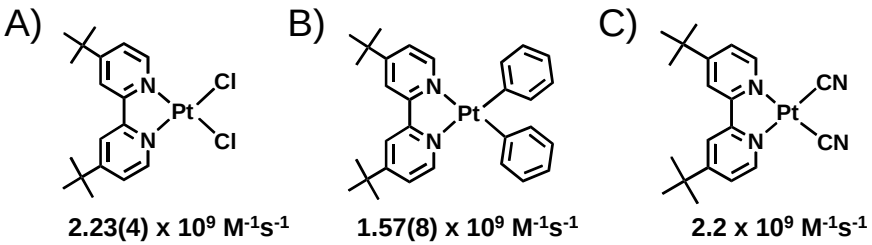

Figure 5.11. Three platinum(II) diimine quencher complexes with different lowest energy excited states; A) ligand field, B) MLCT, and C) π-π^*.

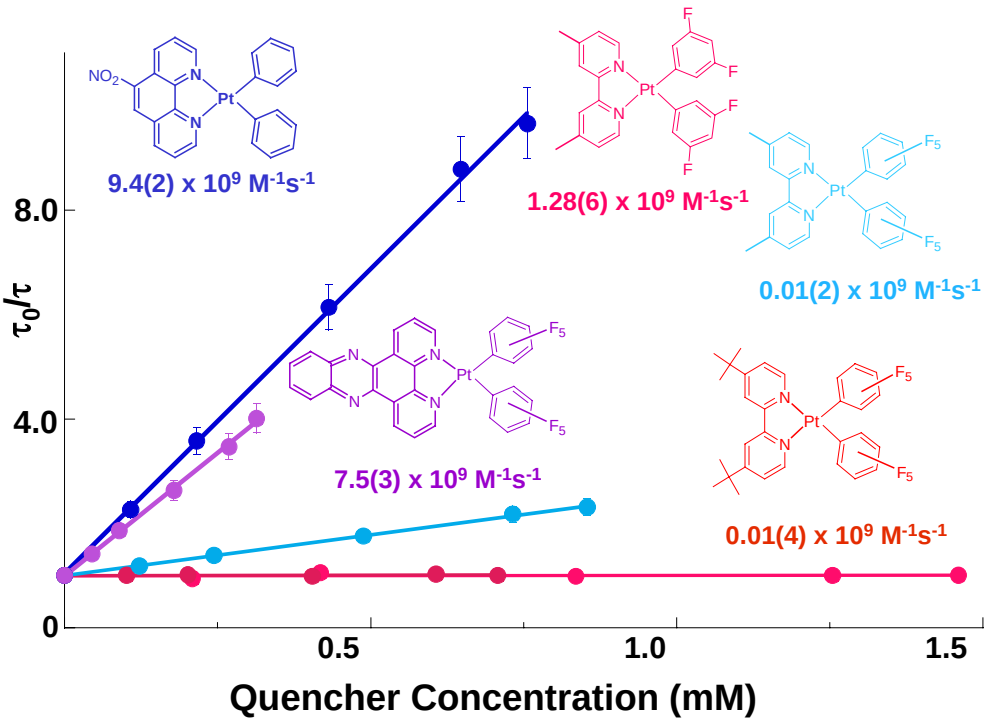

Figure 5.12. Stern-Volmer plots showing the influence of electron-withdrawing groups on cross-quenching. Error bars represented as ± 2σ. For some points, the error bars are hidden by larger size of data points.

References

1. Demas, J. N. *Excited State Lifetime Measurements*; Academic Press: New York, 1983.

2. Connick, W. B.; Geiger, D.; Eisenberg, R. *Inorg. Chem.* **1999**, *38*, 3264-3265.

Chapter 6
Quenching Mechanism

I. Introduction

Since the observation of self-quenching by Che and coworkers[1] in 1989, there has been growing interest in understanding the stabilizing intermolecular interactions involved in excimer formation. Toward this goal, we have investigated how the steric and electronic properties of the quencher influence the cross-quenching reaction. Throughout these studies, we have considered several possible quenching mechanisms, including energy transfer, outer-sphere electron transfer and exciplex formation. From a series of experiments and data analyses discussed in Chapters 4 and 5, it was concluded that, for nearly all investigated cross-quenching reactions, energy- and electron-transfer quenching did not play a significant role. In addition, only platinum(II) diimine complexes proved to be effective quenchers, resulting in cross-quenching rates on the same order of magnitude as those of self-quenching reactions, as might be expected for a similar quenching mechanism. These observations lead to the conclusion that the cross-quenching reactions with the platinum(II) diimine quenchers (Q) most likely involve formation of an exciplex (MQ*), in analogy to that proposed for self-quenching reactions:

$$M^* + Q \rightarrow MQ^* \rightarrow M + Q$$

A closer analysis of these data can be expected to provide insight into the interactions stabilizing the exciplex. In interpreting these results, we have considered three logical and plausible modes of association, namely via (*i*) diimine-diimine, (*ii*) metal-metal (*iii*) or a combination of both interactions. In fact, a simplified molecular orbital model indicates that all three modes of association are favorable, though it is not obvious that one is necessarily more favorable than the other two. At first glance, it is tempting to conclude that a combination of

these interactions (case *iii*) stabilizes the exciplex, since only quenchers with both a platinum center and a diimine ligand resulted in rapid quenching. However, as we will show in this chapter, a close examination of the data supports the view that metal-metal interactions are most important in stabilizing the exciplex.

The evidence begins with the observation that steric bulk on the diimine and ancillary ligands of the quencher strongly influence the rate of quenching for the bipyridine and phenanthroline quenchers. Interestingly, steric bulk near the metal center has the greatest impact. On the other hand, several sterically unhindered quenchers with ancillary ligands having relatively electron-withdrawing groups are found to be very ineffective quenchers, suggesting an electronic effect on exciplex formation. Because the ancillary ligands are directly bonded to the platinum center, rather than the diimine ligand, their electronic properties are expected to have a significantly greater impact on metal-metal interactions than on diimine-diimine interactions. For this reason, we examine the charge-transfer interactions believed to favor association of ground-state complexes, and extend this analysis to exciplexes. This analysis supports the view that decreased σ-donor strength of the ancillary ligand destabilizes the exciplex, resulting in the observed slower quenching. We close this chapter by contrasting these results with those obtained for platinum(II) dppz quencher complexes. The quenching behavior is quite different for the latter complexes, suggesting a different mechanism.

II. Bipyridine and Phenanthroline Quenchers

According to the accumulated data presented in Chapter 5, energy transfer can be dismissed as a possible quenching mechanism for all quenchers due to the careful selection criteria of quenchers described in Chapter 4. Each of the chosen quenchers has a higher lying lowest excited state ($E_{0,0}$ >2.1 eV) than that of the chromophore, making energy

transfer quenching endergonic. Similarly, outer-sphere electron transfer can be excluded as a possible mechanism for bipyridine and phenanthroline quenchers (except for $Pt(5\text{-}NO_2phen)Ph_2$ discussed later in the chapter) based on the driving force for electron-transfer as determined from electrochemical measurements. As discussed in Chapter 5, no direct correlation between driving force and cross-quenching rates was apparent for the bipyridine and phenanthroline quenchers. However, the theory of outer-sphere electron transfer predicts a parabolic dependence of the electron-transfer rate on driving force for reactions that have similar reorganization energies and electronic factors. The preceding considerations lead to the conclusion that the quenching mechanism for the bipyridine and phenanthroline quenchers most likely involves exciplex formation. However, the question still remains, namely, what are the interactions stabilizing the exciplex?

To gain further insight into the stabilizing interactions, qualitative molecular orbital diagrams for three types of excimers (Chapter 2) are illustrated in Figure 6.1. Each diagram represents the energetic benefits for a particular mode of association. The first diagram illustrates an excited state analogous to that of organic aromatic excimers. The other two diagrams are analogous to an excited state having $d\sigma^*(Pt)\rightarrow\pi^*$(diimine) character as observed for emissive stacked platinum(II) diimine complexes.[2,3] For each excited dimer a formal bond order (B.O.) can be calculated; diimine-diimine B.O.=1, Pt-Pt B.O.=0.5, and combination B.O.=1. From these values, it can be seen that association of the metal complexes is favored in the excited state over the ground state (B.O.=0), though relative bond orders do not necessarily reflect the relative strengths of these interactions, and it is not obvious that one is more favorable than the others. On the other hand, these diagrams suggest very different orbital character for each excited dimer, which could be distinguished in the excimer emission spectra. However, as

discussed in Chapter 2, the evidence is inconclusive. Also, no emission data are available for the exciplexes formed in cross-quenching reactions since there are no reported cases of exciplex emission from platinum(II) diimine complexes. For the Pt(tmphen)(tdt) chromophore this can be attributed to the low energy of the monomer emission, implying that the exciplex emission would lie at even lower energy, to the red of 800 nm, where most conventional mutlialkali photocathode photomultiplier tubes are relatively insensitive. Thus, while the molecular orbital analysis suggests all three modes of association are favorable, it does not definitively point to one over the others. For this reason, we turn our attention to the results of the cross-quenching experiments.

In the case of the bipyridine and phenanthroline quenchers, accumulated evidence suggests that steric bulk around the metal center has a much greater effect on the rate of quenching than steric bulk on the diimine. This conclusion rests on the premise that steric bulk near the point(s) of closest contact between the chromophore and quencher in the exciplex will destabilize the exciplex and reduce the observed rate of quenching. This reasonable notion is in keeping with principles of chemical reactivity and supported by studies of other exciplex formation reactions.[4-6] For example, as previously, discussed in Chapter 5, Pt(2,9-dmphen)Ph_2 (2.42(5) x 10^9 $M^{-1}s^{-1}$) is a less efficient quencher than Pt(phen)Ph_2 (4.48(9) x 10^9 $M^{-1}s^{-1}$) and Pt(4,7-dmphen)Ph_2 (4.39(9) x 10^9 $M^{-1}s^{-1}$) (Figure 6.2). Negligible change in the quenching rate is observed as methyl groups are added to the periphery of phenanthroline, as for Pt(4,7-dmphen)Ph_2. However, a much more significant change is noted as the methyl groups are placed in positions (Pt(2,9-dmphen)Ph_2) near the platinum metal center. The crystal structure of Pt(2,9-dmphen)Ph_2 indicates that steric demands of the methyl groups result in large distortions. The dihedral angle formed by the best fit plane for the diimine N=C-C=N atoms and the plane

defined by the platinum center and two bonded carbon atoms is 31°,[7] as compared to 0° expected for a planar complex. This distortion is anticipated to inhibit intermolecular diimine-diimine interactions as well as Pt-Pt interactions. In addition, these methyl groups are expected to further protect the platinum center by restricting rotation of the phenyl ligands about the Pt-C bonds. Also, of the bipyridine and phenanthroline quenchers, the slowest rates (0.02(3)-0.1(6) x 10^9 $M^{-1}s^{-1}$) were observed for complexes containing mesityl ligands. From crystal structures[7-11] and electrochemical studies[7-9,12,13] of these and similar complexes, it can be inferred that the mesityl ligands sterically shield the metal center from external attack in the axial position. This shielding is evident in the electrochemistry of $Pt(bpy)(Mes)_2$, as discussed in Chapters 3.

It is noteworthy that steric factors influence the formation of exciplexes by other inorganic and organic chromophores.[4-6] However, the steric dependence of the cross-quenching rates discussed here is modest in comparison. For example, the emission from anthracene is quenched by dimethylaniline in cyclohexane through a charge-transfer interaction. Increasing phenyl substitution on the anthracene decreases the quenching rate by three orders of magnitude.[4] The rate is dependent on the degree and position of substitution. For example, a greater decrease is reported for 1,4,5,8-tetraphenylanthracene (k_q = 0.02 x 10^8 $M^{-1}s^{-1}$) than for 1,4-diphenylanthracene (k_q = 8.5 x 10^8 $M^{-1}s^{-1}$). The fact that the rate is much slower for the 9,10-disubstituted anthracene (k_q = 0.5 x 10^8 $M^{-1}s^{-1}$) than for the 1,4-disubstituted anthracene is consistent with the notion that the central ring is involved in the charge-transfer interaction. Significant changes in rate are also observed for quenching of the emission from

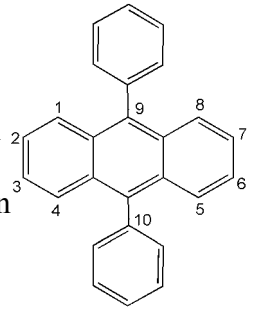

9,10-diphenyl anthracene

$Cu(2,9\text{-dmphen})_2^+$ by substituted pyridines binding to a vacant coordination site of the copper center. For example, the quenching rate for 2,6-dimethylpyridine ($k_q < 10^6$ $M^{-1}s^{-1}$) of the copper complex is more than three orders of magnitude slower than that of pyridine ($k_q = 10^9$ $M^{-1}s^{-1}$).[5,6]

The weaker steric dependence of the cross-quenching rates as compared to the preceding examples may indicate longer intermolecular interactions for the platinum diimine systems. Indeed, the changes in rate with increasing steric bulk near the metal center are more dramatic than the changes associated with increasing steric bulk of the diimine ligand, as expected for a metal-metal interaction. From the accumulated data, we conclude that metal-metal interactions play an important role in association. In the next section we examine the electronic factors that should favor metal-metal interaction and compare this model to the experimental results.

III. Electronic Factors Influencing Metal-Metal Association

Up until now, we have focused our attention on the effect of sterics on quenching. In this section we examine how the electronic properties of the ligands influence exciplex formation. Our approach is dictated by the observation that sterically unhindered quenchers with ancillary ligands having electron-withdrawing groups are found to be very ineffective quenchers. Because the ancillary ligands are directly bonded to the platinum center, rather than the diimine ligand, their electronic properties are expected to have a significantly greater impact on metal-metal interactions than on diimine-diimine interactions. In support of this notion, we previously found (Chapter 3) that switching between various anionic ancillary ligands (Cl^-, Ph^-, Mes^-, $C_6F_5^-$) had a relatively small effect (0.48 V) on diimine ligand reduction potential and that the observed rates did not seem to correlate with electron-transfer driving force. For this reason, we begin by examining the charge-transfer interactions believed to favor ground-state association and how the electronic properties of the ligands will influence these interactions. The approach converges

on the molecular orbital picture developed previously, but also offers some important new insights.

Aullón and Alvarez[14] suggest there are three important interactions involved in non-covalent metal-metal association of complexes with π-acidic ligands such as a diimine group (Figure 6.3). These are (1) four-electron repulsion between the d_{z^2} (Pt) orbitals, (2) the attractive donor-acceptor interaction between the d_{z^2}(Pt) orbital of one metal and p_z(Pt) orbital of the other, (3) the metal-mediated donor-acceptor interaction between the d_{z^2}(Pt) orbital of one metal and the empty π* orbital of the π-acidic ligand(s) of the other complex (Figure 6.3).[14] The reason the charge-transfer interactions (1) and (2) stabilize the associated complexes can be understood as follows. These favorable charge-transfer interactions correspond to excited states, whereby charge is transferred from one complex to the other, resulting in a stable charge-transfer complex represented by the wavefunction Ψ_{CT}. On the other hand, the actual associated complexes are not in an excited state. They form a ground-state complex, which in the absence of any stabilizing force is described by two monomer wavefunctions represented by $\Psi_{(Pt)}$. However, this ground-state wavefunction will mix with the excited states resulting in a small fraction (α) of stabilizing charge-transfer character in the wavefunction (Ψ) describing the dimer:

$$\Psi = 2\Psi_{(Pt)} + \alpha\Psi_{CT}$$

As the energy gap between a charge-transfer state and the ground state decreases, the amount of mixing (*i.e.,* the magnitude of α) will increase, further stabilizing the dimer. Thus, the attractive interaction (3) is largely responsible for the tendency of platinum(II) complexes with π-acidic ligands to stack *via* metal-metal interactions in the solid state and fluid solution.

The preceding description indicates that increased π-acceptor character of the ligands will increase the strength of the stabilizing charge-transfer interaction (3), as well as decrease

electronic repulsions between the metal centers because of removal of electron density from the metal center. Both results favor metal-metal association in the ground state. Circumstantial evidence supports this view. For example, comparing $PtCl_4^{2-}$ and $[Pt(CN)_4]^{2-}$ salts, the complex with the more π-acidic ligands, $[Pt(CN)_4]^{2-}$, exhibits the stronger tendency to stack in the solid-state and fluid solution.[15,16]

Gray and coworkers[17] arrived at similar qualitative conclusions concerning ligand π-acidity in their investigation of solid-state structures of platinum(II) diimine complexes. However, in addition, they argued that strong σ-donor ligands tend to destabilize the d_{z^2}(Pt) orbital, enhancing orbital overlap and the interactions between adjacent complexes.[17] This suggestion is consistent with accumulated data and is at least partially supported by the Aullón and Alvarez[14] model, since destabilization of the d_{z^2}(Pt) level strengthens the favorable charge-transfer interactions (2) and (3). Aullón and Alvarez also have suggested that increased σ-donation actually decreases the repulsive interaction (1) because of increased platinum s(Pt) + d_{z^2}(Pt) hybridization. Nevertheless, these same authors conclude that, in contradiction to the qualitative arguments of Gray and coworkers[17] and empirical evidence, increased σ-donation has little impact on the strength of the interaction between the two complexes.

The preceding considerations readily extend to the description of the exciplex, which is expected to have increased excited-state charge-transfer character since it is in an excited state. It is even conceivable that the exciplex is best described as having d_{z^2}(Pt)→π*(diimine) charge-transfer character (interaction (3)), as suggested by Figure 6.1b and 6.1c. Based on relative redox potentials we would anticipate transfer of charge from the Pt(tmphen)(tdt) complex to the quencher complex to be the most favorable of these interactions. Therefore, we anticipate increased ligand π-acidity will strengthen this charge-transfer character and stabilize

the exciplex. As noted by Gray and coworkers for ground-state complexes, increased ligand σ-donation can be expected to further stabilize the exciplex. Moreover, promotion of an electron from the d_{z^2}(Pt) orbital to a ligand-centered orbital will reduce electron-electron repulsion between the metal centers (interaction (1)).

The impact of the stabilization of the exciplex by π-acceptor and σ-donor ligands can be understood in terms of the quenching mechanism developed in Chapter 5 and illustrated in Figure 6.3, whereby the exciplex can relax to give the ground-state complex and quencher, or alternatively, the excited chromophore and ground-state quencher. The latter reaction corresponds to the reverse of the exciplex formation reaction and will become less favorable with increasing exciplex stability. Thus, stabilization of the exciplex will increase the ratio of k_Q/k_B, thereby shifting the (M*+Q)/MQ* equilibrium toward the exciplex and accelerating the apparent rate of cross-quenching. In summary, quenchers with strong π-acceptor and σ-donor ligands can be expected to favor rapid quenching relative to those with weaker π-acceptor and σ-donor ligands.

Generally speaking, the accumulated data are consistent with these predictions. For example, the ligands of inefficient quencher complexes such as $Pt(acac)_2$ and $Pt(dppe)(C_2H_4S_2)$ are relatively poor π-acids. In contrast, the diimine ligands of the efficient platinum(II) diimine quencher complexes are strong π-acceptors with low-lying π* levels. Carrying this argument further, one would expect these electronic properties and the corresponding stabilization of the exciplex to be reflected in the relative cross-quenching rates for the series of quencher complexes with diimine ligands. In Chapter 3, the relative energies of the diimine π* orbitals of these complexes were estimated by measuring their reduction potentials. However, as noted in Chapter 5, we find no general correlation between electron-transfer driving force (which is

directly related to the π* orbital energy) and the cross-quenching rate. Thus, it seems that electronic effects are obscured by steric effects in most cases. However, when we examine quenching reactions with platinum(II) diimine quenchers having relatively electron-withdrawing ancillary ligands, we find quenching is very inefficient. In the next section, we account for these observations in terms of the preceding electronic considerations.

IV. Quenchers with Electron-Withdrawing Groups

The diimine perfluoro phenyl complexes prove to be the least efficient quenchers of all the platinum diimine complexes (~10^7 $M^{-1}s^{-1}$). This result is quite remarkable since Pt(diimine)Ph_2 quenchers are by contrast very efficient (1.6- 4.5 x 10^9 $M^{-1}s^{-1}$). Clearly, steric effects cannot explain these differences. If we consider the van der Waals radii of H (120-145 pm), F (150-160 pm), and CH_3 (200 pm), we see that the radius of fluorine is intermediate to the other two groups, suggesting fluorine groups on the quencher complex should interfere with quenching more than hydrogen but less than methyl. However, when examining Pt(bpy)(3,5-dmPh)$_2$ (3.0(2) x 10^9 $M^{-1}s^{-1}$) compared to Pt(bpy)Ph_2 (3.9(1) x 10^9 $M^{-1}s^{-1}$), only an insignificant change in rate is observed. On the other hand, when the phenyl ring is substituted with fluorine atoms in the same 3 and 5 positions a much slower rate is observed (1.28(6) x 10^9 $M^{-1}s^{-1}$). These observations together suggest that we are observing factors other than steric effects, and we turn to the previously discussed electronic factors to understand these results. The strong σ-donor properties of the phenyl ligands are attenuated in the fluorinated analogs by inductive effects, resulting in weaker σ-donation. Weaker σ-donation effectively reduces electron density at the metal center and stabilizes the d levels, disfavoring the charge-transfer interactions (2) and (3) previously discussed (Figure 6.3). This will disfavor exciplex formation and result in less efficient quenching. In keeping with this interpretation, the difluorinated

complex, Pt(dmbpy)($C_6H_3F_2$)$_2$, exhibits a quenching rate (1.28(6) x 10^9 $M^{-1}s^{-1}$), intermediate to those of the perfluorinated complexes (~10^7 $M^{-1}s^{-1}$) and that of Pt(dmbpy)Ph_2 (2.6(1) x 10^9 $M^{-1}s^{-1}$). The *meta*-substituted difluorophenyl ligands are better σ-donors than perfluorophenyl ligands, but slightly worse σ-donors than unsubstituted phenyl. Nevertheless, it is evident the impact of fluorine substituents at the *meta* positions is small. This result is consistent with σ-donation being dominated by resonance effects, since field effects largely dominate with *meta* substituents.

The influence of weaker σ-donation can be observed not only in the variations in quenching rates, but also in the electrochemical and absorption data of these complexes. For example, the complex with the weakest σ-donor ligands, Pt(dmbpy)(C_6F_5)$_2$ (-1.37 V) is more easily reduced than either the Pt(dmbpy)($C_6H_3F_2$)$_2$ (-1.54 V) or Pt(dmbpy)Ph_2 (-1.75 V). In the absorption spectroscopy, the various σ-donor properties also can be seen. The maximum of the metal-to-diimine charge transfer band shifts to longer wavelength with increasing σ-donor strength: (Pt(dmbpy)(C_6F_5)$_2$ (369 nm), Pt(dmbpy)($C_6H_3F_2$)$_2$ (395 nm), and Pt(dmbpy)Ph_2 (424 nm). However, it must be stressed, as noted in Chapter 5, there is no correlation between diimine reduction potential and quenching rate. In fact, the cathodic shift of the reduction potential with increasing fluorination should strengthen favorable charge-transfer interactions such as (3). However, the rates contradict this view, reflecting the influence of the ancillary ligands on the metal center and supporting the view that metal-metal interaction is most important for stabilizing the excimer. Similarly, as noted in Chapter 5, there is no general correlation between MLCT band maximum and quenching rate. Figure 6.3 illustrates this point further by showing the cross-quenching rates as a function of the maximum MLCT energy of the quenchers. No correlation is evident. Thus, the observed quenching data are consistent with an

inner-sphere mechanism that involves interactions such as those discussed in the previous section, rather than just outer-sphere charge transfer.

Conclusive evidence of electronic effects on quenching caused by substitutents on the diimine ligand has been challenging to obtain. As mentioned in Chapter 5, the fastest quenching rate (9.4(2) x 10^9 $M^{-1}s^{-1}$) was observed for Pt(5-NO_2phen)Ph_2, which has an electron-withdrawing group attached to the diimine ligand. Though the rapid quenching is consistent with increased diimine π-acidity, these results are inconclusive because of the possibility of quenching by electron transfer (Chapter 5). The driving force for outer-sphere electron-transfer quenching to give oxidized chromophore and reduced Pt(5-NO_2phen)Ph_2 is estimated at -1.14 V vs Ag/AgCl. Electron-transfer quenching of excited Pt(tmphen)(tdt) in the presence of nitrobenzene[18] (Table 6.1) has a similar driving force (-1.30 V vs Ag/AgCl or -1.10 vs NHE) and occurs at a comparable rate (7.9 x 10^9 $M^{-1}s^{-1}$) (Figure 6.4). Thus, a significant component of the quenching observed with Pt(5-NO_2phen)Ph_2 may involve electron transfer.

V. Dppz Quenchers

The platinum(II) quencher complexes with dppz ligands behave differently than the other platinum(II) diimine quenchers and we find no evidence of steric effects associated with the ancillary ligands. For example, surprisingly, all of the dppz platinum complexes show comparable cross-quenching rates (4.3(2)-7.5(3) x 10^9 $M^{-1}s^{-1}$) that appear to be almost independent of the nature of the anionic ligands. As discussed in Chapter 4, energy transfer can be ruled out as a possible mechanism due to the relatively high energy lowest excited-state of the dppz quenchers relative to the chromophore. From inspection of the electrochemical data for these complexes, it seems unlikely that outer-sphere electron transfer is significantly contributing to quenching, because driving forces for the dppz quenchers (ΔG_{ET} = -0.68-0.71 V) (Figure 6.5)

are lower than those associated with nitrobenzene electron-transfer quenchers investigated by Cummings and Eisenberg (-1.15-1.75 V).[18] From a crude extrapolation of the Cummings and Eisenberg results, the dppz quenchers with their fairly small driving forces are predicted to undergo electron-transfer quenching of the excited Pt(tmphen)(tdt) at a rate of ~8.9 x 10^7 $M^{-1}s^{-1}$. The observed rates are much faster, suggesting outer-sphere electron-transfer quenching does not make a significant contribution to the observed quenching.

It should be noted that the extended aromatic system of the dppz ligand tends to favor π-stacking in the crystal structures of platinum complexes such as Pt(dppz)$(Mes)_2$.[10] Thus, an alternative interpretation of the quenching data involves formation of an exciplex stabilized by diimine-diimine interactions, associated with stacking of the phenazine "tails." It is amazing that with the bulky mesityl ligands around the metal center, Pt(dppz)$(Mes)_2$ (5.3(2) x 10^9 $M^{-1}s^{-1}$), the rate is actually faster than that observed for the less sterically hindered complexes such as in Pt(dppz)Ph_2 (4.3(2) x 10^9 $M^{-1}s^{-1}$). It seems reasonable to expect this apparent tendency to stack in the ground state to be manifested in fluid solution. In fact, static quenching is observed for these complexes, as evidenced by the significant difference in the steady-state and time-resolved quenching rates. In the most extreme case, Pt(dppz)$(Mes)_2$, the difference is 50% (k_{cq}^{ss}=9.3(1) x 10^9 $M^{-1}s^{-1}$ and k_{cq}^{tr}=5.3(2) x 10^9 $M^{-1}s^{-1}$), corresponding to a ground-state association constant of ~780 M^{-1}. In summary, the data suggest quenching of the chromophore by dppz quenchers occurs by a different mechanism than that of the bipyridine and phenanthroline quenchers.

VI. Conclusion

Before this investigation of cross-quenching reactions with the Pt(tmphen)(tdt) chromophore, little information was available on the mechanism of self-quenching of

platinum(II) diimine complexes. As mentioned previously, three interactions were proposed, but no definitive evidence was available to support one particular association over the other. Consequently, cross-quenching reactions were undertaken to elucidate the mechanism of quenching, since initial studies suggested comparable rates to those of self-quenching. From these investigations, we now have a deeper understanding of the mechanism of quenching and the associated intermolecular interactions. Most importantly, we have learned that cross-quenching reactions of Pt(tmphen)(tdt) can be controlled by variation of the steric and electronic properties of the quencher.

At the beginning of our studies, we found that rates of cross-quenching reactions are only comparable to those of self-quenching when other platinum(II) diimine complexes are used as quenchers. Quenchers lacking either a platinum metal center or diimine exhibited negligible effect on the emission intensity of the chromophore. Subsequently, a series of platinum(II) diimine complexes were investigated as possible quenchers. These quenchers were divided into three classes based on their ligands: complexes with bipyridine and phenanthroline ligands, complexes with electron-withdrawing ligands, and complexes with the dppz ligand. Several mechanisms of quenching have been considered, including energy transfer, outer-sphere electron transfer, and exciplex formation. From the results detailed in Chapters 4 and 5, we concluded that quenching of the emission from Pt(tmphen)(tdt) chromophore by other platinum(II) diimine complexes occurs most likely by an inner-sphere process, such as exciplex formation.

The accumulated data from the three classes of quencher complexes suggests metal-metal interaction plays an important role in stabilizing the exciplex. Some of the slowest quenching rates were observed when the metal center was surrounded by steric bulk for the bpy and phen class of quenchers. Mesityl complexes with the general formula Pt(diimine)$(Mes)_2$ represent the

most extreme cases examined, and these quenchers exhibited the slowest quenching rates (~10^7 $M^{-1}s^{-1}$). The methyl groups of the mesityl ligands are positioned large mesityl groups located above and below the coordination plane of the metal center, effectively hindering metal-metal association. This results support the view that quenching occurs by association to form an exciplex.

The complexes with fluorinated complexes also were relatively ineffective quenchers (~10^7 $M^{-1}s^{-1}$). This result cannot be contributed to steric effects, because sterically-hindered quenchers such as Pt(bpy)(3,5-dmPh)$_2$ exhibit a faster rate of quenching than the less sterically-hindered Pt(dmbpy)($C_6H_3F_2$)$_2$ complex. The fluorinated phenyl ligands are weaker σ-donors than their phenyl counterparts. Weaker σ-donation is expected to serve to destabilize metal-metal association, resulting in slower rates of quenching. Therefore, the evidence suggests that the electronic properties of these quenchers strongly influence the rate of observed quenching.

The behavior of the dppz quenchers leads to a different type of conclusion. For these quenchers, the observed quenching rate is fast and relatively insensitive to the properties of the ancillary ligand. Both energy transfer and outer-sphere electron-transfer have been ruled out as possible quenching mechanisms. Therefore, the accumulated evidence suggests that the mechanism of exciplex formation may be different for different types of platinum(II) diimine complexes based upon electronic properties. For example, the quenching of Pt(tmphen)(tdt) chromophore with a lowest triplet MMLLCT state, is consistent with metal-metal association. However, for another chromophore such as Pt(dpphen)(CN)$_2$ chromophore with a lowest π-π* excited state this may not be the case. Two separate studies by Vogler and George and Weinstein have been carried out with the Pt(dpphen)Ph$_2$ complex.[19,20] Both studies suggest the

diimine-diimine interaction as the dominant mode of association for this complex. Unfortunately, it is difficult to fully address this issue in adequate studies with a range of quenchers and at the same time confidently rule out energy transfer quenching due to the higher energy of the lowest excited state this chromophore ($E_{0,0} \geq 2.7$ eV).

In summary, the accumulated evidence from cross-quenching studies of the Pt(tmphen)(tdt) chromophore indicates metal-metal interactions are important for exciplex formation. Most importantly, from these studies, we have learned how to control the self-quenching behavior of platinum(II) diimine complexes. Specifically, in order to control this behavior, it is necessary to hinder the dominant metal-metal interaction of exciplex formation in the Pt(tmphen)(tdt) chromophore through utilization of bulky substituents near the metal center or quencher complexes with weaker σ-donor ancillary ligands. This systematic approach is predicted to allow for use of this wonderful class of luminescent complexes to be successfully used in a variety of applications.

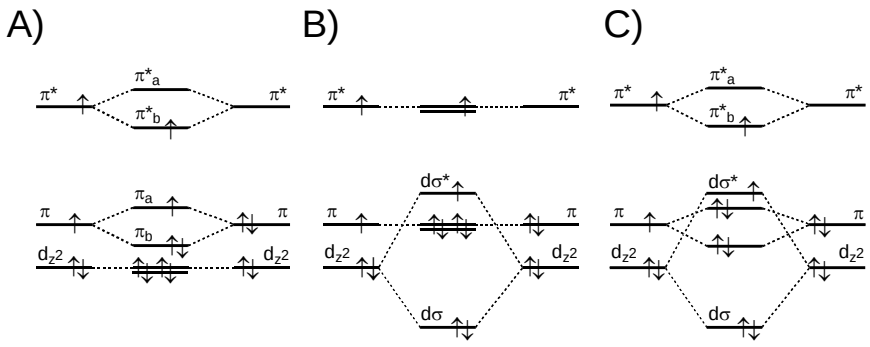

Figure 6.1. Qualitative orbital energy level diagrams for an excimer stabilized by A) diimine-diimine interactions, B) metal-metal interactions, and C) both types of interactions.

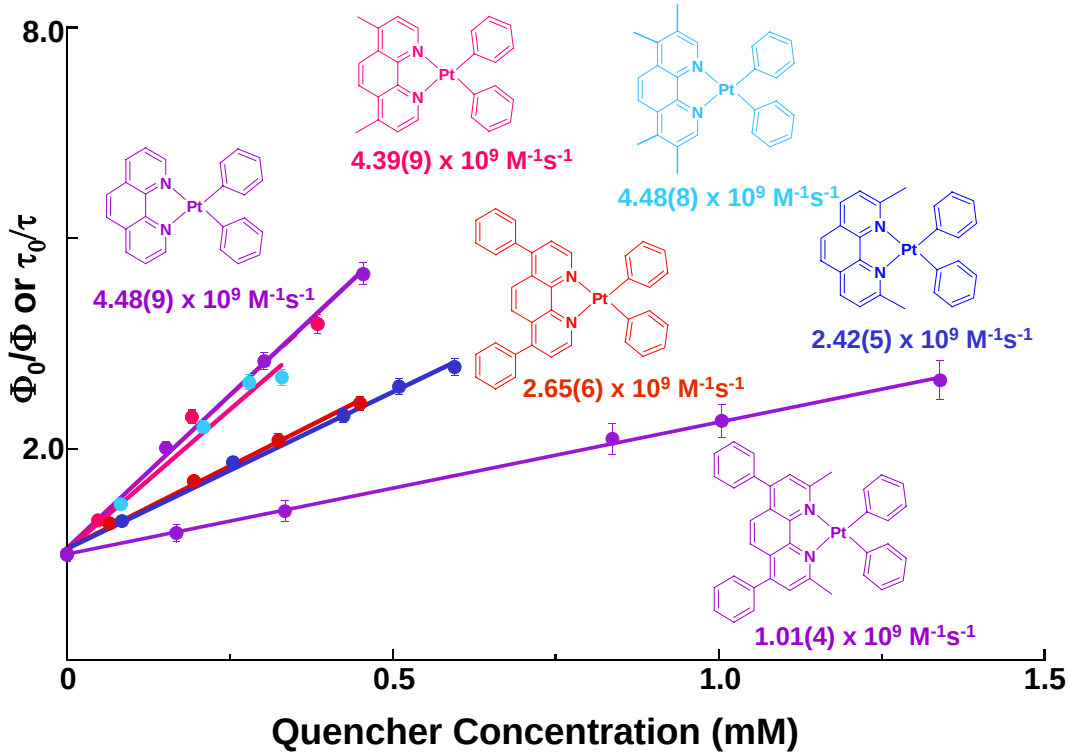

Figure 6.2. Stern-Volmer plots showing the influence of substituents on the 1,10-phenanthroline ligand. Error bars represented as ± 2σ. For some points, the error bars are hidden by larger size of data points.

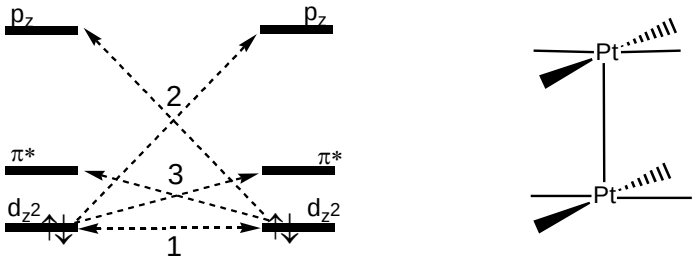

Figure 6.3. Electronic interaction model for ground-state metal-metal association of square planar platinum(II) diimine complexes.

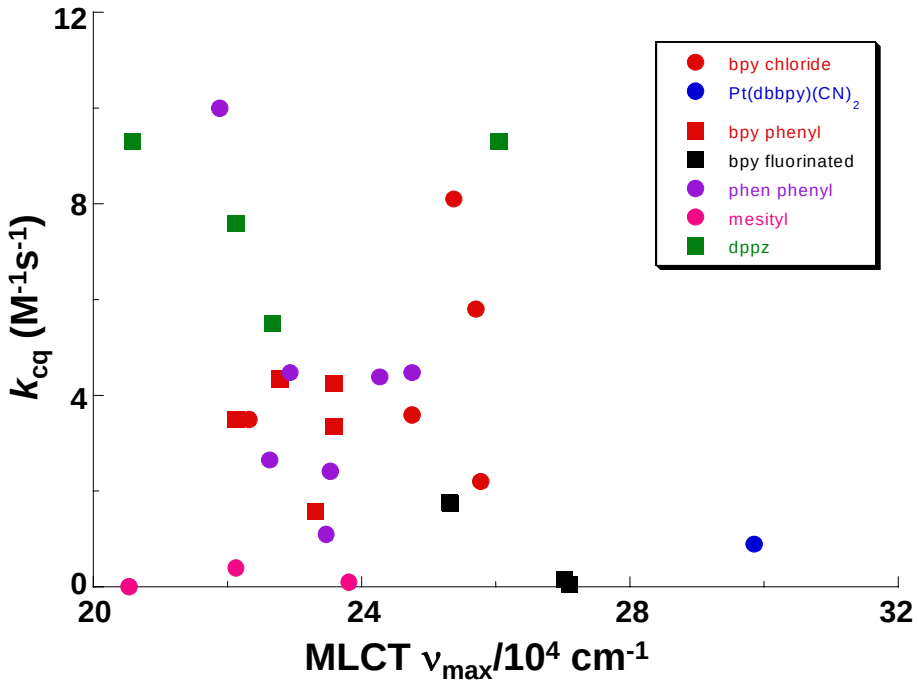

Figure 6.4 MLCT energy vs cross-quenching rate.

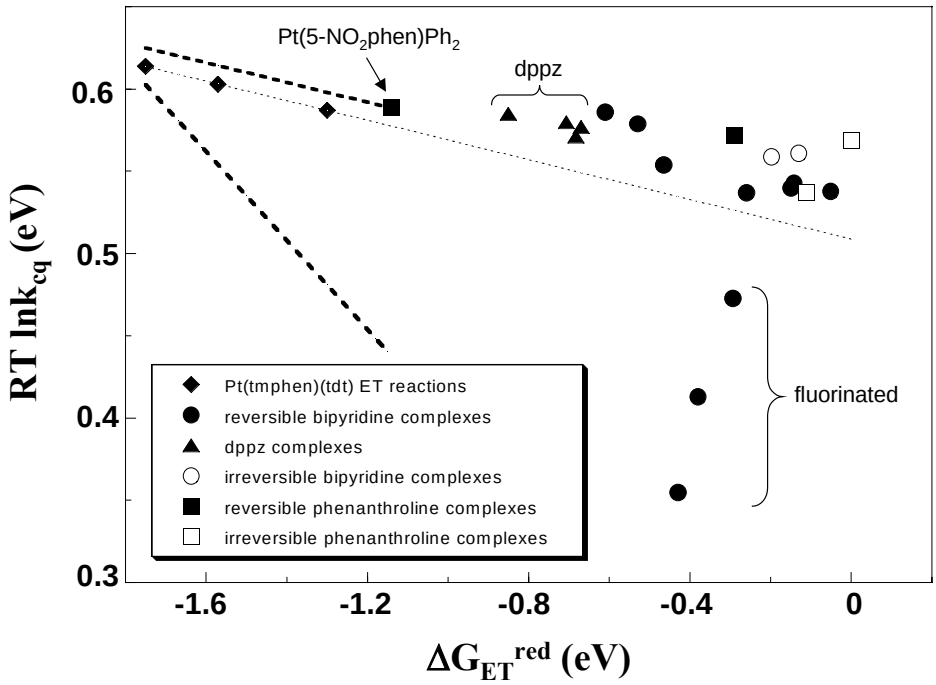

Figure 6.5. Pt(tmphen)(tdt) cross-quenching rate dependence on electron-transfer driving force ΔG_{ET}^{red} for photoinduced reduction of the quencher including Cummings and Eisenberg's electron-transfer quenching of excited Pt(II) diimine dithiolate complexes with nitrobenzene, nitrobenzaldehyde, and dinitrobenzene. Heavy-dashed lines bracket all rate constants reported by Cummings and Eisenberg. The light dashed line represents a linear fit to the electron-transfer data for Pt(tmphen)(tdt). It is significant that the majority of the cross-quenching rates lie above the extrapolated fit, suggesting that outer-sphere electron transfer does not make a significant contribution to the cross-quenching reaction.

Table 6.1 Electron-driving forces and corresponding quenching rates for Pt(II) diimine(tdt) complexes.

Chromophore	Quencher	Rate (10^9 $M^{-1}s^{-1}$)	ΔG_{ET} (NHE)[a]	ΔG_{ET} (Ag/AgCl)
Pt(tmphen)(tdt)	$Pt(dppz)Ph_2$	4.5(2)		-0.68
	$Pt(dppz)(3,5\text{-}dmPh)_2$	6.7(2)		-0.71
	$Pt(dppz)(Mes)_2$	5.3(2)		-0.67
	$Pt(dppz)(C_6F_5)_2$	7.5(3)		
	$Pt(5\text{-}NO_2phen)Ph_2$	9.4(2)		-1.14
Pt(tmphen)(tdt)	Nitrobenzene	7.9	-1.1	-1.30
	Nitrobenzaldehyde	15	-1.38	-1.57
	Dinitrobenzene	23	-1.55	-1.75
Pt(bpy)(tdt)	Nitrobenzene	0.8	-0.98	-1.18
	Nitrobenzaldehyde	6.3	-1.28	-1.48
	Dinitrobenzene	11	-1.45	-1.65
Pt(dbbpy)(tdt)	Nitrobenzene	0.95	-1.0	-1.20
	Nitrobenzaldehyde	7.6	-1.3	-1.50
	Dinitrobenzene	12	-1.48	-1.67
Pt(Clphen)(tdt)	Nitrobenzene	0.05	-0.95	-1.15
	Nitrobenzaldehyde	1.0	-1.25	-1.45
	Dinitrobenzene	8.2	-1.42	-1.61

References

1. Che, C.-M.; Wan, K.-T.; He, L.-Y.; Poon, C.-K.; Yam, V. W.-W. *J. Chem. Soc., Chem. Commun.* **1989**, 943-945.
2. Miskowski, V. M.; Houlding, V. H. *Inorg. Chem.* **1991**, *30*, 4446-4452.
3. Miskowski, V. M.; Houlding, V. H.; Che, C.-M.; Wang, Y. *Inorg, Chem.* **1993**, *32*, 2518-2524.
4. Lishan, D. W.; Hammond, G. S.; Yee, W. A. *J. Phys. Chem.* **1981**, *85*, 3435-3440.
5. McMillin, D. R.; Kirchoff, J. R.; Goodwin, K. V. *Coord. Chem. Rev.* **1985**, *64*, 83-92.
6. Horvath, A.; Stevenson, K. L. *Coord. Chem. Reviews* **1996**, *153*, 57-82.
7. Klein, A.; McInnes, E. J. L.; Kaim, W. *J. Chem. Soc., Dalton Trans.* **2002**, 2371-2378.
8. Klein, A.; Kaim, W. *Organometallics* **1995**, *14*, 1176-1186.
9. Klein, A.; Kaim, W.; Waldhor, E.; Hausen, H.-D. *J. Chem. Soc. Perkin Trans.* **1995**, *2*, 2121-2126.
10. Klein, A.; Scheiring, T.; Kaim, W. *Z. Anorg. Allg. Chem.* **1999**, *625*, 1177-1180.
11. Dungey, K. E.; Wwright, L. L.; Thompson, B. D.; Walsh, R. D.; Pennington, W. T. *J. of Chem. Crystall.* **2003**, *33*, 425-429.
12) Klein, A.; Hausen, H. D.; Kaim, W. *J. Organomet. Chem.* **1992**, *440*, 207-217.
13. Fees, J.; Ketterle, M.; Klein, A.; Fiedler, J.; Kaim, W. *J. Chem. Soc., Dalton Trans.* **1999**, 2595-2599.
14. Aullon, G.; Alvarez, S. *Chem. Eur. J.* **1997**, *3*, 655-664.
15. Gliemann, G.; Yersin, H. *Struct. Bonding* **1985**, *62*, 87-153.
16. Lechner, A.; Gliemann, G. *J. Am. Chem. Soc.* **1989**, *111*, 7469-75.
17. Connick, W. B.; Marsh, R. E.; Schaefer, W. P.; Gray, H. B. *Inorg. Chem.* **1997**, *36*, 913-922.

18. Cummings, S. D.; Eisenberg, R. *J. Am. Chem. Soc.* **1996**, *118*, 1949-1960.

19. Pettijohn, C. N.; Jochnowitz, E. B.; Chuong, B.; Nagle, J. K.; Vogler, A. *Coord. Chem. Rev.* **1998**, *171*, 85-92.

20. Kuimova, M. K.; Mel'nikov, M. Y.; Weinstein, J. A.; George, M. W. *J. Chem. Soc., Dalton Trans.* **2002**, 2857-2861.